Advancing Management and Control of Enclosed Spaces through Human-Centered Artificial Intelligence

by

Min Deng

A dissertation submitted in partial fulfillment
of the requirements for the degree of
Doctor of Philosophy
(Civil Engineering)
in the University of Michigan
2023

Doctoral Committee:

Professor Carol C. Menassa, Chair
Professor Vineet R. Kamat
Professor SangHyun Lee
Professor Kathy Velikov

Min Deng

mindeng@umich.edu

ORCID iD: 0000-0002-5301-8541

Dedication

To my mother and father,

who are the best parents in the universe

Acknowledgments

I would like to express my sincere gratitude to my academic advisor, Prof. Carol Menassa for her guidance and support during my doctoral study. During my Ph.D. study with Prof. Menassa, I not only learned how to conduct good research but also gained experience regarding academic presentations. In addition, Prof. Menassa also provided me with valuable experience in teaching, mentoring, grant writing, and servicing. With the provided opportunities, I equipped myself with competitive background and capabilities to pursue my future career.

I would like to sincerely thank Prof. Vineet Kamat for his co-advising during my Ph.D. journey. He always could provide meaningful insights from different perspectives which allowed me to rethink my research with diverse views. His inspiration and guidance helped me overcome difficulties through my research topics.

I want to thank Prof. SangHyun Lee, who invited me as the guest lecturer in his seminar and provided constructive advice to help reshape my dissertation. I am also deeply appreciative of Prof. Kathy Velikov for her valuable comments regarding the structures of my studies.

I would also like to thank Dr. Da Li, Dr. Julian Brinkley, Aaron Gluck, and Yijin Zhao who provided significant support to my research project and living while I was performing the experiments at Clemson University.

I am grateful to my colleagues and friends, Dr. Xi Wang, Bo Fu, Hongrui Yu, Hang Song, and Somin Park, who always provide their first support to my life and research. They were always available for me to share my happiness and sorrows. They provided advice and assistance when I was struggling with my research and felt upset about life.

I would like to acknowledge the financial support for this dissertation received from the U.S. National Science Foundation (NSF) (CBET 1349921, CBET 1804321), Center for Connected and Automated Transportation (CCAT) (69A3551747105), Rackham Graduate Student Research Grant provided by Rackham Graduate School, and the John L. Tishman Fellowship from the Department of Civil and Environmental Engineering.

Last but not least, I would like to take this opportunity to express the deepest gratitude to my beloved parents and elder sisters, for being my inspiration and motivation through my last four years of study, and for their endless love and care.

Table of Contents

List of Tables

List of Figures

Abstract

People are expected to spend the majority of their time in enclosed spaces (man-made environments where people can live and work) in modern life. The maintenance of safe and healthy environments in these spaces is of paramount importance to human comfort, productivity, and health. Poor management of such spaces might not only adversely affect human well-being but also lead to extra energy consumption and thereby deteriorate the effectiveness of sustainability initiatives in urban areas. This dissertation proposes a human-centered artificial intelligence (AI) framework for the efficient operation and maintenance of sustainable enclosed spaces that can positively impact the well-being and productivity of the occupants. Specifically, the research focuses on two main enclosed spaces where people in developed countries are expected to spend most of their time doing various tasks, buildings, and Autonomous Vehicles (AVs).

As a departure point, human-centric data is incorporated with environmental conditions in a holistic way to enhance human-building interaction and improve the efficiency of building management. A generic framework for human-centric real-time monitoring and management of the indoor environment is developed. Since different individuals might have distinct preferences for indoor environments, the concept of activity-based workplaces (ABW) is also incorporated into the framework. At first, a joint optimization approach for thermal comfort and energy consumption is used to demonstrate the feasibility of the developed framework. Based on the prediction models and the optimization algorithm, people with distinct characteristics are assigned to different indoor spaces. Meanwhile, the room conditions such as temperature, humidity, and lighting levels are adjusted autonomously. The results indicate that the appropriate adoption of

personal models can significantly improve the occupants' thermal comfort in the building while a large amount of energy can be saved.

Second, the scope of indoor well-being is not only limited to human comfort but also extended to mental health and productivity. To obtain the fundamental knowledge, experiments regarding the effects of wearing masks and lighting conditions on mental states such as work engagement and mental health of the occupants based on physiological sensing are conducted. The results reveal that wearing masks might reduce the mental workload (MW) and task performance of the occupants while the effects of lighting levels vary across different subjects. To better incorporate the mental states into the developed framework, personal prediction models for the work engagement are established based on the experimental results using machine learning techniques. A case study concerning both thermal comfort and work engagement is given to demonstrate the scalability of the framework. As a result, the framework is proven to be feasible regarding the improvement of human well-being while maintaining a low energy consumption of the buildings.

Based on similar human sensing technologies, the scope of the research has been extended from buildings to AVs aiming at safer driving environments. In L3 AVs, the driver is expected to be doing secondary tasks similar to those performed by occupants in the buildings such as reading, texting, and working on a laptop. However, humans still need to take over vehicles in some situations due to the limitations of automation technologies. Therefore, the states of the drivers such as how they are engaged in these tasks are essential as they will determine the success of any takeover event. A systematic analysis regarding the effects of takeover behaviors on human physiological responses is conducted. To conduct the experiment, different takeover scenarios are designed in the simulation program. A driving simulator is used for the experiment while the data

from the human subjects and vehicles are collected. The correlation between different physiological features from humans, takeover scenarios, and vehicles is investigated. Prediction models for takeover readiness are then tested. The results reveal that takeover readiness can be reflected in the physiological data and takeover scenarios.

In general, this research provides a new paradigm regarding how humans can be involved in the loop of control of enclosed spaces for smart decision-making. The proposed framework, algorithms, and discoveries can serve as fundamental theories to help with future research to investigate how this knowledge can be extended in the context of smart and connected communities and cities.

Chapter 1 Introduction

Aiming at better operations, the future built environment needs to collect a variety of types of data to help with the management of resources, assets, and services. The well-being and safety of people should be their priority in future built environments [1]. There are mainly two types of enclosed spaces of man-made environments where people can live or work in the future: 1) buildings and 2) Autonomous Vehicles (AVs) (the drivers can do secondary tasks similar to those performed by occupants in buildings). Since people are expected to spend most of their time in these spaces [2, 3], developing management strategies for indoor environmental conditions and advancing mechanisms of interactions with the occupants of these spaces is very important. To achieve efficient human-centric control of enclosed spaces, personal human data is the key due to the distinct characteristics of different people [4, 5]. Failure of incorporating personal characteristics may result in undesirable outcomes such as unsatisfied indoor environments and extra building energy consumption [6, 7].

This research aims to develop scalable approaches to bring humans into the loop for smart decision-making and controls of enclosed spaces. Specifically, this research explores the implementations of personal human data in different themes. As a core idea, the human Digital ID (DID) which refers to a digital replica of human biographic data, environment preferences, and personal prediction models that can be used to help with the evaluation of their indoor experience is proposed and defined. Based on DID, the first theme integrates personal data into the joint optimization of thermal comfort and energy consumption of the buildings. The second theme extends thermal comfort to a broader definition of human well-being by investigating the effects

of indoor environments on the mental states of the occupants. The third theme implements similar human sensing technologies in improving the safety of AVs. The overview of the research is shown in Figure 1.1.

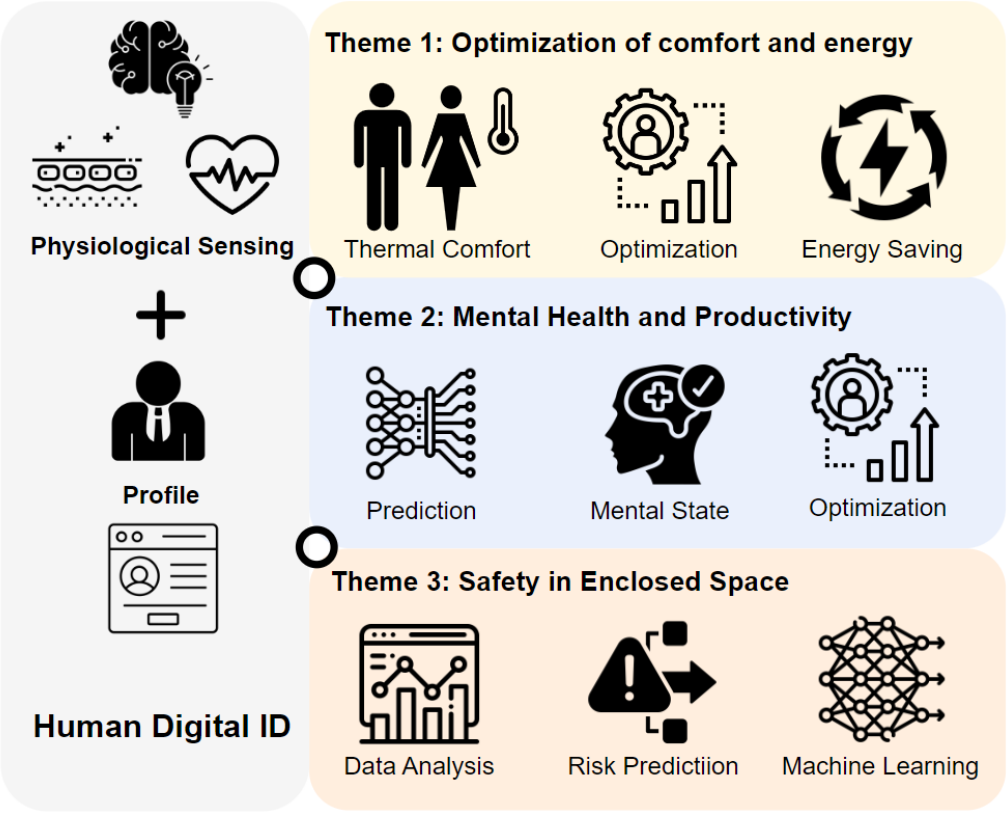

Figure 1.1. Research Overview

1.1 Importance of the Research

Comfortable and safe enclosed spaces (i.e., indoor spaces of building and AVs) play a vital role in a human's daily life and is crucial to the improvement of the well-being and safety of humans [8-10]. Human-in-the-loop (HITL) control is key to smart decision-making in these spaces for better operations. Failure to incorporate feedback from individuals may lead to undesirable outcomes regarding human comfort, work engagement, productivity, and safety in buildings and AVs.

For example, in terms of buildings, a survey shows that only half of the occupants are satisfied with their indoor environments [11]. One major reason behind this is that the conventional methods for indoor environment control rely on adaptive comfort models and standards [12, 13], which adopt one-size-fits-all approaches that assume all the occupants have similar preferences [14] resulting in an indoor environment that can only satisfy a small proportion of occupants [11]. However, it is well established that different people have distinct preferences for indoor environments resulting from differences in age, gender, and physiological features to name a few [4, 15]. On the other hand, these approaches may also easily lead to overheating or overcooling of the indoor space, thereby resulting in extra building energy consumption. As a result, the Heating, Ventilation, and Air Conditioning (HVAC) systems, which maintain the indoor environment at comfortable levels account for approximately 50% of the total energy usage in residential and commercial buildings in developed countries [16].

Similarly, human involvement still plays an important role in current AV designs due to limitations in relevant technologies [17, 18], and failure to incorporate the human states in AVs could lead to severe consequences. For example, in "Level 3 Conditional Automation", instead of always focusing on the roadway, the drivers are given some freedom in performing secondary tasks similar to those performed by occupants in the buildings. However, these activities lead to additional challenges in the timely takeover of the vehicles since the drivers might be highly distracted from the secondary tasks and not able to promptly be aware of the road conditions or respond to an alert in a timely manner [19]. Failure to take over control of the vehicles can lead to unexpected traffic accidents. Therefore, it is essential to know the states of the drivers while they are in the AVs such that the systems could provide alerts accordingly. To achieve this, a systematic understanding of the effects of takeover behaviors on driver's states is thus of significant

importance to allow better interaction between humans and vehicles so as to achieve safer driving environments.

To address these problems, it is important to first understand the effect of these environments on occupants, and then use the obtained knowledge to provide close-loop controls with the help of state-of-the-art technologies such as physiological sensing, Internet of Things (IoT), and AI.

Apart from the commonly investigated well-being indicators such as thermal comfort, the mental states of occupants also play important roles in well-being of the occupants. For example, work engagement ("a positive, fulfilling, work-related state characterized by vigor, dedication, and absorption [20]") and mental workload (MW) ("the 'costs' a human operator incurs as tasks are performed [21]") can directly affect the mental wellness [22] and productivity [23-26] of people. Therefore, a comprehensive consideration of human well-being which incorporates not only comfort but also mental states is necessary.

In general, the integration of personal human data into enclosed spaces including buildings and AVs is key to achieving healthy, comfortable, and sustainable communities.

1.2 Background of the Research

In this section, the importance of man-made enclosed spaces and their current situations are discussed. Specifically, the current strategies and challenges regarding the monitoring and control of indoor environments in buildings are introduced and discussed. In addition, it is expected that in the future AVs, the drivers can perform different tasks similar to those performed by occupants in buildings, thus the background of human involvement in AVs regarding the safety aspect is also explored.

1.2.1 Current status of the management of indoor environment

A good indoor environment is essential for the occupants in many aspects. It can potentially have a significant impact on their well-being and lead to the improvement of their productivity [27-29] and vice versa [30-32]. In order to have better management of the indoor environment, many studies have focused on developing smart building management platforms [33]. The rapid growth of high-speed commercial internet [34], advances in building management systems (BMSs) [35], as well as personal electronic devices such as smartphones [36], have supported the concept of a smart building [37]. A smart building aims to automatically control the building systems to address energy waste and improve the indoor environment quality based on smart sensors [38]. The sensors were installed in different locations in the building to collect environmental data such as temperature and humidity [39-47]. In addition, technologies such as Wi-Fi, WSN, 5G, and LP-WAN [33, 48, 49] were applied to allow for seamless data communication. With the sensing data, real-time visualization platforms for indoor environments were developed, which aimed to provide the building manager with a more efficient decision-making process. For example, Revel et al. [50] developed a low-cost thermal comfort monitoring system by means of the Predicted Mean Vote (PMV) index of multiple positions calculated through the collected environmental parameters such as temperature, relative humidity, and air velocity. Chang et al. [51] presented a framework to achieve colorful visualization of indoor temperature and humidity associated with adaptive thermal comfort values, which used Dynamo to import real-time sensing data into Autodesk Revit through the Arduino microcontroller. In addition to thermal comfort, other factors such as acoustic comfort were also investigated. In addition, different platforms were developed to evaluate the real-time indoor air quality. A battery-free device was designed by Tran et al. [52] to monitor the concentration of VOC, air temperature,

relative humidity, and atmospheric pressures of the indoor environment. Similarly, Kim et al. [53] developed an integrated monitoring system with multiple sensors to evaluate real-time indoor air quality. By examining the level of seven gases (i.e., ozone (O3), particulate matter (PM), carbon monoxide (CO), nitrogen oxides (NO_2), sulfur dioxide (SO_2), carbon dioxide (CO_2), and the volatile organic compound (VOC)), the system was able to provide a timely alert regarding the air quality.

Even with those efforts being paid to improve the indoor environment, a survey involving more than 52,000 people in 351 office buildings showed that only half of the occupants are satisfied with their indoor environments [11]. One major reason behind this is that the conventional methods for indoor environment control rely on adaptive comfort models and standards [12, 13], which adopt one-size-fits-all approaches that assume all the occupants have similar preferences [14] resulting in an indoor environment that can only satisfy a small proportion of occupants [11]. However, it is well established that different people have distinct preferences for indoor environments resulting from differences in age, gender, and physiological features to name a few [4, 15]. For example, it is suggested that females prefer higher room temperatures than males [54] and the thermal sensation of people in different age groups (under 25 years old, 26-45 years old, and over 65 years old) are statistically different [55]. In addition, it is shown that the occupants' physiological features such as brain signal [23, 56, 57], skin conductance level (SCL), heart rate (HR), and skin temperature (ST) may vary across individuals under the same indoor environment (i.e., temperature and lighting conditions) [57]. Therefore, it is essential to consider the individual differences in the decision-making of the building systems.

1.2.2 Active-based workplaces

To meet occupants' diverse preferences for the indoor environment, previous studies have focused on approaches regarding individual indoor experiences. The idea of active-based workplaces (ABWs) [58] was proposed to offer people more flexible workplaces. The utilization of ABWs aims to provide flexible workplaces for the occupants depending on their personal preferences (e.g., the location and microclimate of the workplace) [59]. It has shown an advantage in improving people's performance [60], physical activity, and relationships with co-workers [61] compared with traditional offices. A review involving 36,039 participants also highlights the benefits of ABW particularly in improving communication, control of time, and workplace satisfaction [62]. Recently, some efforts have already been paid to integrate the ABW with smart building systems. For example, a robust system named *OccuSpace* was developed by Rahaman et al. [63] for workplace management. The system allowed the occupants to use the statistical features of the Received Signal Strength Indicator (RSSI) of Bluetooth card beacons to predict the utilization of the shared workplace. Similarly, Sood et al. [14] presented a platform with a mobile interface for the occupants to find suitable workplaces by collecting their experience feedback at different indoor workplaces.

However, the application of ABW needs precise control of the indoor environment, as a poor indoor space management strategy may lead to extra energy consumption [64] and insufficient indoor comfort improvement for the occupants [65]. Therefore, to maximize the gains from ABW, a human-centric smart decision-making system is required. In addition, a comprehensive survey regarding the worker perspectives on incorporating AI into office spaces is conducted. The results show that it is expected that future buildings should be able to interact with the occupants and create better indoor environments for individuals [48].

1.2.3 Real-time monitoring of the indoor environment

To achieve the efficient control and management of the indoor environment considering the feedback of individuals, real-time estimation of the occupants' states is the key to mapping personal behavior patterns and performance to improve the comfort level and well-being of each individual [28]. Prediction models for human comfort as references for the decision-making of the indoor environment have been investigated in several studies. For example, Ho et al. [66] developed a platform that could connect real-time indoor air quality to a personal health reporting system through a mobile app. The system was able to analyze the data and give alerts to the occupants once the concentration of air pollution exceeded a certain threshold. Moreover, after collecting subjects' thermal comfort feedback and physiological data under different environmental conditions, Li et al. developed [36, 67, 68] different approaches including smartphone applications and thermal camera-based frameworks to estimate the occupants' personal thermal comfort. Based on the developed personal thermal comfort models, a dynamic determination of the optimum room condition mode was achieved. Similarly, Ma et al. [69] applied an ANN model which took human parameters (e.g., clothing type, activity type, human relative position, gender, age, height, and weight) and environmental parameters (e.g., air temperature and air humidity) as inputs to train a personal prediction model for thermal comfort.

Based on the existing technologies, research has started to focus on occupant-centric environmental control. For example, Kim et al. [5] have proposed a unified modeling framework to achieve smart control of indoor thermal environments based on personal prediction models. The framework discussed the data collection, model selection, and learning process of the systems, as well as the architecture for the integration of models in thermal control. In addition, a review conducted by Yang [70] summarized the concepts of making the HVAC control based on occupant

information. The utilization of occupant-related data in improving the performance of HVAC systems has been identified. However, these frameworks only focus on thermal comfort and have not explored the capabilities of incorporating other indoor experiences. In addition, there is no case study to demonstrate how the proposed systems work. In order to further improve the indoor experience of the occupants, it is essential to develop a generic framework with an illustrative case study.

1.2.4 The importance of enclosed spaces in buildings and AVs

Besides buildings, another type of enclosed space where people may spend most of their time doing similar daily work in the future is AVs. AVs are expected to contribute to half of the new vehicle market by 2045 [71]. Successful adoption of AVs can reduce drivers' stress and fatigue, curb traffic congestion, and improve safety, mobility, and economic efficiency. The present driving automation systems, including the Tesla Autopilot and Cadillac Super Cruise, are primarily categorized as "Level 2 Partial Automation" (L2) [72]. At this level, the driver is required to continuously monitor the road and take full control immediately when the system reaches its limits. Incidents of failure to take over can result in fatal injuries, such as the tragic Tesla crash in California [73]. As manufacturers transition towards the more sophisticated "Level 3 Conditional Automation" (L3), where drivers are not obliged to actively monitor the dynamic driving environment when the automated system is engaged (i.e., hands-off and eyes-off), such situations are likely to become even more challenging [72]. Instead, they can engage in various secondary tasks, such as texting and relaxation. Nevertheless, in L3, drivers must still be capable of taking over and assuming manual control within a few seconds of being notified to avoid any possible accidents [72]. Since drivers are not consistently and actively involved in driving, they might not be able to rapidly restore situational awareness and effectively take control of the vehicle [19, 74].

This leads to a lack of interaction between the driver, which raises significant safety concerns for L3 automation, potentially impeding its acceptance by society.

Existing studies have extensively explored methods to monitor and evaluate a driver's physical and psychological condition, such as fatigue, attention, and drowsiness, in both manual driving and L2 automation. However, current techniques such as onboard sensors and cameras [75, 76] for monitoring a driver's state are built upon the assumption that drivers must stay focused on the driving task constantly, while driver engagement is not required in L3 automation, which makes these approaches obsolete. Therefore, the investigation of the feasibility of using multimodal physiological features collected from drivers in L3 AVs to estimate takeover readiness is essential for driving safety.

1.3 Research Objectives

The overall objective of this research is to define and integrate the concept of human DID (i.e., personal human data) to achieve more efficient management and control of enclosed spaces so as to improve the comfort, health, productivity, and safety of people while optimizing energy usage.

The specific objectives of this dissertation are as follows:

- Propose and define a brand-new concept of human Digital ID (DID) as the fundamental theory for human-centered advanced management and control of enclosed spaces.
    - Decide the important information that can reflect the personal characteristics that correlated to indoor experiences.
    - Develop a generic framework that demonstrates the potential implementation of DID in smart buildings.

- Based on DID, develop a comprehensive and scalable framework to jointly optimize the indoor well-being of the occupants and energy consumption.
    - Develop the joint optimization algorithm which can be extended to the different indoor experiences of the occupants.
    - Test the optimization algorithm using a case study.
- Conduct experiments to further understand the correlation between human physiological responses and indoor environments as the basis of extending the scope of human well-being optimization.
    - Understand how wearing masks might affect the mental states and performance of the occupants.
    - Understand the effects of lighting conditions on the work engagement of the occupants while they are performing cognitive tasks.
- Explore the possibilities of obtaining personal models for human mental states (e.g., work engagement) as auxiliary tools while managing and controlling indoor environments.
    - Establish the prediction models for work engagement using easily measurable physiological data.
- Adopt similar physiological sensing technologies to AVs for safer driving environments.
    - Conduct a systematic analysis of the effects of takeover behaviors on physiological responses.
    - Explore the potential of predicting the takeover readiness

1.4 Dissertation Outline

This dissertation is a compilation of peer-reviewed scientific manuscripts which describe the research on advanced management and control of enclosed spaces through human-centered Artificial Intelligence. The remainder of the dissertation is organized as follows:

Chapter 2 introduces the definition and potential implementations of the new concept of DID, which is expected to be integrated with recognition, prediction, recommendation, visualization, and feedback systems to form a general framework. It is scalable and can be integrated with any algorithms and techniques, which can serve as a fundamental framework for future smart buildings.

Chapter 3 proposes a framework to optimize thermal comfort while achieving energy savings through room assignment and indoor environmental control as a case study of implementing the concept of DID. The proposed framework integrated learning-based building energy models and personal thermal comfort models with the concept of the Large Neighborhood Search (LNS) algorithm. The proposed optimization method can thus be of significant value for building managers to decide the room assignment and environmental conditions of the buildings.

Chapter 4 investigates the effect of wearing a mask on the physiological responses and task performance of those who work in office environments during the pandemic period. The two most commonly used masks (i.e., cloth and surgical masks) are chosen for evaluation. The work engagement, MW, SCL, HR, as well as the overall performance of the subjects while they are completing simulated office tasks are collected and analyzed. This study provides a valuable reference for those who need to wear a mask while working.

Chapter 5 investigates the effect of lighting level on occupants' work engagement by studying the frontal asymmetry index (FAI) measured by electroencephalography (EEG).

Statistical analysis is performed to investigate the work engagement of the occupants under three typical lighting levels (i.e., 200 lux, 500 lux, and 1000 lux) while they are performing cognitive tasks. In addition, this study also proposes a method to predict the engagement level for each subject based on the lighting level and their GSR, HR, and ST using machine learning algorithms. This opens the possibility of using easily measurable physiological parameters to estimate human brain activities and predict their work engagement under different lighting scenarios.

Chapter 6 illustrates a case study regarding how to integrate thermal comfort and work engagement with their corresponding personal prediction models. The indoor temperature and lighting levels are used as two example environmental parameters that can be controlled in the buildings so as to maximize the thermal comfort and work engagement of the occupants at the same time. A Unity-based program is developed to demonstrate the real-time visualization platform of the states of the occupants.

Chapter 7 provides a comprehensive analysis of the effects of takeover behaviors on the commonly collected physiological data. A program for conditional automation is developed based on a game engine and applied to a driving simulator. The analysis of the data across different subjects is also conducted, which emphasizes the importance of considering standardization or normalization of the data when they are further used as input features for estimating takeover readiness. Overall, the findings in this chapter provide a deep understanding of the pattern of changes in physiological data during the takeover periods, thus serving as references for using these variables as predictors of takeover readiness and performance in future studies.

Chapter 8 concludes the dissertation and summarizes the significance and contributions of the research, followed by a discussion of future research direction.

Chapter 2 Definition and Potential Implementations of Human Digital ID

2.1 Introduction

In support of human-centered AI, a new concept of human Digital ID (DID) is proposed as the core of the real-time human-centric monitoring framework. As per definition, the concept of DID refers to a digital replica of human biographic data, environment preferences, and personal prediction models that can be used to help with the evaluation of their indoor experience. The systems and information flow of the framework are shown in Fig. 2.1. The DID supports interactions in different connected systems that are important for the decision-making and control of indoor spaces. These systems include (1) recognition systems; (2) prediction systems; (3) visualization systems; (4) feedback systems; and (5) control systems. The information stored in DID serves as the personal prediction model to estimate the personal comfort or indoor environment preference of the occupant. After the occupant is recognized by the recognition system, the profile for the specific individual is obtained. In the prediction system, the personal DID combines with real-time environmental data to estimate the human state (e.g., thermal comfort, visual comfort, mental state). In addition, to sufficiently represent the collected and predicted information, a virtualization platform is implemented as a tool for real-time monitoring and decision-making. The details of each system are discussed in the following sections.

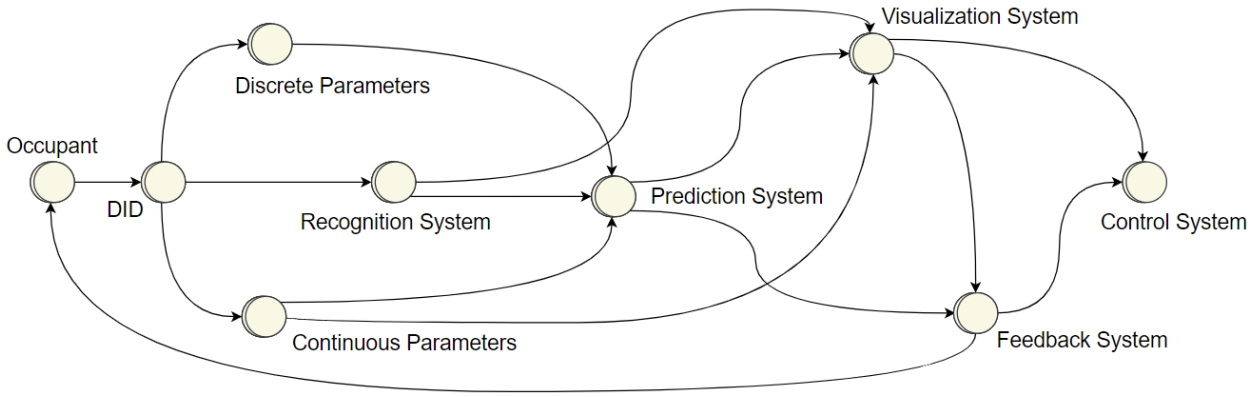

Fig. 2.1. Components and information flow of the DID-based system

2.1.1 Digital ID (DID)

2.1.1.1 DID data components

The information contained in DID for an individual is shown in Fig. 2.2. Human information can be categorized into two major categories: (1) dynamic parameters; and (2) static parameters. Dynamic parameters include the parameters that continuously change over time such as clothing type, location, activity intensity, and physiological data (e.g., GSR, HR, and ST), when available. In contrast, the static parameters do not change significantly within a short period of time, such as human physical parameters (e.g., age, gender, height, and weight), general environmental perceptions (e.g., preference for temperature, humidity, and lighting level), lifestyle (e.g., level of physical activity), and long-term working style (e.g., sedentary or long-standing). In practice, the dynamic parameters can be obtained through wearable or non-intrusive sensors [36, 67]. The static parameters are used to categorize the profiles of different people and do not need to be collected continuously. In addition, personal prediction models are also considered a part of DID. They refer to the mathematical models (e.g., standardized equations and learned models from machine learning) that are capable of predicting the occupants' state such as thermal comfort, visual comfort, and work engagement. The prediction models use static or dynamic parameters, sometimes combined with environmental parameters, to make the estimation. For example, human

activity level and clothing type associated with room temperature and humidity are generally considered good features for predicting thermal comfort [69, 77].

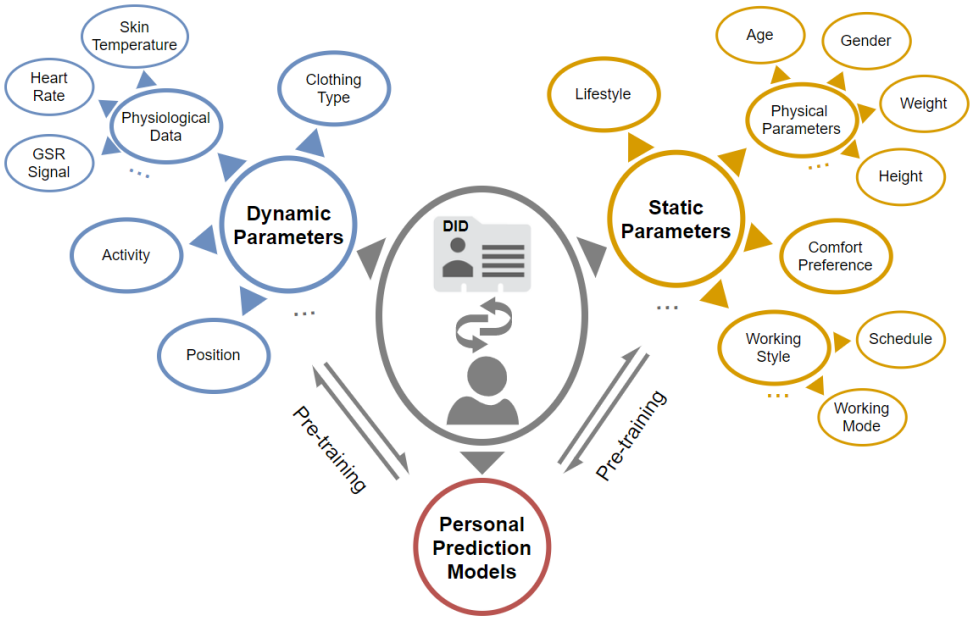

Fig. 2.2. Components of Digital ID

2.1.1.2 A framework to establish and update the DID database

A framework for the establishment and update of the prediction models is proposed as shown in Fig. 2.3. Based on the functionalities of the building, a target group of people is determined. For example, for an educational building with study rooms, the target group of people is students while for an office building the target group of people should be the employees. An initial database is established by collecting the data from the target group. For this study, the educational building is used in the case study, thus the data is mostly collected from students. The static parameters of the people including age, gender, weight, height, thermal preference, and lighting preference are collected. Based on the collected information, further processes of the data are conducted to establish the personal prediction models for occupants' states (e.g., thermal comfort, visual comfort, sound comfort, odor comfort, and work engagement).

However, the existence of personal models for all the occupants cannot be assumed, due to the lack of data or because someone is a new occupant. Therefore, for the new occupants without existing DID databases, public databases will be applied to give the initial guess of their state. Public databases usually contain a large number of datasets collected from different studies. Based on the databases, general prediction models can also be well-trained, thus they serve as potential sources to initialize the system for new occupants. A good example of a public general database being used in this study is the ASHRAE Global Thermal Comfort Database II [15], which will be described in detail in the case study. While the initial guess of the human state is conducted, the occupants will give feedback to the system and allow the establishment of their personal database. An example approach to collecting feedback is through a mobile app developed in previous studies [14, 36, 78]. The collection of feedback can not only apply to new occupants but also be feasible for existing occupants so as to update their existing databases.

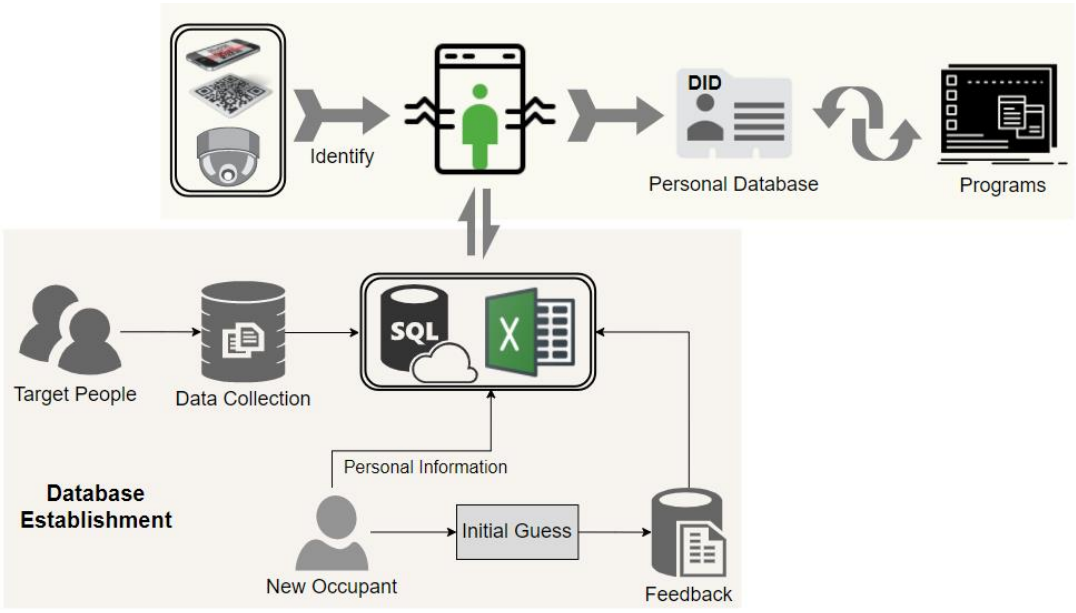

Fig. 2.3. The schematic diagram for the establishment, access, and update of the database

2.1.1.3 DID data storage and exchange

All data of the DID is stored in a local or cloud database. In this study, a text file on the local disk is used to store the personal information of any occupant, while there is no restriction on the data storage and other approaches such as SQL database. Within the database, each individual has a separate sub-database that contains the previously mentioned information. The database is dynamic as the information of the human changes over time. When the database is needed by the system, it is accessed by scripts that are based on computer programs developed in languages such as python, java, C++, and MATLAB (depending on the program platforms). In this study, the back-end programs are mostly written in python. For example, when the system needs to estimate the thermal comfort of the occupants using the environmental parameters (e.g., temperature and humidity), the specific thermal comfort prediction model is accessed and applied to make the estimations. Note that there can be multiple models to estimate the same human state, and they take different input features. For instance, temperature and humidity are often used as the input features for thermal comfort [36, 79] while personal physiological data such as ST and HR are also useful predictors of thermal comfort [36]. The required information from the database thus depends on real-world scenarios.

2.1.2 Recognition system based on DID

To track the human state, a recognition system based on DID is proposed as shown in Fig. 2.3. Once a person enters the building, the system will recognize the occupant so as to match him/her with the corresponding DID database (if it exists). One example of the identification method is the QR code. If the QR code is attached to a phone or an identity card, the occupants only need to swipe the card or an identifiable marker on the phone, which they would typically have to do at the entrance of office buildings. Alternatively, computer vision techniques can be

another method to recognize occupants through indoor surveillance cameras [80]. As both QR scanning and vision-based human recognition are mature techniques in the real world and have been widely used, details of human identifying processing will not be discussed in this chapter as they are out of the scope of this study. Once the DID of the occupant is recognized, the database becomes an open resource for the systems. However, for the new occupants, recognition is considered to fail, and a new database will be generated at the back end of the systems, newly collected data from the specific occupants will be allocated into the database.

2.1.3 Prediction system

The proposed system can deal with the different scenarios: (1) existing occupants with their DID databases well established; (2) new occupants without DID databases or without enough data to deliver accurate personal prediction models. For the first scenario, it is assumed that there is enough data collected from the occupants, and the mathematical models have been established. Therefore, the existing personal database is used to estimate the occupants' states.

However, for the second scenario, there is no personal database for the programs to access. Therefore, it is proposed to conduct the initial guess based on the public open-source database. The process of the model training is shown in Fig. 2.4. For an existing public database with occupants' information, corresponding environment parameters, and associated comfort feedback (e.g., ASHRAE Global Thermal Comfort Database II), a general prediction model can be established using machine learning. Take the thermal sensation as an example, the input includes personal information such as age, gender, weight, height, and clothing level. The environmental parameters include temperature and humidity, while the outputs are the thermal sensation indices (e.g., integer numbers range from -3 to 3). Here, it is considered the baseline prediction model.

However, an alternative method is proposed to establish separate models based on the profiles of humans. Based on the findings in previous studies [81-83], one hypothesis here is that people with similar profiles tend to have similar perceptions and preferences of the environment. Therefore, human profiles are assigned into different categories according to their static parameters such as age, gender, weight, and height. This method requires the new occupants to enter their basic information right after they enter the building through the same app as mentioned in the previous section. For each category of the human profile, a prediction model is established. The categories are distinguished by human profile, and several pre-defined categories are used to establish the initial prediction models based on the data collected in different indoor environments (IE). When the building is used for a specific group of people, the establishment of the initial database can thus be based on data from the target group of people. The potential benefit of this method is that fewer datasets are required to establish the prediction model for a specific group of people.

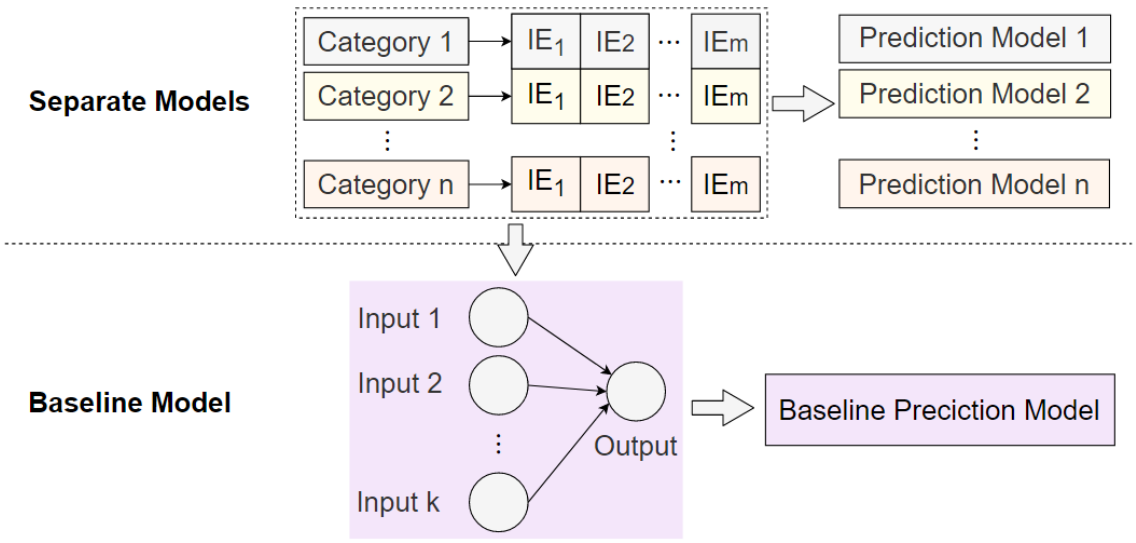

Fig. 2.4. The proposed method for model training

2.1.4 Human-centric visualization system

Different from indoor environment monitoring, the visualization platform required for DID needs to be human-centric. It should be able to show the state of individuals, such as their location in the building, comfort levels, and preferences of the indoor environment. It can help the building manager to provide a better strategy for indoor environment control. To keep the privacy of the occupants, the visualization system contains no identifiable personal information (e.g., name, age, gender, height, weight) and only the building managers can access it. A comprehensive comparison of existing platforms that allow real-time visualization of the built environment is provided. BIM platforms such as Revit are commonly used in previous studies [38, 45]. The developed interactive interfaces achieved through the Application Programming Interfaces (APIs) using C# programming can show the status quo of the indoor environment such as temperature and humidity [40, 43, 84-86]. However, due to the model updating mechanism, most of the BIM platforms are not suitable for real-time visualization of moving components such as human subjects, because it requires the model to update from time to time, which may crash the models. To be specific, any modifications of BIM models in Revit will cause a reload of the entire model.

In contrast, game engines such as Unity can not only be efficiently connected to BIM models but also provide functionalities that allow human models to update their locations with high frequencies (e.g., >100Hz). In addition, data connection and visualization interfaces can also be achieved using C# scripts. The game engine is thus considered the most practical platform. Therefore, in this study, Unity is used as the tool for developing the real-time visualization platform. The Revit model is converted to FBX. Format and pre-processed by the 3D Max (retain some semantic information) and then imported into Unity. In addition to the building model, human models are also created to represent the occupants. Separate programs are written in C#

scripts to allow the data exchange between the local data files. The scripts will read the local data file which contains the environmental parameters (e.g., temperature and humidity) and human state (e.g., thermal sensation). These data files are generated from the back-end programs (written by python) mentioned in previous sections.

2.1.5 Feedback system

The feedback system includes recommendations for the occupants based on the DID. With a variety of smart sensors installed in different locations of the buildings, real-time environmental data such as temperature and humidity are readily available. In this study, the real-time environmental data is collected and stored in the text files, which are not only connected to the Unity visualization platform but are also being used to provide feedback based on the results from the prediction system. After processing the obtained information, recommendations are sent to the occupants or the building managers. The notifications regarding the recommendation are delivered through a mobile app to the occupant, thus they can know the most suitable places for them to visit.

With the capability of estimating the comfort levels of the occupants in different aspects, a recommendation system regarding the best-fit rooms for the occupants is proposed. A composite index is designed to represent the overall comfort score of each room. The indoor environment comfort metric for an occupant includes different aspects such as thermal comfort (TC), lighting comfort (LC), sound comfort (SC), and odor comfort (OC). The score for each aspect can be predicted using a method that is similar to the estimation of thermal sensations (i.e., range from -3 to 3). In order to evaluate the environment of the room in a more straightforward way, a linear method is proposed to evaluate the overall comfort index. A schematic diagram of the linear method is shown in Fig. 2.5. As shown in Eq. (2.1), a normalized score for each comfort level is

first obtained. Based on the preference of the occupants, different weights are assigned to each type of indoor comfort. The weights in the case study are obtained by questionnaires. To normalize the final score, the sum of the weights should be 1 as indicated in Eq. (2.2). The Comfort Score Index (CSI) of a room can thus be represented as Eq. (2.3), which ranges from 0 to 1 (the higher the better). However, a higher final score does not necessarily mean the IEQ for a specific room is good in every aspect. For example, a room may achieve the highest final score but has a score of zero for specific comfort types. Therefore, a constraint of scores (p) for individual comfort types is added to the final choice. The problem can then be written as shown in Eq. (2.4). Based on the strategy, the best-match rooms will be assigned for the occupants based on DID.

$$g(C_{ij}) = \frac{|C_{j\_bound}| - |C_{ij}|}{|C_{j\_bound}|} \tag{2.1}$$

$$\sum_{j=1}^{n} W_j = 1 \tag{2.2}$$

$$f(TC_i, LC_i, OC_i, SC_i, \cdots) = \sum_{j=1}^{n} W_j \cdot g(C_{ij}) = \sum_{j=1}^{n} W_j \cdot \frac{C_{j\_bound} - |C_{ij}|}{C_{j\_bound}} \tag{2.3}$$

$$\max f(TC_i,\ LC_i, OC_i, SC_i, \cdots), \quad s.t. \quad g(C_{ij}) \in [p, 1] \tag{2.4}$$

Where C_{ij} refers to jth parameters (e.g., TC, LC, OC, and SC) in ith room, W_j represents the weight of a specific indoor comfort type for the occupant.

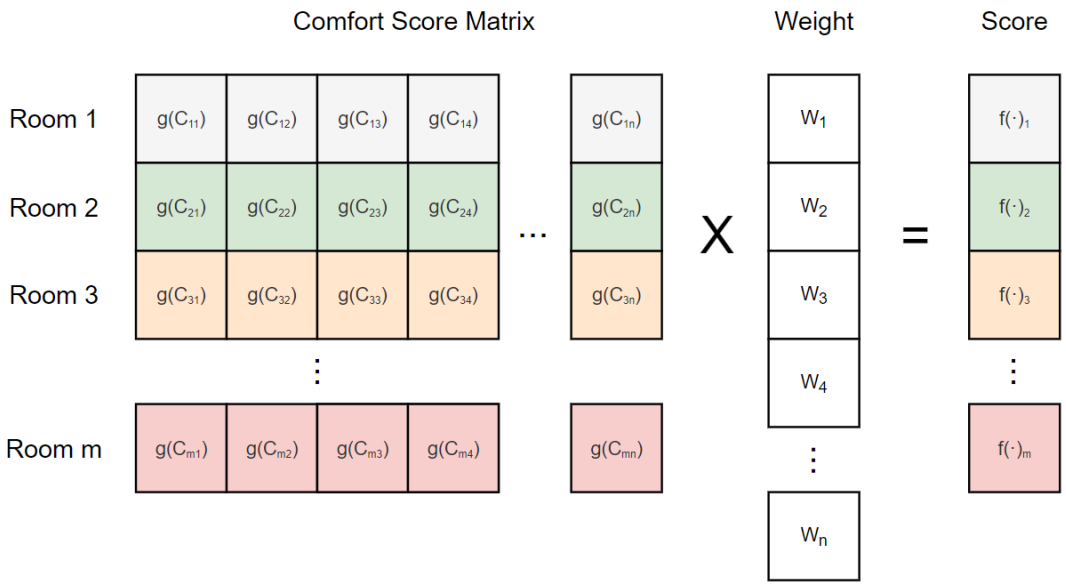

Fig. 2.5. Computation of the scores for building rooms

2.1.6 Control System

The feedback system provides a valid reference for the building control system. On one hand, the predicted human state of the occupants is used as a signal sent to the control terminal regarding the adjustment of the indoor systems. For example, given the occupants are feeling warm, the corresponding signal will be a trigger to lower the temperature setpoint. The final decision can be transferred to a smart thermostat (e.g., NEST) to control the indoor environment. Similarly, a signal that reflects that the occupants feel the room is too bright can drive the dimming of the lighting systems. On the other hand, the real-time monitoring of the occupants' state provides more insights into the interaction between the occupants and the building. A more flexible control strategy can then be applied by the building manager based on the results of the systems and the visualization platform.

Chapter 3 Joint Optimization of Thermal Comfort and Building Energy

3.1 Introduction

Thermal comfort is considered one of the most important factors for evaluating the indoor environment due to its significant effects on occupants' indoor satisfaction [87, 88], health [32, 89], and productivity [10, 90]. Although a significant amount of energy has been used in buildings to maintain the thermal environments through the Heating, Ventilation, and Air Conditioning (HVAC) systems [16], only 38% of the occupants are thermally satisfied with their current workplaces [91]. One of the main reasons is the distinct thermal preferences across different people (e.g., some people prefer a warmer environment while some others prefer a cooler environment), resulting in variations in their thermal perception under the same thermal environment [4, 15]. However, the conventional environmental control systems are typically designed based on design standards [12, 38] or adaptive models (e.g., predicted mean vote) [77, 92], which fail to consider individual differences and always adopt one-size-fits-all temperature and humidity [14].

To address this problem, Personal Conditioning Systems (PCS) were proposed to control the thermal conditions of micro-environments surrounding each individual [93]. The performance of PCS was examined by conducting parallel subject tests in a personal environment laboratory, which shows that PCS could significantly improve thermal comfort. In addition, it was pointed out that PCS could address thermal comfort and energy consumption simultaneously [79]. For example, a suite of minimum-power PCS devices was developed by [94]. The devices were proven to be useful in improving the subjects' thermal comfort and achieving a certain amount of energy-saving (1.5% to 20.7% by heating devices and 15.3% to 34.1% by cooling devices). Despite the

capabilities of the PCS, it may not be practical to install PCS for all spaces in the buildings as it requires additional equipment thereby leading to extra maintenance and cost. In addition, PCS is not flexible enough when people need to walk around the building as it typically requires a device to be attached near an individual [95].

This raises an important question: how we can satisfy an individual's thermal comfort without additional equipment? Flexible workplaces that allow occupants to stay in indoor spaces that suit their preferences and lifestyles have been proposed [58, 60, 62] as a promising approach to achieving this objective. To help with the decision-making of the optimal workplace assignment, an accurate estimation of occupants' thermal comfort is crucial. Regarding individual comfort, personal models that provide an estimate of the individuals' states are continuously being emphasized across different aspects [57, 69, 96, 97] due to higher accuracies. Therefore, personal thermal comfort models are used in this study to perform the optimization. This study uses these typical parameters of the indoor environment (e.g., temperature and humidity) and human factors (e.g., age, gender, height, weight, and clothing level) as the inputs of the personal thermal comfort prediction models. In addition, as the idea of energy-efficient buildings keeps gaining attention among stakeholders [98-100] due to their large proportion of carbon emissions [101], the energy savings strategies for the building are also considered in this study.

To extend our preliminary study [65] which proposes a framework that can group different occupants and match them with best-fit rooms for thermal comfort, the objective of this study also provides suggestions for optimal thermal environmental parameters which can achieve energy-saving for the building while maximizing the thermal comfort of the occupants. This chapter makes the following contributions: (1) a novel framework is proposed to match the occupants with the rooms with optimal indoor thermal environments; (2) energy-saving of the building is achieved

while optimizing the thermal comfort of the occupants; (3) the feasibility of the framework is validated by a case study with different scenarios.

3.2 Related Work

First, existing literature regarding the approaches to flexible workplaces is reviewed to identify the knowledge gap and departure points for this study. Second, related studies for personal thermal comfort models are reviewed to provide the fundamental theory for performing the optimization process.

3.2.1 Flexible personal indoor workplace and environment

Allocation of the workplace based on personal preferences has been investigated in several previous studies. For example, the idea of the ABW offers flexible workplaces for the employees depending on the task they will perform [59]. Prior studies have shown that compared with traditional office space allocations, people perform tasks much better after they are relocated to an ABW [60]. [61] conducted an experiment to investigate the effect of ABW on employees' health and work outcomes. The results revealed that ABW could lead to meaningful improvements in people's workday sedentary time, physical activity, eating behaviors, and work satisfaction. In addition, a systematic review involving 36,039 participants regarding the effect of ABW on health and work performance was done by [62], which further confirmed the positive effects of ABW in workplaces.

In addition, based on the concept of ABW, a human-centric indoor monitoring and control framework developed by [102] showed the capability of assigning occupants to specific rooms based on their preferences for the indoor environment. The case study showed that the thermal comfort of the occupants could be improved with the allocation of appropriate workplaces. [63] developed a robust system named OccuSpace to predict workplace occupancy. The system was

developed to help with the management of workplace utilization to improve the occupant's indoor experiences. Similarly, a platform with a mobile interface to match occupants to suitable ABWs was introduced by [14], which requires prior feedback from the occupants regarding their experience at each workplace in the building. By demonstrating how the data could be utilized to group occupants, the study is a stepping stone for future research. However, there exist some limitations to current approaches for ABW. For example, due to the constraints of real buildings such as the capacity of rooms, the occupants may not always be able to find seats in the most suitable room that fits their preferences. In addition, the existing ABW approaches have not considered the impact of ABW on the energy performance of the buildings.

3.2.2 Personal thermal comfort estimation

Due to the distinct perceptions of the thermal environment across different individuals, previous studies investigated personal thermal comfort models using different algorithms [103]. For example, [104] developed prediction models for personal thermal comfort based on Gaussian Process regression, which improved the individual prediction accuracy by 74% compared to the Predicted Mean Vote (PMV) calculation. Similarly, [69] applied an Artificial Neural Networks (ANN) model to establish the personal thermal comfort models, which took both the individual profiles and environmental parameters as the input features. The results showed that 92.9% of the predicted values were more accurate than conventional PMV. Furthermore, to develop more accurate personal prediction models, the occupants' heating and cooling behaviors were integrated with a PCS by [105]. The results indicated that the median accuracy of the prediction models was 0.73, which was significantly higher than the conventional comfort models (0.51 for PMV and adaptive).

In addition to environmental parameters and individual profiles, personal physiological parameters measured by wearable sensors were also used as the training dataset for the personal prediction models of thermal comfort. For example, [106] developed personal thermal comfort models using the measured temperature and heart rate of people. The results showed a median prediction accuracy of 78% and revealed that the ST of the ankle was more predictive than the temperature at the wrist. Similarly, an Internet of Things (IoT) based system was developed by [107] for estimating personal thermal comfort. Low-cost sensors were used to collect environmental data as the inputs of the prediction models. The results showed an improvement in prediction accuracy compared to industry standards. Moreover, [108] introduced a learning-based model to predict individual thermal preferences in transient conditions. The method collected the temperature of different human body parts (i.e., arms, torso, and head) as the inputs. By using all the proposed features, the overall prediction accuracy was higher than 80%. In summary, the feasibility of using personal models for different individuals in this study can be supported by the existing techniques. However, the personal models have not been well integrated into the building HVAC system for optimization of indoor management strategies.

Overall, the fragmented implementations of ABW and thermal comfort prediction models identify this study's research gaps and highlight the importance of a comprehensive strategy that can make full use of the existing technologies for decision-making of room assignment and indoor environmental control.

3.3 Methodology

In this study, an optimization framework is developed to maximize the thermal comfort of the occupants while reducing the energy consumption of the buildings through flexible workplaces. As shown in Fig. 3.1, to jointly consider energy consumption while optimizing

thermal comfort, the corresponding energy prediction models are needed. To obtain the analytical energy consumption of each room, iterative energy consumption simulations are conducted with a variety of indoor environmental settings such as room temperature (RT) and relative humidity (RH). In this case, a dataset containing the energy consumption of each room with their corresponding indoor environmental parameters is collected, thus the analytical energy prediction models of each room can be obtained through machine learning algorithms. The obtained energy prediction models and the thermal comfort prediction models are incorporated into the optimization algorithm. Iterations of room assignment and adjustment of room environmental settings are conducted until the optimal result is achieved.

In a general case, assume there are m occupants in a building who are seeking suitable rooms, while there are n rooms ($n < m$) with controllable thermal environments, the goal is to help the occupants find suitable rooms that can maximize their thermal comfort. Simultaneously, an optimal set of room conditions that can minimize energy consumption should be found. Since continuous and discrete parts are contained in both the decision variables and the objective function while the estimation of thermal comfort and energy consumption are based on learned non-parametric models, this optimization problem is considered non-trivial.

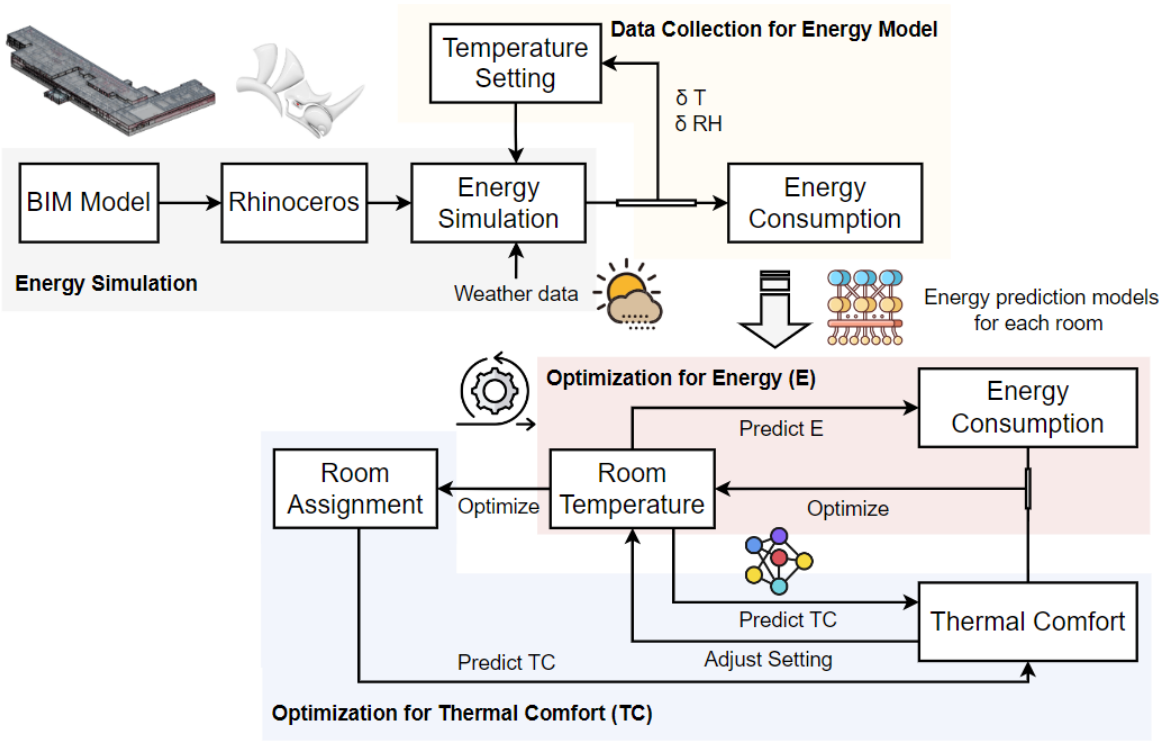

Fig. 3.1. Overview of the Optimization Framework

To help with understanding the problem, a schematic diagram is created and shown in Fig. 3.2. Ranges of comfort zones of different individuals are represented by circles in a coordinate system of temperature and relative humidity. Using the connections between the rooms and occupants to represent the function losses, their sum should be minimized. The RT, RH, and room assignments are perturbed and optimized at the same time. As a result, individuals with similar thermal preferences will be assigned to the same rooms with optimal environmental settings for both thermal comfort and energy consumption. The details of the optimization algorithm are explained in the following sections.

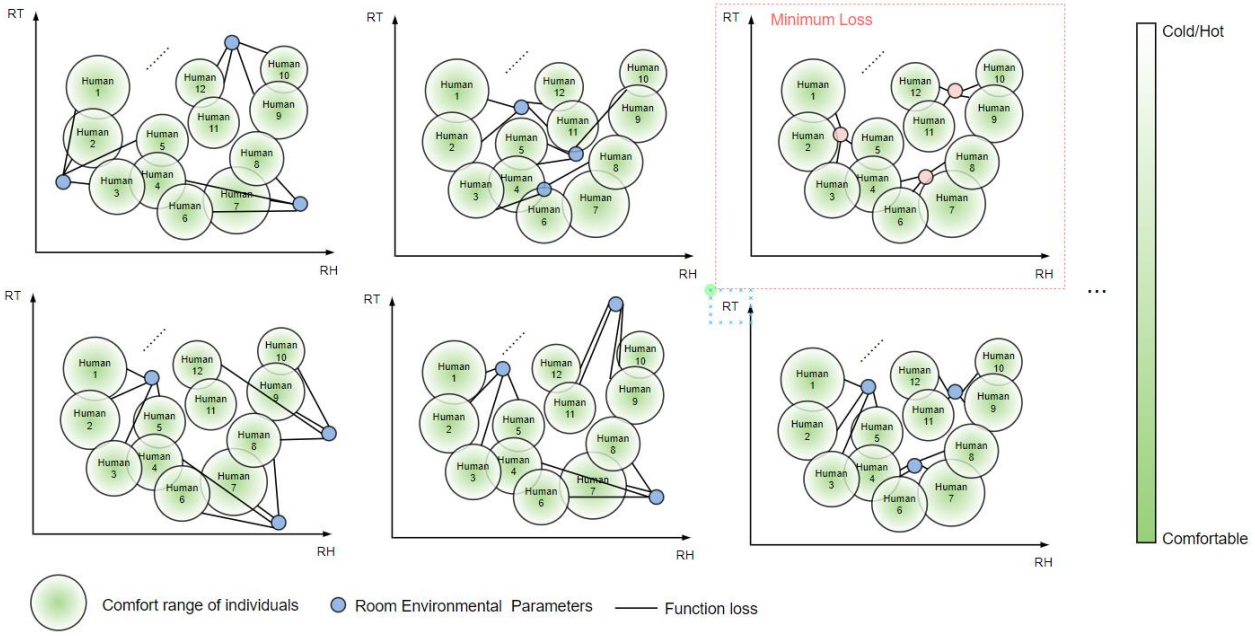

Fig. 3.2. The overview of the optimization problem

3.3.1 Mathematical representations of the optimization problem

The optimization problem is formulated Mathematically where the thermal comfort of the occupants and the energy consumption are jointly considered. Binary variables x_{ij} are added to indicate the match of occupants and rooms: $x_{ij} = 1$ when occupant i $(1 \leq i \leq m)$ is matched with room j $(1 \leq j \leq n)$; otherwise, $x_{ij} = 0$. A discrete 7-scale metric with discrete numbers (i.e., -3, -2, -1, 0, 1, 2, 3) [12] is used to represent thermal comfort, which is correlated with multiple indoor environmental parameters including RT, RH, and the human factors (e.g., clothing level and metabolic rate). Suppose an occupant i $(1 \leq i \leq m)$ is assigned to room j $(1 \leq j \leq n)$, the estimated thermal comfort TC_i, with respect to the indoor environmental parameters, can be represented as follows:

$$TC_i = \sum_{j=1}^{n} g_i(T_j, H_j) x_{ij} \tag{3.1}$$

Here, the $g_i(\cdot)$ represents the (non-linear) function of the thermal comfort for occupant i, which returns $\{-3,-2,-1,0,1,2,3\}$, while T_j and H_j are the RT and RH of room j, respectively. Instead of using any analytic function, $g_i(\cdot)$ is a learning-based model. In terms of the optimization process, the function for $g_i(\cdot)$ is preferred to be differentiable, such as ANN and Support Vector Machines (SVM). In this study, all the indoor thermal parameters (i.e., T_j, H_j, V_j) are assumed continuous and controllable with given ranges, and the overall thermal comfort of the occupants needs to be optimized. Therefore, the sum deviation, F_C, in Eq. (3.3) is penalized. Note that c_i is applied as the weight of any specific occupants.

$$f_i(T_j, H_j, V_j) = \left| g_i(T_j, H_j, V_j) - 0 \right| \tag{3.2}$$

$$F_C = \sum_{i=1}^{m} c_i \sum_{j=1}^{n} f_i(T_j, H_j) x_{ij} \tag{3.3}$$

Similarly, using $h_i(T_j, H_j)$ to represent the energy consumption of room j, the objective function can be written as Eq. (3.4), where the thermal comfort of the occupants and energy consumption are jointly optimized. The left part is copied from Eq. (3.3). The decision variables include x_{ij}, c_i, and T_j, H_j $(1 \le i \le m, 1 \le j \le n)$. α is used to adjust the weight between thermal comfort and energy consumption during the optimization. The capacity of the rooms is limited by (3.5.1), where C_j represents the capacity of room j. Since everyone can only be matched to one room, the constraint (3.5.2) is added. Constraints (3.5.3), (3.5.4), and (3.5.5) set up the ranges of the variables. The minimum and maximum room temperatures are defined by T_j^{min} and T_j^{max}. Similarly, the range of the relative humidity is defined by H_j^{min} and H_j^{max}.

$$\min_{x_{ij}, T_j, H_j} \alpha \sum_{j=1}^{n} \sum_{i=1}^{m} c_i f_i(T_j, H_j) x_{ij} + (1-\alpha) \sum_{j=1}^{n} h_i(T_j, H_j) \tag{3.4}$$

subject to

$$0 \leq \sum_{i=1}^{m} x_{ij} \leq C_j \tag{3.5.1}$$

$$\sum_{j=1}^{n} x_{ij} = 1 \tag{3.5.2}$$

$$x_{ij} \in \{0, 1\} \tag{3.5.3}$$

$$T_j^{min} \leq T_j \leq T_j^{max} \tag{3.5.4}$$

$$H_j^{min} \leq H_j \leq H_j^{max} \tag{3.5.5}$$

3.3.2 Optimization algorithm

The Large Neighborhood Search (LNS) is a technique that improves an objective by iteratively solving non-trivial sub-problems in the neighborhood of the current solution [109], and it is capable of solving scheduling problems efficiently [110-113]. Therefore, LNS is proposed to solve this joint optimization problem, which consists of two main steps: (1) match the individuals with rooms by solving an LP problem, and (2) adjust the environmental parameters (i.e., RT and RH) of the rooms. The technique of solving Integer Linear Programming (ILP) using an equivalent LP problem has been proven efficient in other problems such as classroom assignments [114] and task allocation [115]. However, none of the previous studies have adopted a similar technique to optimize indoor room assignment and environmental control for thermal comfort, which highlights the novelty of the developed algorithm in this study.

Based on the technique of LNS, in each iteration, the original problem shown in Eq. (3.4) is decoupled into two main separate steps as shown in Fig. 3.3, and the corresponding pseudocode is shown in Algorithm 1. The first step tries to find the most suitable rooms for the occupants based on their thermal preferences and the current room conditions. In the first step, the thermal

parameters of the rooms (i.e., T_j and H_j) are temporarily fixed, thus the objective function in Eq. (3.4) can be replaced by Eq. (3.6). Due to the only variables of x_{ij} and the linearity of both the objective function and its constraints, it is an ILP problem. For this specific problem, the constraints (3.5.3) can be replaced with $0 \leq x_{ij} \leq 1$, followed by solving the reduced LP by Simplex-based algorithms. It is guaranteed that the solutions to x_{ij} will be integers.

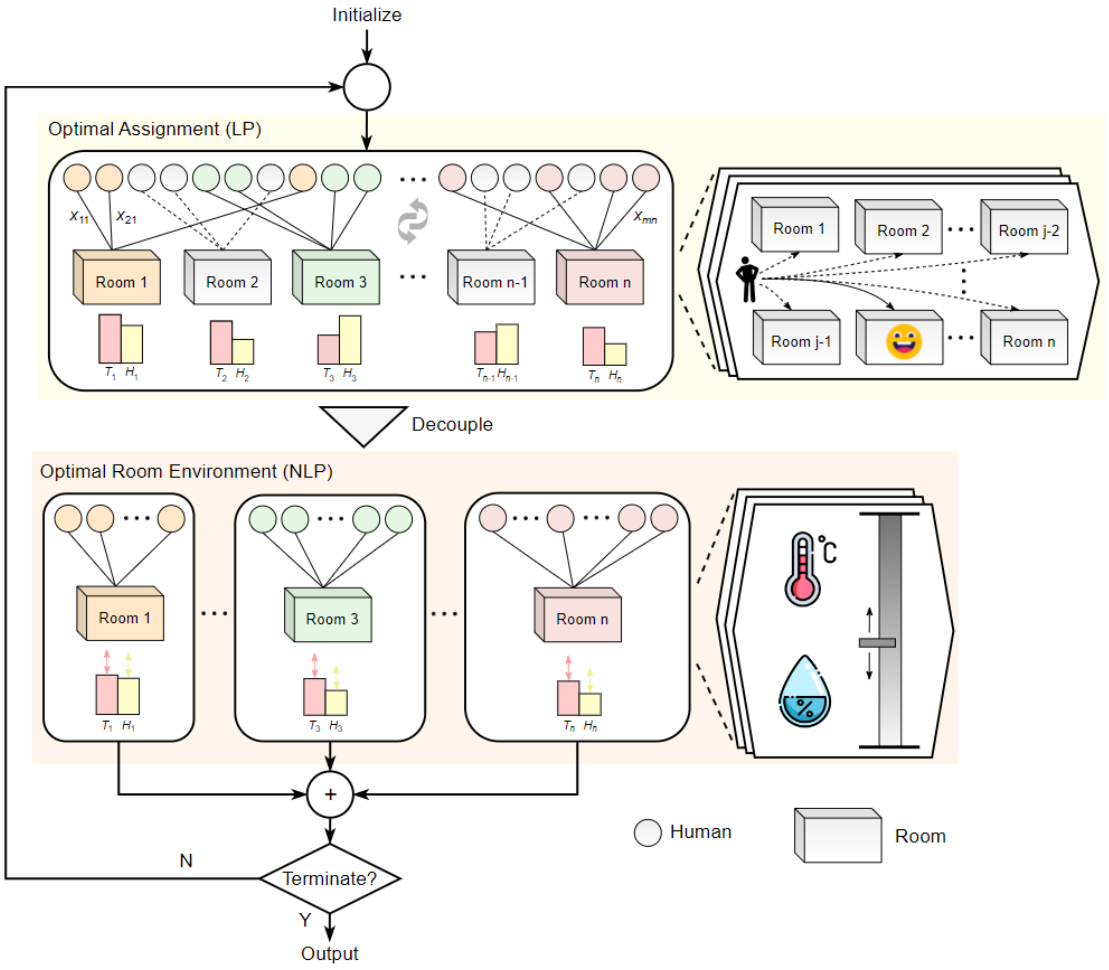

Fig. 3.3. The proposed algorithm for optimizing room assignments and environmental settings

Algorithm 1: Large Neighborhood Search for Thermal Comfort

Input: initial room parameters T_j^0, H_j^0 $\forall j = 1, \cdots, n$

initial room assignment x_{ij}^0 $\forall i = 1, \cdots, m, \quad \forall j = 1, \cdots, n$

Output: optimal room parameters T_j^*, H_j^* $\forall j = 1, \cdots, n$

optimal room assignment x_{ij}^* $\forall i = 1, \cdots, m, \quad \forall j = 1, \cdots, n$

$F^* = +\infty$
for $l = 1, \cdots, l_{\max}$ **do**
  // Step1: optimize x_{ij}, while T_j, H_j are fixed
  // Simplex-based algorithm
  Solve the linear program: $\min_{x_{ij}^l} \sum_{j=1}^{n} \sum_{i=1}^{m} c_i f_i\left(T_j^{l-1}, H_j^{l-1}\right) x_{ij}^l$
  Update x_{ij}^l
  // Step2: optimize T_j, H_j, while x_{ij} are fixed. Rooms are decoupled
  for $j = 1, \cdots, n$ **do**
    // Trust-region algorithm
    Solve the nonlinear program: $\min_{T_j^l, H_j^l, V_j^l} \alpha \sum_{i=1}^{m} c_i f_i\left(T_j^l, H_j^l\right) x_{ij}^l + (1-\alpha) h_i\left(T_j, H_j\right)$
    Update T_j^l, H_j^l
  end for
  $F^l = \alpha \sum_{j=1}^{n} \sum_{i=1}^{m} c_i f_i\left(T_j^l, H_j^l\right) x_{ij}^l + (1-\alpha) \sum_{j=1}^{n} h_i\left(T_j, H_j\right)$
  if $F^l < F^*$ **then**
    $F^* = F^l, T_j^* = T_j^l, H_j^* = H_j^l, x_{ij}^* = x_{ij}^l \quad \forall i = 1, \cdots, m, \quad \forall j = 1, \cdots, n$
  end if
  if the termination condition is reached **then**
    return T_j^*, H_j^*, x_{ij}^*
  end if
end for

The matching between people and rooms can be regarded as a bipartite matching problem. In the linear program formulation (standard form: $\min \mathbf{c}^{\mathrm{T}}\mathbf{x}$ such that $\boldsymbol{A}\mathbf{x} \leq \mathbf{b}$ and $\mathbf{x} \geq \mathbf{0}$) of a bipartite matching problem, the matrix $\boldsymbol{A}$ is totally unimodular [116]. Therefore, all the corners of the polytope defined by the constraint Ax⩽b are integers. A Simplex algorithm-based solver can efficiently find the solution of the linear program by searching through the corner points. As the solution is one of the corners, it is guaranteed to be integral. Therefore, this step will be conducted efficiently with a polynomial algorithm. Based on the personal models and the room conditions,

the algorithm tries to find the best-fit rooms for the occupants in terms of thermal comfort by solving the LP problem.

$$\min_{x_{ij}} \sum_{j=1}^{n} \sum_{i=1}^{m} c_i f_i(T_j, H_j) x_{ij} \tag{3.6}$$

subject to

$$0 \leq \sum_{i=1}^{m} x_{ij} \leq C_j, \tag{3.7.1}$$

$$\sum_{j=1}^{n} x_{ij} = 1, \tag{3.7.2}$$

$$x_{ij} \in \{0, 1\} \tag{3.7.3}$$

After finding the optimal matching of occupants and rooms in step 1, the second step of the algorithm tries to find the optimal indoor thermal parameters (i.e., T_j and H_j) with the determined room assignments (x_{ij}). The optimization concerning different rooms is thus decoupled and Eq. (3.6) is split into n separate Non-Linear Programming Problems (NLP), and each of them has variables of T_j and H_j. The overall thermal comfort and the energy consumption in each room are jointly optimized as in Eq. (3.8) by modifying T_j and H_j within the limited ranges. In addition, α is added for a trade-off between thermal comfort and energy consumption. A gradient-based algorithm could thus be applied to solve the n problems. In this study, a trust-region algorithm is chosen.

$$\min_{T_j, H_j} \alpha \sum_{i=1}^{m} c_i f_i\left(T_j, H_j\right) x_{ij} + (1 - \alpha) h_i\left(T_j, H_j\right) \tag{3.8}$$

subject to

$$T_j^{min} \leq T_j \leq T_j^{max} \tag{3.9.1}$$

$$H_j^{min} \leq H_j \leq H_j^{max} \tag{3.9.2}$$

Since both steps explore the solutions in the feasible regions, when considered together, they form an LNS algorithm. The large nonlinear problem is decomposed into smaller easily solvable sub-problems by the LNS algorithm. In each iteration, better solutions for room assignments and indoor thermal parameters are found by solving the LP and NLP, respectively. The optimal solutions are found when the algorithm converges. The optimality and iteration steps of the optimization are empirically evaluated due to the complexity of the functions. The results show that this algorithm can output a near-optimal solution and make a smooth trade-off between thermal comfort and energy consumption. It is worth noting that the proposed algorithm is fully scalable and can be applied to other similar problems. For example, the f_i in the above equations can be replaced by functions of other indoor experiences such as visual, acoustic, and work engagement [57], and the corresponding indoor environmental parameters T_j and H_j should also be modified accordingly.

3.4 Case Study

To demonstrate the proposed framework and verify the developed algorithm, a case study is presented. In the case study, the GG Brown Building at the University of Michigan is selected as the target building, and 12 rooms on the first floor are randomly selected to help demonstrate the optimization algorithms. The Revit model of the GG Brown Building is shown in Fig. 3.4. The energy model of each selected room is obtained by applying the Nonlinear Polynomial Regression (NPR) on the results from multiple energy simulations. The obtained NPR models are in the analytical form that can be inserted into the objective function as described in Eq. (3.8). In addition to the energy models for rooms, the thermal comfort prediction models for the occupants are also

needed. When applying the machine learning methods for thermal comfort models, there are two typical scenarios: (1) there is no personal data for the occupants regarding their preferences of thermal environments, and (2) the feedback of different thermal environments has been collected from the occupants. For the first scenario, a public thermal comfort database is used to simulate the thermal comfort prediction models based on the profiles of the occupants. For the second scenario, personal thermal comfort models can be used. Details of the case study are presented in the following sections.

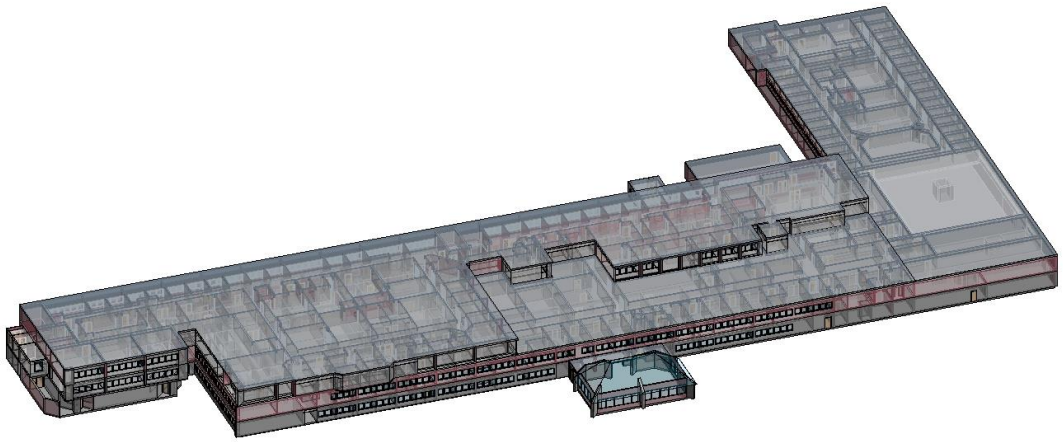

Fig. 3.4. The Revit model of the GG Brown Building

3.4.1 Prediction models for energy consumption

The layout of the first floor of GGB is shown in Fig. 3.5, and the locations of the 12 selected rooms are highlighted and labeled. The areas and capacities of the rooms are listed in Table 3.1. The capacities of rooms are estimated using the occupant density of 20 people per 100 m^2 which is estimated from the usage of the office building and is aligned with the previous study [117]. The indoor environments of these rooms are fully controlled by the central heating, ventilation, and air conditioning (HVAC) system through thermostats.

Fig. 3.5. The layout of the GGB first floor

In order to obtain the analytical models of the energy consumption with respect to RT and RH, a learning method is applied as shown in Fig. 3.6. An energy model of the building is established in Rhino 7 with separate zones for different rooms. The two environmental plugins, Ladybug and Honeybee for Grasshopper for Rhino are used to conduct the energy simulation of the building. Each simulation can provide the separate hourly energy consumptions of each selected room with respect to the given settings of RT and RH. In this case, each simulation gives 8760 datasets corresponding to each hour for one year. For each hour, the outdoor weather condition, the energy consumption of each room, and the corresponding RT and RH can be obtained. Heating season is used to demonstrate algorithms since heating is much more often required for the building due to its location. The ranges of the RT and RH are set from 18 °C to 28 °C and 20% to 70%, respectively. They are decided by giving enough buffer zones of the suggested settings of 20 °C to 24 °C for RT and 30% to 60% suggested by ASHRAE standard [12]. The intervals of the RT and RH are 1°C and 10%, respectively. In this case, a dataset containing the

energy consumption and corresponding RT and RH of each room is collected. NPR methods are used to fit the analytical models for energy consumption of each room with respect to RT and RH when given a specific outdoor weather condition. With the degree of freedom of 5, the errors of the NPR models for different rooms are calculated using Eq. (3.10) and (3.11) and the results are shown in Table 3.1. The results indicate that the models have very small errors regarding the prediction.

$$RMSE = \sqrt{\frac{1}{n}\sum_{i=1}^{n}(e_i - \hat{e})^2} \tag{3.10}$$

$$\text{Error} = \frac{RMSE}{\bar{e}} \tag{3.11}$$

Where e_i refers to the observed value and $\hat{e}$ refers to the predicted value, $\bar{e}$ is the average energy consumption of the room.

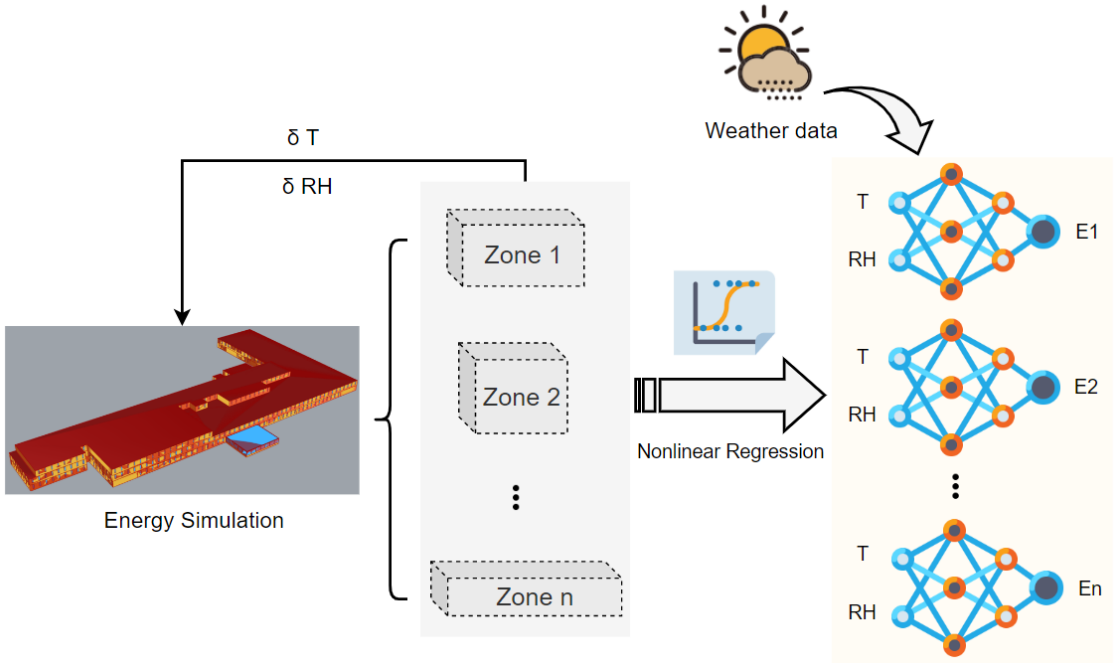

Fig. 3.6. Learning method for the energy models of each building room

Table 3.1. Details of the selected rooms

Room ID	1	2	3	4	5	6	7	8	9	10	11	12
Area (m^2)	72.7	69.3	65.6	56.5	35.0	128.4	58.1	66.6	75.6	21.3	38.3	21.0
Capacity	15	14	13	11	7	26	12	13	15	4	8	4
NPR Error (%)	0.8	1.2	0.9	0.4	0.4	2.0	1.1	0.6	1.3	0.5	0.5	0.8

3.4.2 Thermal comfort models using public database

To obtain the personal thermal comfort prediction models, $g_i(\cdot)$ is trained using ASHRAE Global Thermal Comfort Database II [15]. The database contains approximately 107,583 datasets on thermal comfort, which has a web-based tool to allow end-users to export the data using a filter. The thermal sensation is used here to indicate thermal comfort as it is the most widely used subjective thermal metric [103]. It uses a 7-scale metric (discrete number from -3 to 3) to indicate people's thermal feelings ranging from cold, cool, slightly cool, neutral, slightly warm, warm, and hot, respectively.

In addition to the thermal sensation, the database is manually filtered based on other features contained in each dataset. The datasets that contain the environmental thermal parameters (i.e., RT and RH) and typical human factors (i.e., gender, age, height, weight, clothing level, and metabolic rate) are selected. The detailed information regarding the selected datasets is summarized in Table 3.2. To obtain the $f_i(T_j, H_j)$ in the optimization, two typical differentiable learning-based algorithms: SVM and ANN are applied. Note that there is a slight difference between the $f_i(\cdot)$ here and the defined one in Eq. (3.2). Eq. (3.2) is the conceptual idea of the overall thermal comfort penalty. However, it is challenging to incorporate the $f_i(\cdot)$ in Eq. (3.2) into the optimization since it is discrete. Therefore, it is replaced with the output defined in Fig. 3.7. As the goal of this function is to minimize the deviation of the thermal sensation from 0, thus the sign associated with 0 is set as negative while all others are positive. The symbols "+" and

"−" indicate that when the predicted results are −3, −2, −1, 1, 2, and 3, the function loss will increase while the loss will be reduced if the predicted results are 0. In addition, different weights are assigned to the values of thermal sensation as indicated by S_i. The function loss described in Fig. 3.7 is thus formulated as the weighted sum of the possibilities of the predicted output values that reward the thermal sensation of 0 while penalizing the non-zero ones. In addition, the function becomes continuous and can be easily processed for optimization.

Compared with the general prediction models, the accuracies of using similar profiles to simulate the personal thermal comfort models have been proven to be higher [102]. The accuracies of SVM and ANN for predicting thermal sensation are tested based on the selected datasets. The SVM applied the radial basis function (RBF) kernel as it gives the best performance among all kernels using the test datasets. The ANN applied in this study has three hidden layers. There are 4 neurons in the first layers and 8 neurons in the second and third layers. The accuracies indicated by the fraction of correct predictions are used to compare the performance of these two types of models. The average tested accuracies of SVM and ANN are 0.706 and 0.540, respectively. Therefore, the SVM is selected to help demonstrate the proposed algorithm.

Table 3.2. Details of the selected datasets

Count	5339
Age range	16 ~ 70
Gender	Male/Female
Height (cm)	122 ~ 206
Weight (kg)	35 ~ 116
Clothing Level (Clo)	0.04 ~ 1.49
Air Temperature (°C)	13.9 ~ 37.9
Relative Humidity (%)	10.4 ~ 95.3

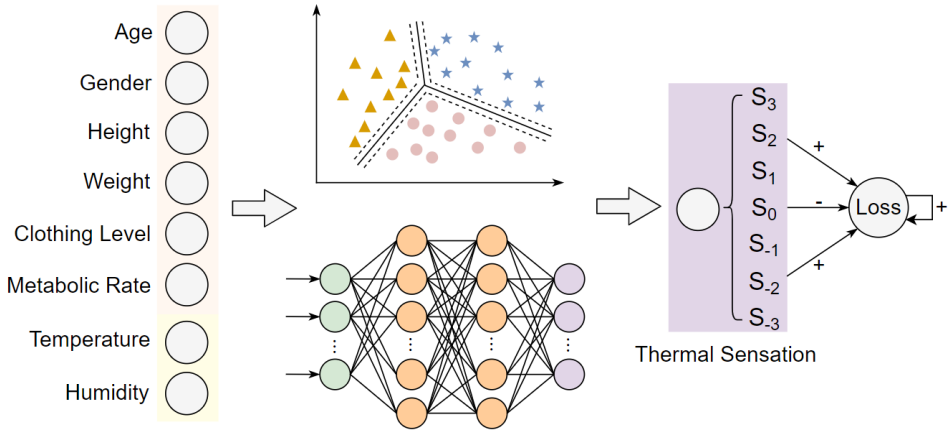

Fig. 3.7. Process for computing the function loss

3.4.2.1 Initialization of the optimization

The initial parameters of the indoor thermal environments are assigned random values within the defined ranges (i.e., 18 °C to 28 °C and 20% to 70% for RT and RH, respectively). Based on the ASHRAE database, the profiles of 100 people are randomly selected to demonstrate the occupants of a building. The capacities of the rooms follow the values in Table 3.1. The outdoor weather condition during the heating season is randomly selected based on the. EPW weather file.

3.4.2.2 The trade-off between thermal comfort and energy consumption

As described in the methodology, the proposed algorithm not only concerns the thermal comfort of the occupants but also tries to achieve energy savings. Based on Eq. (3.4), there is a trade-off between the cost of thermal comfort and the cost of energy consumption of the building, represented by α. When the cost ratio (α) is set to 1, all effort is paid to optimize the thermal comfort of the occupants without considering the energy consumption. In contrast, if α is set to be 0, all effort is paid into the optimization of the energy consumption without considering the thermal comfort of the occupants. In practice, the weight assigned to thermal comfort and energy consumption is likely to require empirical decision-making. Therefore, the trade-off between the thermal comfort of the occupants and the energy consumption of the building is investigated. The

algorithm is tested with different cost ratios (α) of the weights so as to provide comparative insights regarding the trade-off.

The results are plotted as shown in Fig. 3.8. When the cost ratio (α) is 0, the cost (loss in the objective function) of the objective function is high for thermal comfort and low for energy consumption, which indicates that the optimization is done for energy consumption without considering the thermal comfort of the occupants. Meanwhile, the number of occupants with a thermal comfort of 0 is very low. With the increase in the ratio, the cost of energy consumption goes up while the cost of thermal comfort drops quickly. As a result, when the ratio is 1, the relative values of the cost for thermal comfort and energy consumption are reversed, indicating that the algorithm only optimizes the thermal comfort of the occupants without considering the energy consumption.

In this example, a good trade-off can be obtained by setting the cost ratio (α) to 0.7 where the comfort cost almost converges while there is still a great potential for energy savings. As a result, all of the occupants can be thermally comfortable while a large proportion of energy consumption is saved.

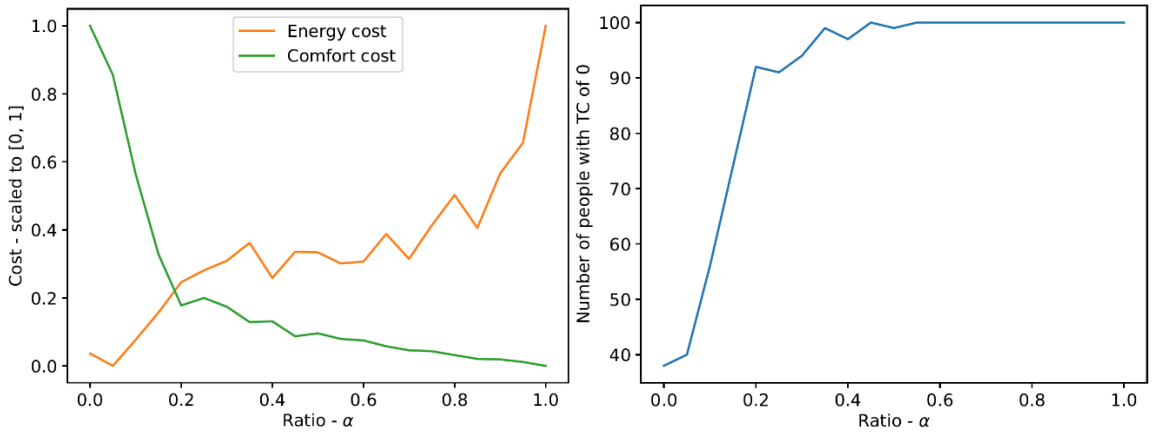

Fig. 3.8. The trade-off between thermal comfort and energy consumption

3.4.2.3 Static Scenario

To demonstrate the performance of the optimization results with a suitable trade-off for thermal comfort and energy consumption, the case study with $\alpha = 0.7$ is used. In this section, the number of people in the buildings is still set to 100 and is assumed to be static (no people leave or come in). Fig. 3.9 shows the changes in the allocation of occupants after applying the optimization algorithm. The circles are used to represent the occupants. To track the movement of the occupants, each circle is assigned a number tag from 1 to 100. Colors are designed to indicate the thermal states of the occupants. The grey color means the occupant is comfortable (with a thermal sensation of 0) while the red color indicates that the occupant is not thermally comfortable. It can be seen that a large proportion of the occupants would be thermally uncomfortable. After applying the optimization algorithm, the allocation of the occupants changes significantly, and all the circles become grey as a result of the neutral thermal sensation of the occupants. In addition to the changes in room parameters, the energy consumption saving penalty can also be reflected in rooms 4 and 6. These two rooms are recommended empty thus no heating is required to achieve additional energy savings.

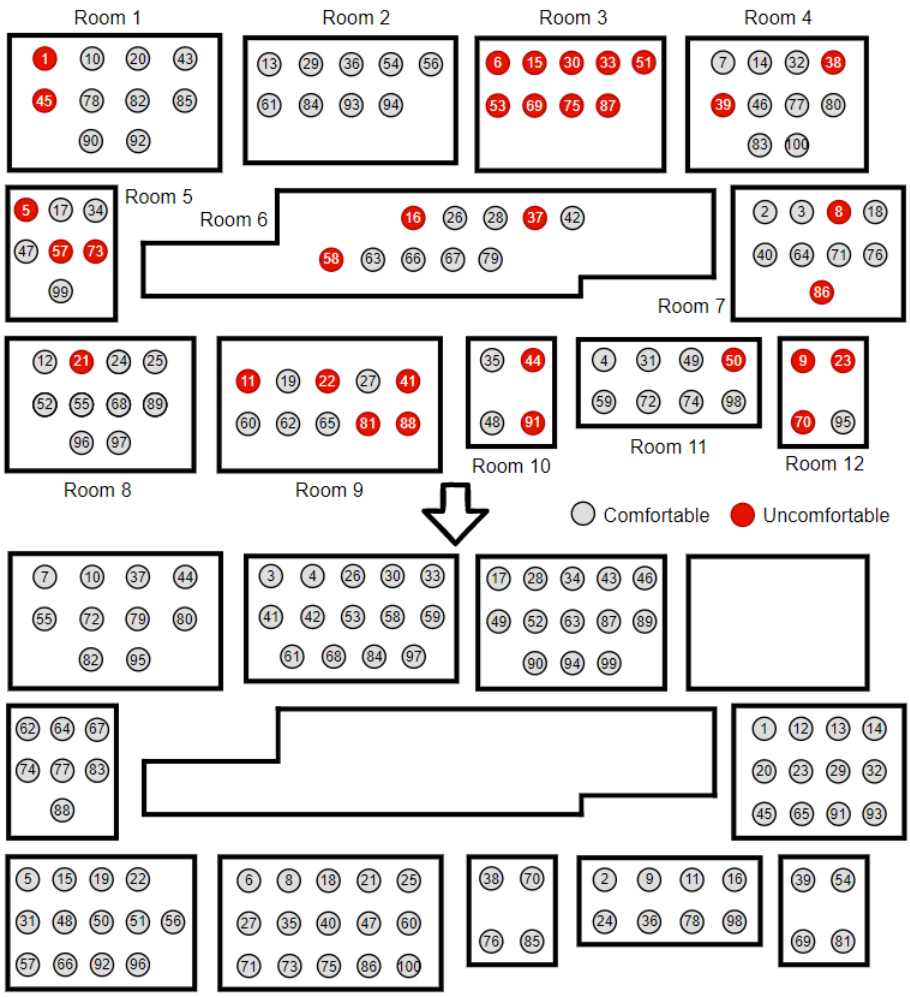

Fig. 3.9. Optimization of room assignment

The detailed distribution of predicted thermal sensation of the 100 occupants before (with randomly assigned rooms) and after applying the optimization is shown in Fig. 3.10. It can be seen that the original distribution of thermal sensation ranges from −3 to 3. Only 67 out of the 100 occupants would have a thermal sensation of 0. A large number of occupants (25) would consider the room environment slightly cool, 2 occupants would feel cool, and 1 occupant would feel cold. In contrast, 3 of the occupants would feel slightly warm, 1 of the occupants would feel warm, and 1 would feel hot. The overall thermal comfort of the occupants is optimized after applying the proposed algorithm. The results indicate that all 100 occupants would have a thermal sensation of 0.

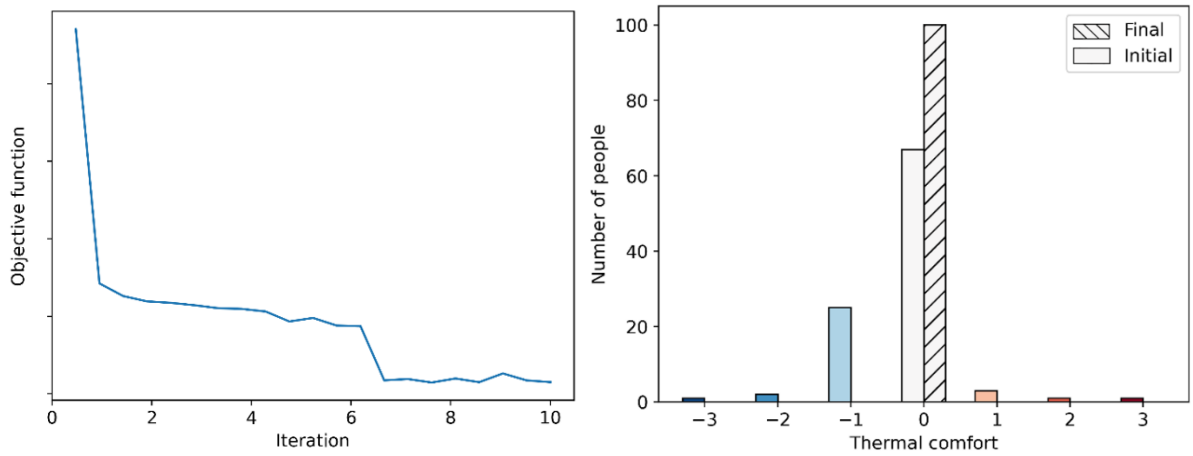

Fig. 3.10. Distribution of thermal sensation before and after optimization

The changes in indoor environmental parameters (i.e., RT and RH) and energy consumption before and after applying the optimization algorithm are shown in Table 3.3. From the initial randomly assigned values, RT and RH in each room are updated to match the preferences of the occupants being assigned.

Table 3.3. Changes in room conditions after optimization

Room ID	**1**	**2**	**3**	**4**	**5**	**6**	**7**	**8**	**9**	**10**	**11**	**12**
Before Optimization												
RT (°C)	22.3	25.6	18.5	20.6	19.5	19.8	25.6	27.7	20.7	20.2	26.2	21.0
RH (%)	57.2	65.1	62.6	59.4	69.6	66.1	46.9	20.8	23.4	34.0	31.1	47.7
Energy (wh)	10363	12958	7984	8470	5240	17306	9407	8795	6921	2935	6295	3341
After Optimization												
RT (°C)	23.7	21.4	18.0	N/A	18.3	N/A	23.7	23.6	18.0	18.0	24.8	19.2
RH (%)	58.6	68.7	41.1	N/A	69.2	N/A	40.5	22.9	25.8	33.5	40.4	47.2
Energy (wh)	11287	10497	6496	N/A	4837	N/A	8008	7355	6037	2557	6433	2983

To further illustrate the capability of energy consumption saving of the algorithm with maximized thermal comfort, the results (i.e., energy consumption and thermal comfort) under three scenarios are compared: (1) the settings of the indoor environmental parameters follow ASHRAE standard [12] (i.e., 22 °C for RT, 45% of RH); and (2) the optimized indoor environments with α

= 1; and (3) the optimized indoor environments with α = 0.7 (corresponding to results in Table 3.3). Table 3.4 shows the comparison results. When following recommended setting by the ASHRAE standard (scenario 1), many occupants (27) would feel slightly cool (−1), and some occupants (3) would feel cool (−1). Only 70 of the occupants would have a thermal sensation of 0. Assume the proportion of the energy savings (ES) based on Eq. (3.12). When the algorithm is applied without considering the energy consumption (scenario 2), the thermal comfort of the occupants can be optimized (all 100 occupants would have a thermal sensation of 0) while the energy consumption will increase by 30.1% compared with scenario 1. However, when the energy penalty is incorporated in the optimization (scenario 3), 22% of the energy consumption can be saved (compared with the settings following ASHRAE) with the optimal results of thermal comfort.

$$ES = \frac{E^o - E^*}{E^o} \tag{3.12}$$

where E^o represents the original energy consumption while $E^*$is the energy consumption after optimization

Table 3.4. Comparison of thermal comfort and energy saving

Scenario	**Thermal Comfort Distribution (# of people)**							**ES (%)**
	−3	**−2**	**−1**	**0**	**1**	**2**	**3**	
1	0	3	27	70	0	0	0	0
2	0	0	0	100	0	0	0	−30.1
3	0	0	0	100	0	0	0	22

3.4.2.4 Dynamic Scenario

The previous section uses a case study that assumes a fixed number of people in the building. However, in the real world, people may leave or enter the building. Therefore, the scenario when the number of people in the building is dynamic is also examined. An illustrative pattern of people flow in the building is used in the case study and is shown in Fig. 3.11. It is

assumed that initially there are 60 people in the building with the random allocation and room indoor conditions are also randomized, and then the optimization is carried forward with people suddenly increasing or decreasing. The program randomly selects 10 people to leave first, and then it randomly adds 30 and 20, to the building at different timestamps. Each time when people leave or enter the building, a new optimization is conducted to optimize the thermal comfort of existing occupants in the building. In addition, during each optimization process, the original occupants are assumed to stay in their original rooms.

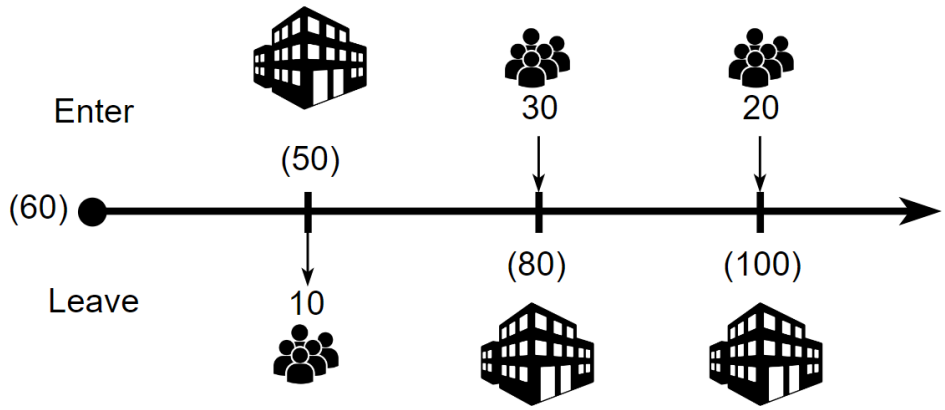

Fig. 3.11. Simulated people flow into the building during the optimization

Suppose the total number of occupants in the building after the change is m, and $m = m_0 + \Delta m$, where m_0 is the original number in the building and there are Δm people entering the building. When $\Delta m > 0$ (entering), the algorithm needs to generate the optimal room assignment for the Δm new people (occupants $m_0 + 1 \leq i \leq m$) and adjust the room parameters to optimize the thermal comfort of all the m people in the building. Suppose originally, occupant i ($1 \leq i \leq m_0$) is in the room a_i, the objective described above is encoded as a combination of the optimization problem described in Eq. (3.4) and (3.5) and a new constraint in Eq. (3.13), where the first $\min\{m_0, m\}$ people are already in their selected rooms. With the constraint (3.13), the room assignment only happens for occupants i ($\min\{m_0, m\} + 1 \leq i \leq m\}$.

$$x_{ij} = \begin{cases} 1, & j = a_i \\ 0, & j = 1, \cdots, a_i - 1, a_i + 1, \cdots, n \end{cases} \qquad (1 \le i \le \min\{m_0, m\}) \qquad (3.13)$$

Fig. 3.12 (left) shows the curves for the convergence of the objective function for the dynamic optimization. The optimization process is divided into different stages, and each of them corresponds with a change in occupants. Similar to the static one, the algorithm converges quickly at the beginning and stabilizes after around 10 iterations for each stage. The iteration numbers 10, 20, and 30 refer to the timestamps when people leave or enter the building. In general, the algorithm still converges rapidly during each stage. The loss of objection function suddenly increases after additional people are randomly added to the building (i.e., at iterations of 20 and 30), it decreases dramatically during the optimization process. Fig. 3.12 (right) describes the number of people with different thermal sensations with respect to iteration number. Similarly, although the number of people who would feel cold or warm suddenly increases, people with a thermal sensation of 0 increase dramatically as the optimization goes forward. Therefore, the proposed algorithm is proven stable even in the case when people leave and enter the building along with time.

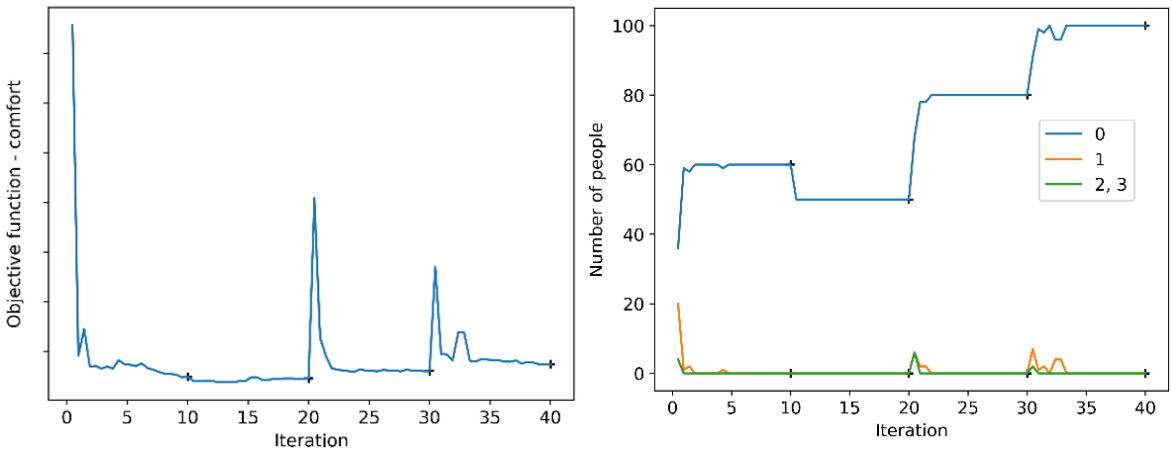

Fig. 3.12. Convergence of objective function and thermal comfort

The final thermal comfort distribution of the occupants before and after the optimization for the dynamic scenario is shown in Fig. 3.13. At the initial stage, there are only 60 occupants with thermal sensations ranging from −3 to 3. Among these occupants, only 36 occupants would have a thermal sensation of 0. A large number of the occupants (19) would feel slightly cool, 1 occupant would feel cool, and 1 occupant would feel cold. In contrast, 1 occupant would feel slightly warm, 1 would feel warm, and 1 would feel hot. However, the optimization process has maximized the overall thermal comfort of the occupants. Eventually, all the occupants would think the thermal environments are neutral for them. The results show that even if the number of occupants increases to 100 after several times of people exchange, a good result regarding the overall thermal comfort of the occupants is achieved.

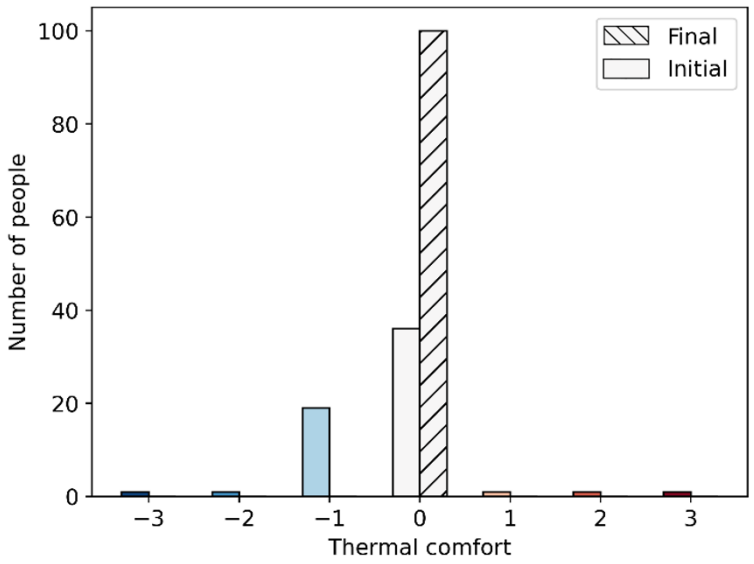

Fig. 3.13. Distribution of thermal sensation before and after optimization

3.4.3 Thermal comfort models using collected personal database

In addition to the public thermal comfort database, the algorithm is also tested using the personal thermal comfort database. During the daily thermal comfort feedback collection, instead of the 7-scale metric, it is very common that the occupants only give feedback regarding the

changes in temperature, which contains only three outputs: cooler, no change, and warmer [118]. Therefore, the personal prediction models based on 3-scale metrics collected from 12 subjects are also applied to verify the scalability of the developed algorithm. Instead of using a single prediction model (which incorporates the personal characteristic as the input features), separate personal thermal comfort models are established based on the personal database using SVM, and the accuracies of the models are listed in Table 3.5. The details regarding the data collection can be found in our previous study [36, 67]. With different outputs of the models, the function loss of the thermal comfort is re-defined as shown in Fig. 3.14.

Table 3.5. Accuracies of the personal thermal comfort prediction models

ID	1	2	3	4	5	6	7	8	9	10	11	12
Acc.	0.952	0.875	0.882	0.941	0.944	0.938	0.889	0.938	0.938	0.944	0.952	0.95

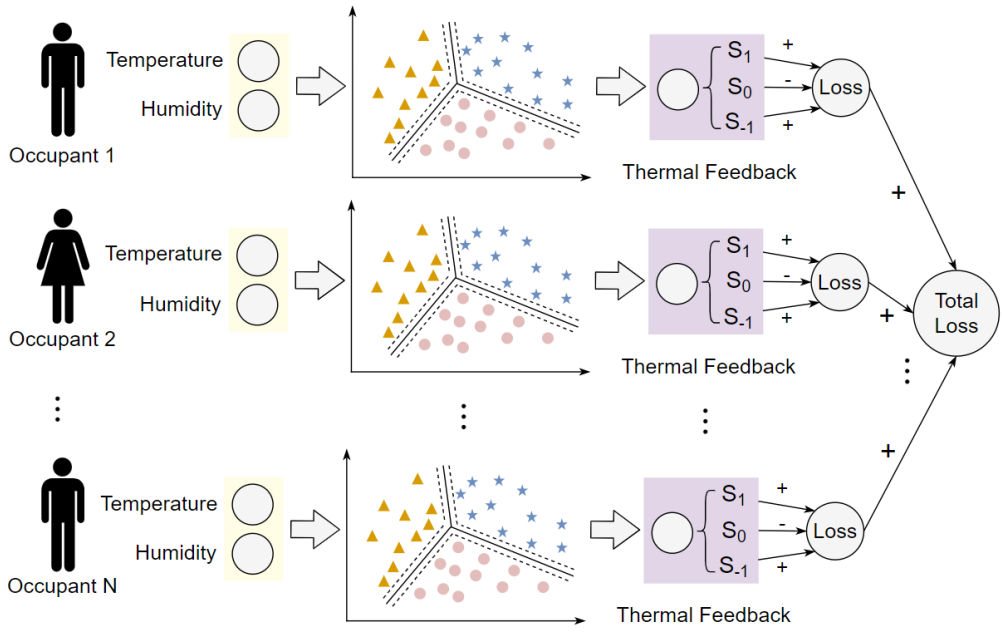

Fig. 3.14. Loss function of thermal comfort based on the 3-scale metric

Due to the limited number of occupants, four small rooms (i.e., 5, 10, 11, and 12) are selected for the test. In this test, $\alpha = 0.75$ is used for the trade-off between thermal comfort and

energy consumption. Other settings of the initialization are identical to the previous section. Fig. 3.15 shows the changes in the allocation of occupants after implementing the optimization algorithm. It can be seen that before the optimization, none of the occupants would consider the indoor environment neutral. However, 11 of them would feel comfortable in the indoor environment. The detailed distributions of their perceptions of the thermal environment before and after implementing the optimization are shown in Fig. 3.16, and the changes in room conditions are shown in Table 3.6.

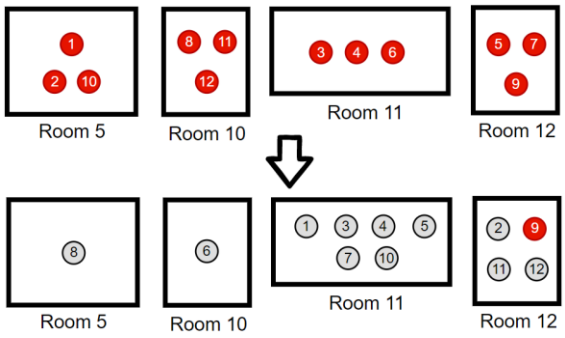

Fig. 3.15. Optimization of room assignment

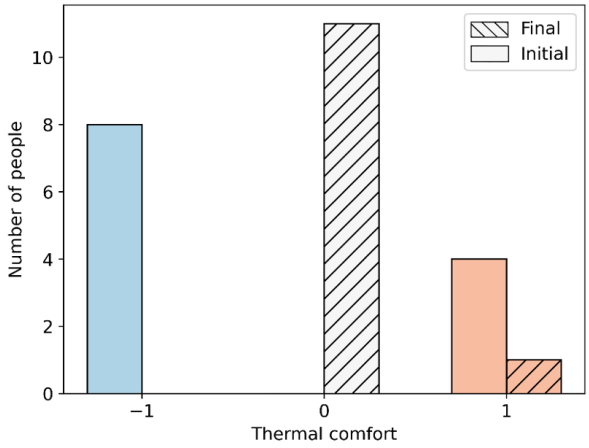

Fig. 3.16. Distribution of thermal sensation before and after optimization

Table 3.6. Changes in room conditions after optimization

Room ID	5	10	11	12
	Before Optimization			
RT (°C)	24.8	22.6	20.5	24.5
RH (%)	61.1	36.0	48.3	27.3
Energy (wh)	6595	3403	5438	3368
	After Optimization			
RT (°C)	18.0	18.0	25.0	27.8
RH (%)	28.6	41.7	20.0	29.9
Energy (wh)	3350	2733	5235	4024

To better understand the superiorities of the optimization, a comparison between the optimization results and the results following the ASHRAE standard is conducted as shown in Table 3.7, where the baseline refers to the ASHRAE standard (i.e., 22 °C for RT, 45% of RH). It can be seen that 9 out of 12 people would feel cold in the indoor environment and the other 3 would feel hot. However, the optimization can make 11 of them feel neutral about the thermal environment. Meanwhile, 14.1% of energy can still be saved due to the appropriate control of the environmental settings.

Table 3.7. Comparison of thermal comfort and energy consumption

Scenario	Thermal Comfort Distribution (# of people)			Energy (wh)
	−1	**0**	**1**	
Baseline	9	0	3	17865
Optimized	0	11	1	15341
	ES%			14.1

3.5 Discussion

In general, after implementing the optimization algorithm, the energy consumption of the building can be saved while the overall thermal comfort of the occupants is optimized. The trade-off between the cost of thermal comfort and energy consumption provides a reference for finding a good balance between them. For example, according to the results based on the public ASHRAE thermal comfort database, with around 22% energy savings, the algorithm can still provide an

optimal solution to make all occupants feel comfortable. When using the data collected from the subjects, although the scales of the outputs of thermal prediction models are different, the algorithm still works well and 14% of energy consumption can be saved while most of the occupants would feel thermally comfortable. In addition, the algorithm is proven to be feasible for a dynamic scenario that which people leave and enter the building from time to time.

However, there exist limitations to the proposed framework. The optimization algorithm is highly dependent on the prediction models for personal thermal comfort and building energy consumption, thus some preliminary studies might be required to ensure it works well for different groups of people and different buildings. Nevertheless, it will not affect the generality and feasibility of the proposed algorithm regarding the optimal room match and indoor environmental settings. In addition, this algorithm aims to provide a new theoretical framework and approach, and additional efforts regarding building management may be required to make it well-equipped for use in real buildings.

3.6 Conclusions

This study proposes a framework to optimize indoor thermal comfort while achieving building energy savings based on LNS. The framework tries to jointly optimize the allocation of the occupants and the settings of environmental parameters in different rooms. To consider the distinct thermal preferences of different individuals, learning-based personal prediction models are incorporated into the objective function. In addition, the penalty for energy consumption is added for achieving energy savings. In general, there are two steps in solving the problem. The first step is to find suitable rooms for each individual based on their personal preferences by solving an LP problem. The second step is to obtain the optimal environmental parameters (i.e., RT and RH) of

different rooms considering both thermal comfort and energy consumption of the building, which is achieved by solving an NLP problem.

To further demonstrate the proposed algorithm, a case study containing is provided. The prediction models for personal thermal comfort are learned using SVM based on either the ASHRAE database or the collected personal database. With the adoption of energy consumption models obtained from energy simulation using NPR, the trade-off between thermal comfort and energy consumption is also analyzed. The results of the two scenarios in the case study show that 22% and 14.1% of energy consumption can be saved while maintaining the thermal comfort of the occupants. The analysis of the trade-off between thermal comfort and energy consumption can be an assistive tool for building managers regarding flexible workplaces and indoor environmental control. Although only thermal comfort is applied in this study, the proposed framework is scalable and can incorporate any predictable indoor comfort metrics.

Chapter 4 Investigating the Effect of Wearing Masks on Office Work in Indoor Environments During a Pandemic Using Physiological Sensing

4.1 Introduction

Due to the spread of the new coronavirus (COVID-19), people's lives have been affected in different ways. Indoor environments are particularly important to slow the spread of the virus, resulting in additional requirements of maintaining good indoor air quality [38, 119, 120] and wearing face coverings in common places like office environments and public gatherings [121, 122]. For example, as recommended by the United States Centers for Disease Control and Prevention (CDC), people should wear masks in public events, gatherings, or anywhere with other people, as masks can provide a barrier to respiratory droplets and thus prevent the spreading of COVID-19 [123]. The Occupational Safety and Health Administration (OSHA) recommends employees wear cloth face covering at work to reduce the spread of the virus and thereby the risk of disease transmission [124]. Similarly, the World Health Organization (WHO) also considers wearing masks as a key measure to suppress the transmission of the pandemic and save lives [125].

To overcome the economic recession during the pandemic period [126], people's working styles have become more and more flexible. For example, employees can choose to work from home and only return to the office seldomly [127]. Nevertheless, not every home has a suitable workplace [126] and home office work requires more online effort and greater concentration during communication, thereby generating visual, auditory, and mental overload [128]. Moreover, it is unavoidable for some employees to go back to the office from time to time to perform professional tasks [129, 130]. Therefore, it is crucial to understand the potential effect of wearing

a mask on people's productivity and wellness while they are performing work in office-type settings.

Although the efficacy of face masks in preventing the spread of respiratory viruses is confirmed by previous research [131], they may also cause some adverse effects on people [132]. For example, wearing an efficacious mask will affect the respiration cycles, and lead to increased expired air retained within the breath zone [133]. The concentration of carbon dioxide (CO_2) in the breath zone will rise significantly after wearing a face mask. This may cause an increase in physiological stress due to the low level of oxygen [134]. In addition, previous studies have shown that wearing a mask for a long time may influence people's health and comfort due to the poor ventilation underneath the mask [132, 134, 135]. Despite some general effects of wearing masks have been studied, there is a lack of systematic investigation to understand the effect of wearing masks on the performance and mental health of individuals who work in office-like indoor environments (the setting, social features, and physical conditions in which people could perform office work [136]). This raises an important question: since wearing masks may adversely impact the breath zone air condition in different aspects, how will it affect the physiological responses (e.g., work engagement, MW, and SCL) and task performance of people while they are performing office work?

To answer this question, an experiment is needed. Based on the literature, specific types of physiological data are correlated with human psychological states. For example, the brain signal is correlated with psychological stress [137], and galvanic skin response (GSR) is proven as a good indicator of detecting emotions [138]. Therefore, instead of collecting data in subjective approaches such as questionnaires, the experiment is designed based on physiological sensing. The experiments are conducted in a controlled lab environment, and computer-based cognitive tasks

are designed for the subjects to simulate typical office tasks. Meanwhile, the subjects' physiological responses and performance are recorded. Based on previous research, work engagement, and MW can directly affect the productivity of the employee [23-26]. In addition, SCL and HR are found relevant to the general changes in autonomic arousal [139-141]. Therefore, these physiological indicators are measured under the scenarios with and without masks. Based on the guideline of CDC and OSHA, the two most common types of masks used during the pandemic, cloth and surgical masks [123, 124] are used in the experiments. The collected experimental data is further analyzed and compared to provide insights into the effect of wearing masks on the subjects. The objectives of this study can thus be summarized as (1) to investigate the effect of wearing different mask types on work engagement; (2) to understand the effect of wearing different mask types on the MW; (3) to investigate the effect of wearing different mask types on other important physiological responses (i.e., SCL and HR); and (4) to compare the task performance of the subjects before and after wearing a mask.

4.2 Related Work

This section provides three main literature review categories to support the motivation and methodology of this study. First, existing literature on the effect of wearing masks on people's life and wellness are reviewed. The research gaps in previous studies are identified based on this literature review. Second, the utilization of physiological data to evaluate people's states is reviewed to support the usage of biosensors in the experiment. Third, to support the design of the cognitive tasks, the conventional methods of evaluating the task performance of office workers are reviewed.

4.2.1 Effect of wearing a mask on people

In order to understand how wearing masks could affect people, different experiments were conducted in previous studies. For example, to investigate the effect of wearing a mask on the social life of people, an experiment was carried out to measure the effect of masks on emotion recognition. The subjects were asked to assess the emotional state (i.e., angry, disgusted, fearful, happy, neutral, and sad) of faces covered by masks. The results showed that wearing face masks would cause huge confusion for people and their ability to perceive others' emotions, which added a negative effect on social interaction [142]. Moreover, potential side effects of wearing masks on people's wellness were studied by Geiss [143], who investigated how wearing face masks affected the CO_2 concentration in the breathing zone. Three types of masks (i.e., surgical mask, cloth mask, and KN95 mask) were tested. The results revealed that after wearing a face mask, the concentration of CO2 (between nose and mouth) increased to a range between 2150 and 2875 ppm, which was significantly higher than the maximum acceptable indoor level of 1000 ppm based on ASHRAE and OSHA standards [12, 124].

In addition, the impact of wearing a mask on physiological stress was explored by analyzing the heart rate variability (HRV). The results indicated that higher stress might be caused by wearing a mask [134]. Another study investigated the influence of wearing masks on people's health and comfort through physiological sensing and questionnaires, suggesting that in a warm environment, wearing a mask for a long time could make people feel hot and humid [132]. Moreover, the effects of wearing N95 and surgical masks were compared. Subjects wearing different types of masks were asked to perform intermittent exercise on a treadmill, which showed that ST and humidity inside the surgical masks were significantly lower than N95 due to better air permeability [135]. Furthermore, the effect of wearing a mask on body temperature and HR during

exposure to electromagnetic fields (EMF) was explored. The results showed that a mask could help stabilize vital body signs within a normal range [144]. Despite the previous studies, it is still not clear how wearing a mask during a pandemic period will affect the mental health, work engagement, and task performance of individuals who work in office-like indoor environments. A better understanding of this can be important for improving the wellness and productivity of office workers.

4.2.2 Measurement of office worker physiological responses

Different methods have been investigated to evaluate office workers' states using their physiological responses. According to previous studies [24-26], higher work engagement could lead to higher productivity. Therefore, studies have tried to correlate work engagement with brain waves as they could be directly measured through an electroencephalography (EEG) headset. For example, using the average overall power of the brain waves as the indicator of the occupants' engagement, Choi et al. [145] found that the best attention of the subjects was associated with the environment that achieved a slightly positive Predicted Mean Vote (PMV). Similarly, researchers have extensively investigated MW as it was also found to be correlated with people's task performance [23, 139, 146, 147]. To obtain the effect of the thermal environment on people's MW, EEG was used in previous studies [23, 139] to directly measure the MW. The results from these studies showed that warmer environments would slightly increase the MW.

In addition, parameters such as SCL, HR, ST, and blood pressure were also measured as major indicators of people's physiological responses. For example, different biosensors were used to collect and compare the SCL, HR, and tympanum temperatures under different thermal environments. Higher levels of SCL were found when people were performing tasks in warmer environments, while no obvious pattern was found in HR and tympanum temperature [139].

Similarly, the effect of long-term indoor thermal history was investigated by comparing the physiological responses indicated by HR, ST, systolic blood pressure, and diastolic blood pressure. The results indicated that indoor thermal history had no significant effect on those physiological responses [148]. Moreover, Deng et al. [57] proposed a method to estimate work engagement and investigate the effect of lighting conditions using easily measurable physiological data including SCL, HR, and ST, which suggested that the effect of lighting conditions varied across individuals. These previous studies confirmed the feasibility of using physiological indicators (e.g., brain waves, SCL, and HR) to evaluate the well-being of office workers. However, none of the studies have tried to investigate the effect of wearing a mask on physiological responses, which is important for those who need to wear masks while working, especially during pandemic periods.

4.2.3 Cognitive tasks to evaluate the performance of the office workers

Cognitive tests that could represent typical office tasks were commonly used to measure the performance of the office worker. Several studies have conducted performance tests to assess the cognitive functions of office workers. For example, to evaluate the cognitive functions of perception, thinking, learning, and memory of office workers under different thermal environments, an experiment was used by Lan et al. [149]. Similarly, cognitive tasks such as number calculation, reading, and reaction were used in several studies to assess the performance of the office worker [150-152]. Some of the studies [8, 150] found significant effects of the indoor environment (e.g., air temperature) on test performance. In addition, the memory test was used to evaluate people's brain activities, which indicated that the amount of cortical spectral activity from frontal areas and parietal was higher during the moments when things were remembered [153]. Moreover, a strategic management simulation software tool was applied to evaluate the decision-making performance of the office worker, suggesting that higher cognitive function scores could

be achieved in green building conditions compared with conventional ones [154]. Regarding the experimental design, these studies provide the support of using cognitive tasks to simulate the daily tasks of the office worker.

Overall, although the physiological measurement and cognitive task have potential, they have not been used to study the effect of wearing masks on individuals who are working in office-like indoor environments. Therefore, in this study, physiological measurement is integrated with cognitive tasks to bridge the identified gap. These methods allow us to simulate office tasks and reasonably evaluate the effect of wearing masks on individuals who work in office-like indoor environments.

4.3 Research Methodology

In this study, a comprehensive framework was developed to investigate the effect of wearing masks on work engagement, MW, SCL, HR, and task performance, as shown in Fig. 4.1. To simulate daily office work, subjects were asked to perform three cognitive tasks including number addition, visual search, and digit recall. Three sections of experiments were conducted: (1) the subject performed cognitive tasks without any mask (baseline); (2) the subject wore a surgical mask to perform cognitive tasks; and (3) the subject wore a cloth mask to perform cognitive tasks. The surgical mask and cloth mask were selected because they were the two most commonly used masks recommended by different authorities [123, 124] at the time of the experiment. The surgical masks used in this study are 3-ply masks that filter against 99% of particles larger than 0.1μm. The cloth masks used in this study are 3-ply 100% cotton masks. As one of the most commonly used colors, blue was chosen for the surgical mask. Black was chosen for cloth masks as it is also one of the most common colors and people trust cloth masks with black color more than others [155]. An EEG headset was used to capture the subjects' brain signals to

obtain their MW and engagement level. Related physiological data including GSR signals and HR were also collected by corresponding sensors. The final results of the tasks were automatically graded to indicate the subjects' performance. Detailed steps of the experiment are discussed in the following sections.

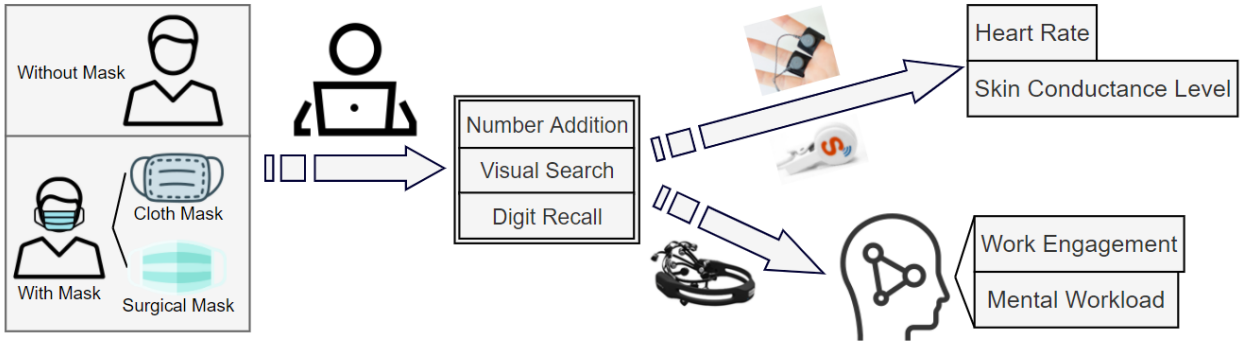

Fig. 4.1. Framework for investigating the effect of wearing masks on physiological data

4.3.1 Subjects and Experimental design

To ensure the generality and reliability of the results, the subjects confirmed that they had no reported mental disorder or physical disability. The selection process made sure there was no restriction on the professional field or personal characteristics such as gender, height, and weight. In total, 20 subjects (9 females and 11 males) aged between 20 and 30 were recruited. All the subjects were graduate students at the University of Michigan who usually spend most of their time doing office-like tasks such as preparing for presentations and working on manuscripts among other tasks. Each subject was asked to come to the lab at the same time for three days, where they spend a total of 80 minutes. On each day, the subjects either did not wear a mask or wear one of the two types of masks. All subjects received a monetary award upon completion of all phases of the experiment. In order to respect the COVID protocols at the time of the experiment (i.e., October 2021), only one subject was allowed in the room per session.

The dimensions of the room and the experimental setup are shown in Fig. 4.2. The room used for the experiment was an office space used by graduate students located in the basement of the Civil and Environmental Engineering building at the University of Michigan. It did not have any windows and was accessible through a single door that was kept closed during the experiment. It was fully controlled by a central Heating, Ventilation, and Air Conditioning (HVAC) system with mixing ventilation. The maximum total airflow rate supplied by two cassette fan coils at the ceiling was 600 m^3/h, with around 10% of outdoor air using recirculation. The same amount of air in the room was exhausted into a return grille. The locations of the fan coils and exhaust grille can be found in Fig. 4.2. The air velocity surrounding the subjects was measured as less than 0.01 m/s (using the ANNMETER AN-856A with the resolution of 0.001 m/s and the accuracy of $\pm$3%+0.1 rdg). The settings of the room environment were consistent during all experimental sessions to ensure identical air velocities and CO2 levels. The environmental parameters were continuously measured using the GC-0010 COZIR sensor with the accuracies of ± 0.2 °C for temperature, ± 3% for relative humidity, and ± 50 ppm for CO2 at a distance of less than 1 meter from the subjects. In addition, a light meter with an accuracy of 1 lux was used to ensure a lighting level of 500 lux. The placement of the COZIR sensor and the positions of the equipment for measuring lighting level and air velocity can be seen in Fig. 4.2. Table 4.1 shows a summary of the measured indoor environments compared with the recommended ones by ASHRAE [12] and U.S. General Services Administration [156].

A guideline was proposed for the subjects to follow to ensure similar initial mental states and good data quality. The guideline includes: (1) try to get enough sleep on the night before the experiment and maintain the same sleeping schedule during the three days of the experiment; (2) avoid eating or drinking foods that might cause excitement (e.g., caffeine, alcohol) during the

experiment period; (3) wear the same level of clothing (trousers, short-sleeved shirt) throughout the experiment; and (4) keep the hair dry and clean before conducting the experiment to ensure proper contact of the EEG electrodes to the scalp. Before starting the experiment, each subject was randomly assigned a unique ID number as the reference for the collected data. This also ensured no personally identifiable information (e.g., name) of the subjects was used during the data collection and analysis. In addition, all experiments followed COVID-19 public health recommendations to ensure the safety of the subjects and the research staff.

Table 4.1. Environmental conditions during the experimental sessions (mean ± standard deviation)

	Air Temperature (°C)	**Relative Humidity (%)**	**Lighting Level (Lux)**	**CO_2 level (ppm)**
Measured	24 ± 0.2	35 ± 5	500 ± 10	450 ± 50
ASHRAE [12]	19.4 ~ 27.8	< 65	500	< 1000

Fig. 4.2. Experiment room dimensions and experimental setup

4.3.1.1 Timeline

Fig. 4.3 shows the details of the experimental timeline for each of the daily sessions. When the subjects reached the lab, they were first given 30 minutes to relax and prepare for the experiment. During this time, the research staff explained the details of the experiment and provided the subjects with instructions. As shown in Fig. 4.2, during the experiment, the subjects needed to

wear sensors to allow the collection of their physiological data (i.e., EEG signal, GSR signal, and HR). The time for each cognitive task was designed to be around 10 minutes. To avoid fatigue, a 10-min break was given between two cognitive tasks. The procedures for the three sessions of the experiment were identical. For one of the sessions, the subjects performed the tasks without any masks. For the sessions with masks, the subjects wore the masks during the whole experiment including the relaxation and preparation periods. The design of the total experiment timeline and the time allocated per cognitive task is consistent with similar studies in the literature. For example, an experiment was designed by Su et al. [157] to investigate the impact of HVAC terminal devices on occupants' thermal comfort and cognitive performance. Three different types of terminal devices were selected as the variables of the three scenarios. The time for performing the cognitive tasks for each scenario was set to be 10 minutes, with a total experimental time of 75 minutes for each subject. Similarly, Lee et al. [158] designed an experiment to investigate the effect of indoor CO2 concentration on cognitive performance and EEG signal, the duration of performing the cognitive task was set to be 5 minutes with a total experimental duration of 30 minutes for each subject. To eliminate the effect caused by the order of the different scenarios, the order of the sessions in this study was fully randomized. The protocol of the experiment was reviewed and approved by the Institutional Review Board at the University of Michigan.

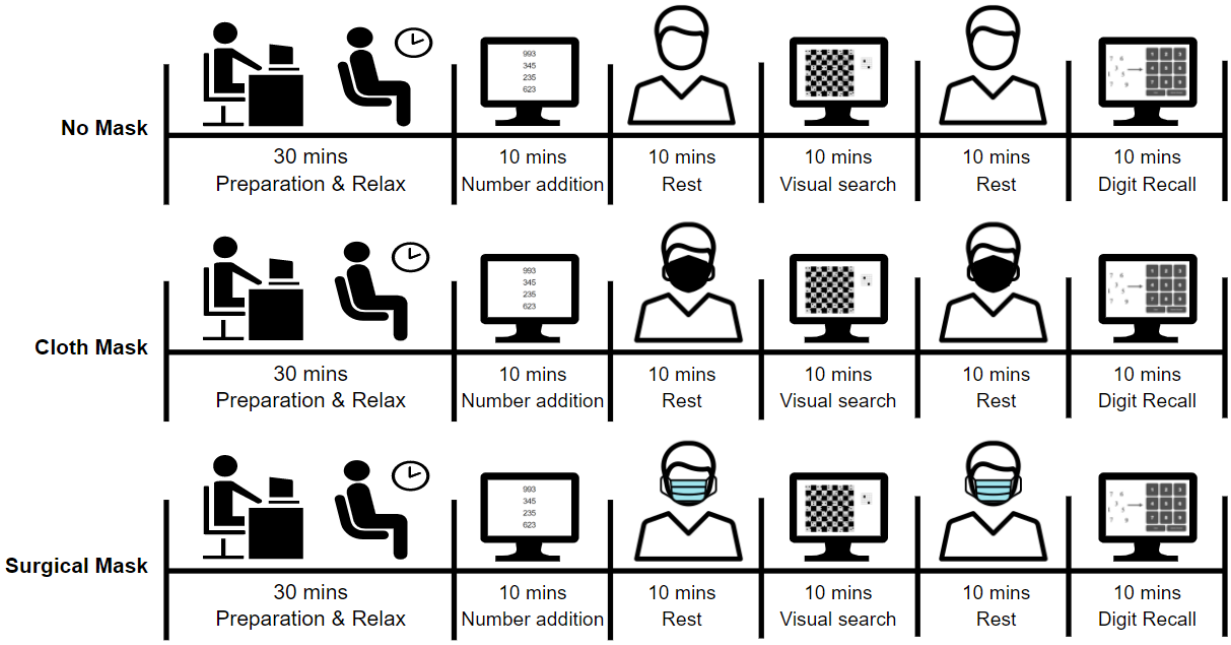

Fig. 4.3. Experimental timeline

4.3.1.2 Design of cognitive tasks

To simulate the common daily tasks, three cognitive tasks were designed. According to previous studies, adding numbers and searching for specific patterns could be used to arouse the thinking and perception of the subject [23, 159-161], and digit recall performance was used to estimate the level of concentration [153]. Fig. 4.4 shows the three designed computer-based cognitive tasks, and the details of the tasks are shown below:

- Number addition: For the number addition task, a few randomly generated numbers are shown on the screen. The subjects are required to calculate the sum of the numbers. After solving one problem, the subjects can continue to the next. The subjects should do the calculation without a calculator as fast as they can. The task has two parts, the first part contains six one-digit numbers while the second part contains four three-digit numbers. The duration for the first part is 4 minutes and the total duration of the task is 10 minutes.

- Visual search: The visual search task contains the target patterns for the subjects to search as fast as they can. The overall interface contains 9×9 grids, 41 of them are white squares while the other 40 are black. Each white square contains 5×5 pieces of small boxes, with two of them being black. There is a target white square shown on the right side of the screen that can match one of the small white squares in the 9×9 grid. The subjects should find the target square in the grid and enter the result in the text box using the index of row and column. After finishing one, the subjects can go to the next. The total duration of the task is 10 minutes.
- Digit recall: The task trying to test the short-term memory of the subjects, which is adapted from a traditional test named the Wechsler Adult Intelligence Scale (WAIS) [162]. During the task, random digits (0 to 9) appear on the screen. There is a time gap of 200 ms between every two digits. Each digit lasts for 800ms on the screen. Once all the digits are displayed and disappear, the subjects are asked to repeat them in the correct order by clicking a number pad. After finishing one, they can click “Continue” to go for the next one. There are two parts to the task, the first part (the easy part) contains 5 digits while the second part (the hard part) contains 11 digits. There are 18 trials for the easy part and 18 trials for the hard part. The total duration of the task is about 10 minutes. During the process, there is a message on the screen to show how many digits will be displayed.

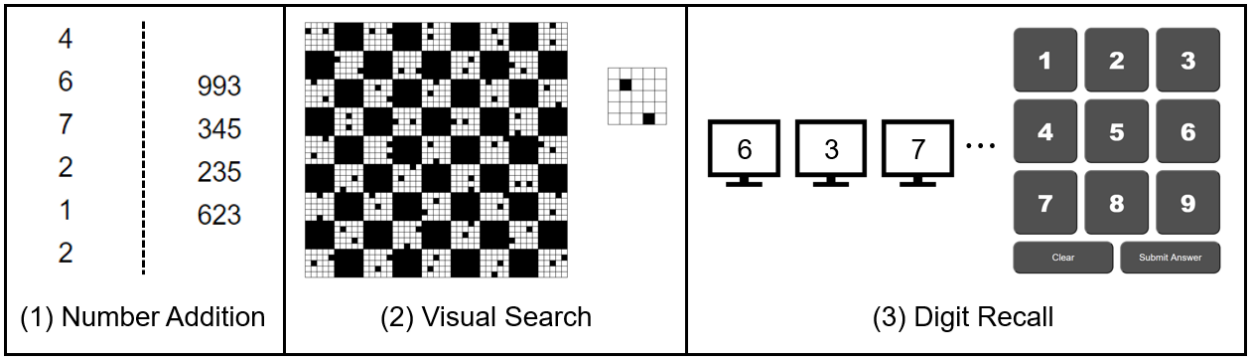

Fig. 4.4. Design interface for cognitive tasks

4.3.2 Physiological data collection and process

4.3.2.1 Measurement of brain waves using EEG

The EEG headset collects the voltage changes caused by brain activities by placing electrodes at specific locations on the scalp surface of humans. The cognitive states of the human can thus be reflected by the collected voltage changes [163]. A low-cost EEG headset, Emotiv EPOC+, was used in the experiment. It contains 14 channels and allows easy setup with only saline solution. The data sampling frequency was 128 Hz. The collected data could be visualized in real-time through a Bluetooth connection and was stored on an ordinary laptop.

The raw data strings obtained from the electrodes were in form of floating-point values with approximately 4200 μV of DC offset, and they normally contain noise [164-166]. The noise normally consists of both extrinsic and intrinsic artifacts. The extrinsic artifacts can be removed using a band-pass filter with a frequency from 0.5 Hz to 65 Hz [167]. The intrinsic artifacts usually contain eye and muscular movements [168, 169] and need more effort to deal with. Therefore, a denoise process was required to pre-process the raw data. Previous studies have proposed several methods for denoising intrinsic artifacts [170-174]. For example, a toolbox was developed to help with the removal of artifacts of EEG signals [171].

Fig. 4.5 summarizes the procedures to process the EEG raw data based on the methods in previous studies. Before conducting any data analysis, the DC offset should be removed, followed by the denoise process. Muscular movement, eye blinking, and eye movement should be removed through the denoise process [168, 169]. EEGLAB was used as the tool to conduct the denoise process in this study. After denoising, Fast Fourier Transform (FFT) was applied to obtain the band power of different frequency ranges. The frequency bands used in this study included Delta (1−4 Hz), Theta (4−8 Hz), Alpha (8−12 Hz), Beta (12−25 Hz), and Gamma (> 25 Hz) [23, 175, 176]. The obtained power of different frequency bands could thus be used to calculate the work engagement and MW.

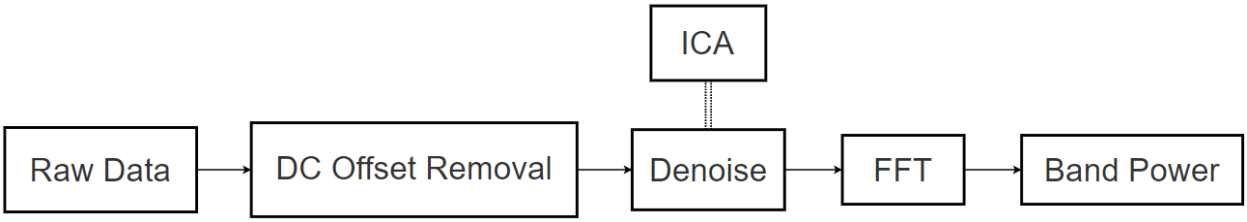

Fig. 4.5. Process of EEG raw data

4.3.2.2 Calculation of work engagement and MW using EEG data

Based on previous studies, the frontal asymmetry index (FAI) could be calculated by alpha power in the right relative to the alpha power in the left cortex to indicate work engagement [177-184]. The frontal asymmetry was found related to motivation and emotion in response to different situations [185]. In addition, it was claimed that higher FAI was associated with positive feelings, motivation, and engagement [20, 186, 187]. Therefore, the work engagement of the subjects was represented by the FAI in this study. FAI could be calculated based on Eq. (4.1) [177, 178]. F3 and F4 electrodes are commonly used to indicate the frontal region and their positions are shown in Fig. 4.6.

Previous studies have shown that higher frontal theta power and lower parietal alpha power were associated with higher MW [188-190]. The frontal power is usually represented by the brain signals from F3 and F4, and parietal power is commonly indicated by P7 and P8 [188-190]. Therefore, the ratio of frontal theta power to parietal alpha power shown in Eq. (4.2) was used as the indicator of MW in this study. Fig. 4.6 shows the positions of the related electrodes for the MW.

$$Frontal\ Asymmetry\ Index = ln\left(\frac{alpha\ power\ of\ F4}{alpha\ power\ of\ F3}\right) \tag{4.1}$$

$$Mental\ Workload\ Index = \frac{F3\ theta\ power + F4\ theta\ power}{P7\ alpha\ power + P8\ alpha\ power} \tag{4.2}$$

Where F3, F4, P7, and P8 refer to signals from the specific electrodes of the EEG headset

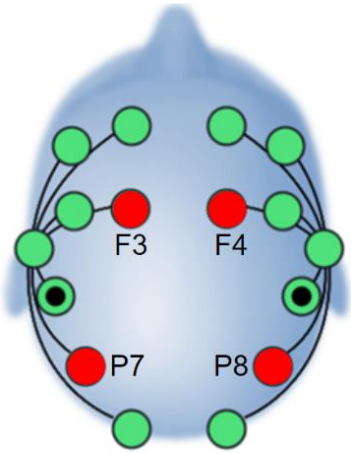

Fig. 4.6. Positions of related electrodes

4.3.2.3 Measurement of SCL and HR

GSR signal can reflect the changes in autonomic arousal [140] and may also affect the activity of the central neural [191, 192], indicating it is correlated to brain activity. The SCL is considered the tonic component of the GSR signal which could be measured directly from the sensors. The usage of SCL to indicate human physiological responses has been confirmed in previous studies [139, 148, 193]. For example, the SCL could reflect sympathetic activity [141,

194, 195]. In addition, previous studies have reported that SCL could be used to reflect the MW [196, 197]. Therefore, SCL was also measured as an accessory of EEG signals [139] in this study. The Shimmer3 GSR+ Unit was used to measure the GSR signals of the subjects, and the tonic component was obtained as the SCL. In addition, several studies have used HR as the physiological indicator for body conditions [36, 69, 198], as it has been proven to be relevant to the emotional well-being of humans [199-202]. Therefore, it is used to help with the analysis of the human physiological responses in this study. As shown in Fig. 4.2, GSR data was collected using Optical Pulse Ear-Clip. During the experiment, the electrodes of the sensors were attached to the subjects as securely as possible to ensure the quality of the collected data.

4.3.3 Data analysis

There was a total of 20 valid datasets from the subjects. The datasets were stored in separate CSV files from different equipment. As the data collection frequency was 128 Hz, there were more than 75,000 data samples for each dataset. To conduct an ANOVA for the dataset of each subject, the original raw data was pre-processed to obtain data points with a specific time window of 8 seconds based on the related studies [182, 203].

4.3.3.1 Within-subject analysis

As the purpose of this study was to investigate the effect of wearing masks on individuals, the analysis was first performed on the datasets of each subject separately. The mean and standard deviation of work engagement, MW, SCL, and HR for each subject were calculated. Repeated measures ANOVA was applied to determine whether there were significant differences in these physiological responses in three mask-wearing scenarios. This was followed by a post hoc test (Tukey's HSD) to find out if there are significant differences between the specific pairs - cloth mask versus no mask, cloth mask versus surgical mask, or no mask versus surgical mask. For each

mask-wearing scenario of the within-subject comparison, datasets for the physiological responses were constructed based on the 8-seconds time windows. Therefore, the post hoc test could be used to determine whether two datasets (for different mask-wearing scenarios) are significantly different.

4.3.3.2 Analysis across all subjects

The general effect of wearing a mask was also analyzed by combining the results from different subjects. However, the ranges of physiological responses vary a lot across different subjects. For example, the SCL of one subject may range from 0 to 1 μS while for another subject it may be between 3 and 5 μS. One reason for this difference is the effect of the psychology of the subjects in the experimental environment [56, 204]. Therefore, to eliminate the distinct ranges of the results caused by personal differences, a standardization of the results, given in Eq. (4.3), was performed before analyzing the general effect of wearing a mask across subjects [205]. The standardized results reflect how much of the standard deviation of the value in one scenario is offset from the mean from the subject's mean value. For example, the standardized value of 1 indicates that the value in this scenario (with a specific mask or no mask) is larger than the mean value of this subject by one standard deviation. The standardized values eliminate the effect caused by the range differences in the physiological data of different subjects and reflect the relative changes of each subject. As for the post hoc test across all the subjects, the mean values of the results for each subject were used, thus for each scenario, 20 data points from 20 subjects were included.

$$Standarized(x_i) = \frac{x_i - \mu}{\sigma} \qquad (4.3)$$

Where x_i is each data point from one specific subject in different scenarios, μ is the mean value of the data points from the specific subject, and σ is the standard deviation of the data points

4.3.3.3 Assumptions of the ANOVA and post hoc test

There are several assumptions to ensure the reliability of ANOVA and post hoc test: (1) each observation of the dataset is independent of every other observation; (2) the residuals of the data are normally distributed; (3) the variances of the differences between all combinations of related groups are equal. Since the experiments were conducted on different subjects on three different days, assumption (1) was true. In addition, the Shapiro-Wilkinson test [206] was conducted to validate the normality of the residuals of the data for both within-subject and across-subjects analysis. For the data across all the subjects, the results showed that the p-values of the datasets were larger than 0.05; thus, there was no sufficient evidence that these datasets did not come from a normal distribution, which supported assumption (2). Similarly, the variances of the differences between different groups of the data were tested using the Brown-Forsythe test [207], and the corresponding p-values were larger than 0.05 for all the datasets, which supported assumption (3). The validation of these assumptions supported the reliability of ANOVA and post hoc test for the across-subject analysis. Regarding the within-subject data, the Brown-Forsythe test also confirmed the similar variances of the datasets. The Shapiro-Wilkinson test suggested non-normal distribution of the residuals for most of the datasets. However, it has often been reported that the violation of normality should not be a serious concern, especially when there are enough data points (e.g., >20) with similar variances [208]. Therefore, the ANOVA and post hoc test were also confirmed applicable for within-subject analysis.

4.4 Results

4.4.1 Comparing the effect of wearing a mask on work engagement (FAI)

Fig. 4.7 shows the average work engagement represented by the FAI for different subjects (subjects 1 to 9 are females and subjects 10 to 20 are males) while they were performing the

cognitive tasks. Based on the data points from the 8-seconds time windows, a p-value of 0.05 was used in this study to determine if there were significant differences between any two pairs of the results. As a result, significant differences were found in most cases while the results varied across individuals. However, the results also indicated that the effect of wearing a mask on people's work engagement varies across individuals. For example, the work engagement of subject 3 with a surgical mask was the highest across all cognitive tasks while the results were the opposite for subject 10. In addition, the effect of wearing a mask was negligible in some scenarios such as the results of subject 14. The post hoc test also indicated that the effects within the subjects might not be always identical for different cognitive tasks. Taking subject 4 as an example, work engagement without masks was the highest for the digit recall task, while it was the lowest for the visual search task.

In addition to the within-subject plots, the results across all subjects were combined to study the general pattern of the effects (Fig. 4.8). For this part, the average values of the results in different scenarios from 20 subjects were used. Due to the significant differences in the range of the results across individuals, the results were standardized based on Eq. (4.3). Repeated measure ANOVA and post hoc test were applied to determine whether the distribution of the results was significant in different scenarios in each cognitive task. Cohen's d effect size was applied to show the difference between the two groups of data. The results are shown in Table 4.2, which revealed that there was no general pattern for the effect of wearing a mask on work engagement.

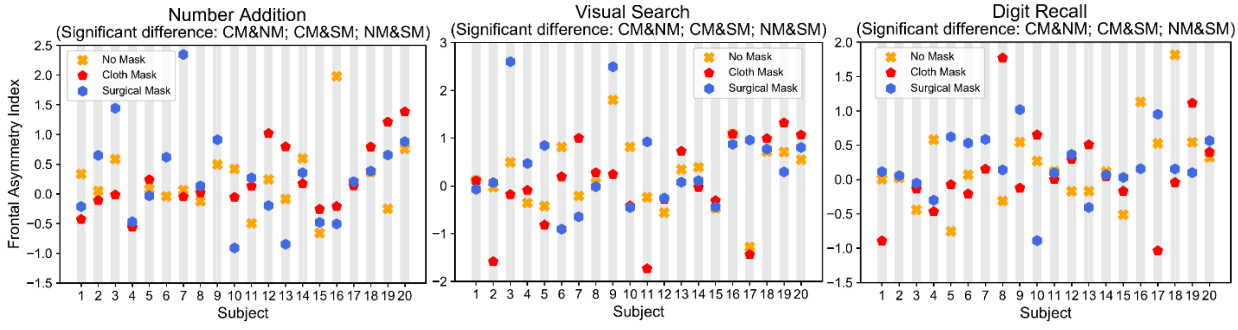

Fig. 4.7. Average FAI of different subjects

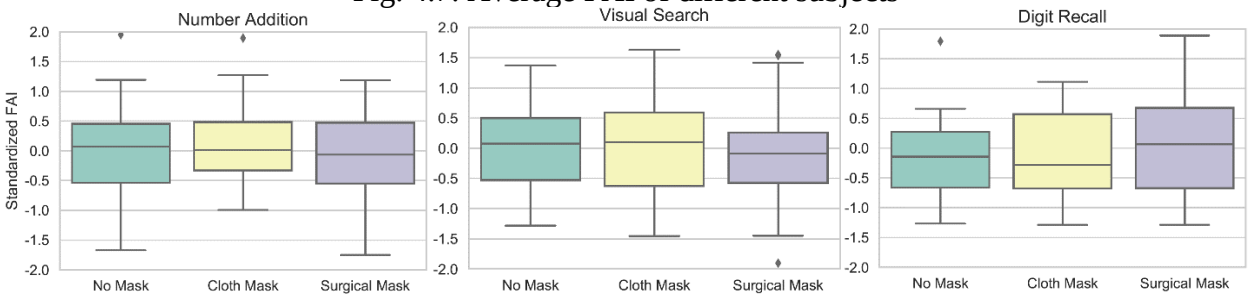

Fig. 4.8. Standardized FAI across all subjects

Table 4.2. Statistical analysis for standardized FAI across all subjects (corresponding to Fig. 4.8)

	Pair	Mean Difference	Effect Size	p-value
Number Addition	CM & NM	0.213	0.162	0.854
	CM & SM	0.390	0.263	0.615
	NM & SM	0.177	0.165	0.9
Visual Search	CM & NM	0.231	0.244	0.766
	CM & SM	0.465	0.381	0.383
	NM & SM	0.234	0.218	0.762
Digit Recall	CM & NM	0.589	0.376	0.378
	CM & SM	0.268	0.193	0.795
	NM & SM	0.321	0.291	0.726

Note: “NM” refers to no mask, “CM” refers to cloth mask, and “SM” refers to surgical mask

4.4.2 Comparing the effect of wearing a mask on MW

Similar to work engagement, the corresponding results for MW were also plotted as per subjects in Fig. 4.9. To maximize the readability, the y-axes of the plots were adjusted according to the range of the results. Significant differences between wearing a mask (either a cloth mask or a surgical mask) and not wearing a mask were also found in MW for most of the subjects (except subjects 8, 13, 14, 15, and 18). The results were also found to be different from person to person. Take subjects 4 and subject 13 as an example, when performing the number addition, the highest MW was associated with wearing a cloth mask for subject 4. However, the MW when wearing a cloth mask was the lowest among the three mask-wearing scenarios for subject 13.

Similarly, the results across all subjects (Fig. 4.10) were plotted to investigate the general pattern of the effects of wearing masks, the same standardization was also performed to eliminate the effects of individual differences. The results of ANOVA and post hoc test were shown in Table 4.3. The results showed that for the number addition, the overall MW of the subjects without wearing a mask was higher than when wearing either a cloth mask (Tukey's HSD: $p = 0.003$, $d = 1.006$) or a surgical mask (Tukey's HSD: $p = 0.023$, $d = 0.78$). No significant difference was found between the surgical mask and the cloth mask. For the visual search, there was no significant difference in MW under different scenarios. As for the digit recall, it was found that the results when the subjects were wearing a cloth mask were lower than without a mask (Tukey's HSD: $p = 0.011$, $d = 0.896$). In general, the results imply that although the effects might vary across individuals, wearing a mask during the pandemic leads to a lower MW while people are performing specific types of tasks (i.e., number addition and digit recall).

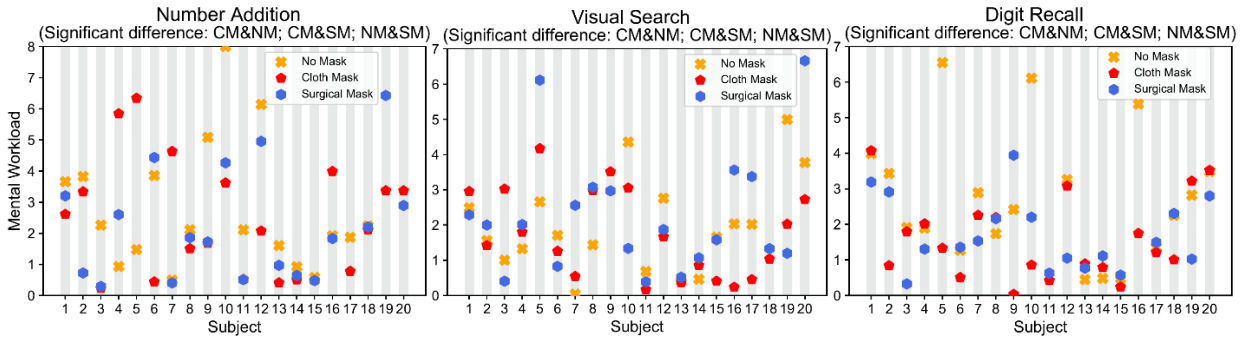

Fig. 4.9. Average MW of different subjects

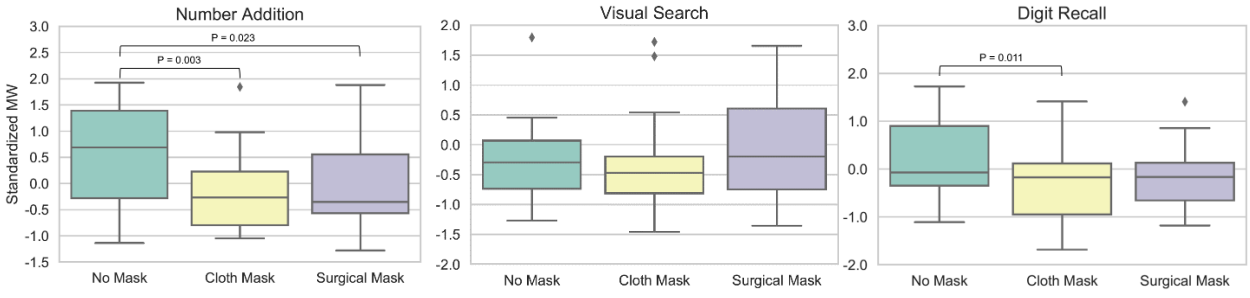

Fig. 4.10. Standardized MW across all subjects

Table 4.3. Statistical analysis for standardized MW across all subjects (corresponding to Fig. 4.10)

	Pair	Mean Difference	Effect Size	p-value
Number Addition	CM & NM	1.068	1.006	0.003
	CM & SM	0.238	0.315	0.699
	NM & SM	0.830	0.780	0.023
Visual Search	CM & NM	1.205	0.367	0.417
	CM & SM	0.440	0.540	0.879
	NM & SM	0.765	0.233	0.684
Digit Recall	CM & NM	0.746	0.896	0.011
	CM & SM	0.293	0.452	0.467
	NM & SM	0.453	0.610	0.167

4.4.3 Comparing the effect of wearing a mask on SCL

As indicated in previous studies, both brain waves and SCL could be used to reflect the MW, thus the results of SCL were also investigated as an accessory to EEG signals. Similarly, the results of SCL analysis under three different mask-wearing scenarios were plotted for each subject (Fig. 4.11). Significant differences were found in most cases while the results varied across individuals. The standardized SCL across subjects was plotted in Fig. 4.12, and the corresponding results of ANOVA and post hoc test were shown in Table 4.4. For number addition, the average standardized SCL without wearing a mask was overall higher than either wearing a cloth mask (Tukey's HSD: $p < 0.028$, $d = 0.737$) or a surgical mask (Tukey's HSD: $p < 0.023$, $d = 0.905$). Similar results were found for both visual search and digit recall tasks. However, there was no significant difference between wearing a cloth mask or a surgical mask. In general, the results indicate that although the effects might vary from person to person, wearing a mask during the pandemic might help reduce the SCL of the subjects for all types of cognitive tasks. If considering the SCL as an indicator of the MW, the results are partially consistent with the MW measured by brain waves.

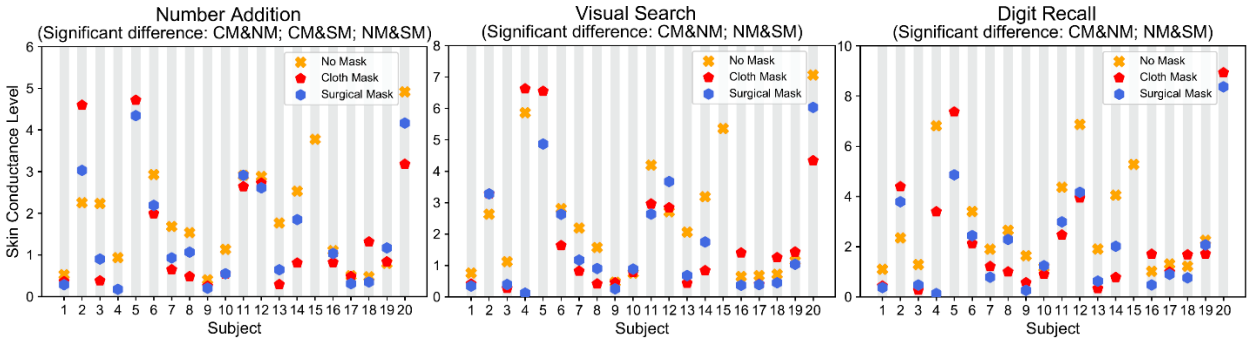

Fig. 4.11. Average SCL of different subjects

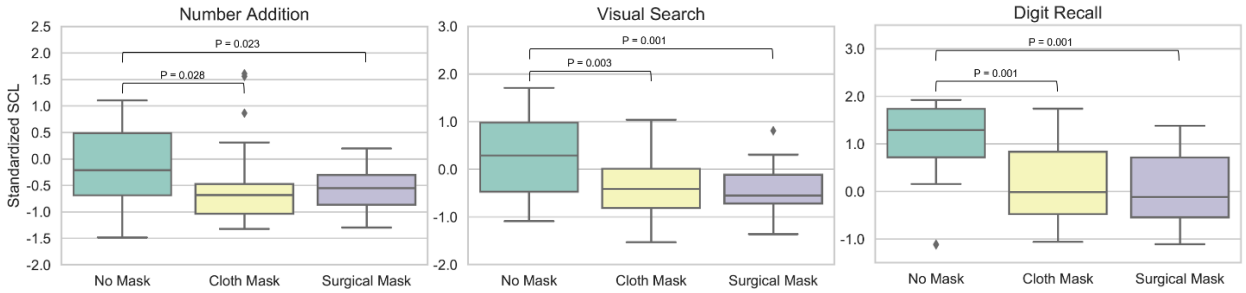

Fig. 4.12. Standardized SCL across all subjects

Table 4.4. Statistical analysis for standardized SCL across all subjects (corresponding to Fig. 4.12)

	Pair	Mean Difference	Effect Size	p-value
Number Addition	CM & NM	0.567	0.737	0.028
	CM & SM	0.019	0.034	0.900
	NM & SM	0.586	0.905	0.023
Visual Search	CM & NM	0.744	0.894	0.003
	CM & SM	0.111	0.199	0.855
	NM & SM	0.855	1.101	<0.001
Digit Recall	CM & NM	1.265	1.193	<0.001
	CM & SM	0.114	0.138	0.900
	NM & SM	1.378	1.292	<0.001

4.4.4 Comparing the effect of wearing a mask on HR

As for HR, Fig. 4.13 shows similar plots for the results as per subject. For most of the cases regarding within-subject comparison, the post hoc test indicated that there existed significant differences between the three scenarios. However, according to the comparison of the standardized results across all subjects shown in Fig. 4.14 and Table 4.5, there was no one-size-fits-all pattern

to conclude the effect of wearing a mask on subjects. For example, the results of HR for subjects 6, 14, 17, and 20 were the highest without wearing a mask, while they were the lowest without wearing a mask for subjects 7, 9, 10, 15, and 16. For subject 1, the effect of wearing a mask on HR could be neglected. In addition, the distributions of the HR under different scenarios were very similar to each other, and the ANOVA analysis confirmed that there was no significant difference among the distributions.

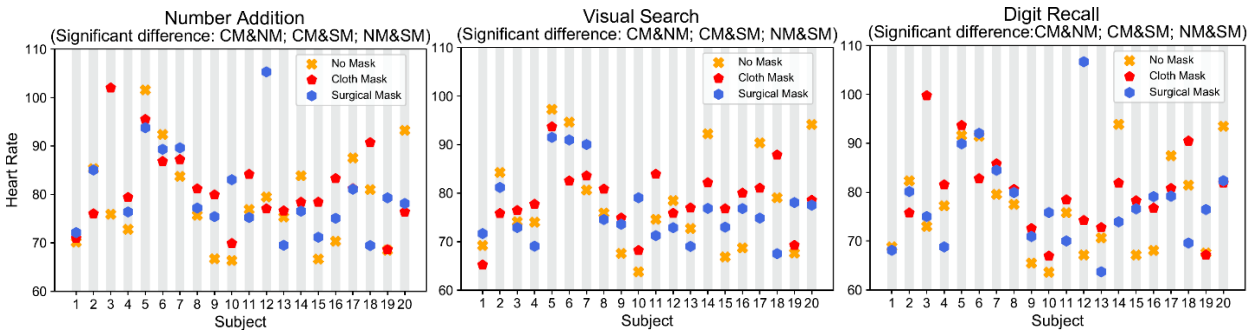

Fig. 4.13. Average HR of different subjects

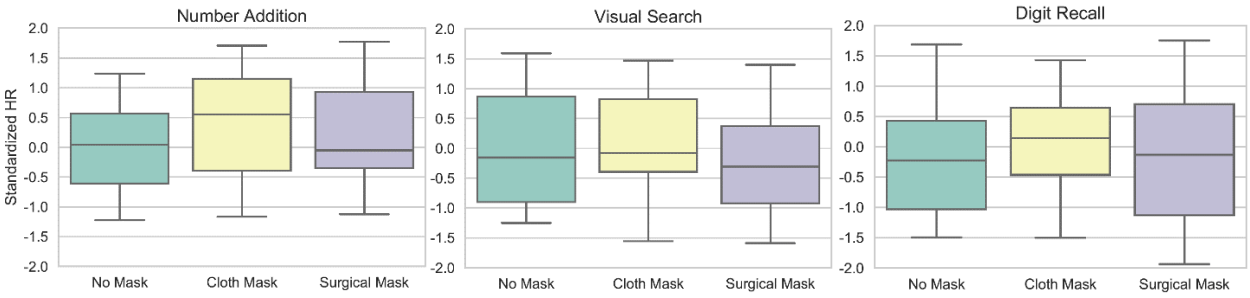

Fig. 4.14. Standardized HR across all subjects

Table 4.5. Statistical analysis for standardized HR across all subjects (corresponding to Fig. 4.14)

	Pair	Mean Difference	Effect Size	p-value
Number Addition	CM & NM	0.337	0.376	0.513
	CM & SM	0.320	0.327	0.544
	NM & SM	0.017	0.018	0.900
Visual Search	CM & NM	0.108	0.123	0.900
	CM & SM	0.339	0.385	0.475
	NM & SM	0.231	0.246	0.688
Digit Recall	CM & NM	0.128	0.137	0.900

	CM & SM	0.088	0.091	0.900
	NM & SM	0.040	0.043	0.900

4.4.5 Comparing the effect of wearing a mask on task performance

Apart from the physiological responses, the task performance of the subjects under different cognitive tasks is shown in Fig. 4.15 to Fig. 4.18. The corresponding results of ANOVA and post hoc test for Fig. 4.16 and Fig. 4.18 are shown in Table 4.6 and Table 4.7, respectively. As seen from the plots for within-subject analysis (Fig. 4.15 and Fig. 4.17), similar to the physiological responses, the effect of wearing a mask on task performance (correct number and correct rate) varied across different individuals. In addition, some subjects' task performance was more sensitive to the effect of wearing masks than others.

However, after performing the standardization of the correct number and correct rate of the tasks following Eq. (4.3), general patterns were found based on the statistical analysis across all subjects. For the correct number of the tasks, Fig. 4.16 indicated that wearing a surgical mask could reduce the correct number of the number addition task compared with no mask (Tukey's HSD: $p < 0.001$, $d = 0.873$) and wearing a cloth mask (Tukey's HSD: $p < 0.001$, $d = 0.864$), while no significant difference was found between no mask and cloth mask. As for the visual search, the correct number of the tasks was higher when not wearing a mask than wearing either a cloth mask (Tukey's HSD: $p = 0.005$, $d = 1.001$) or wearing a surgical mask (Tukey's HSD: $p < 0.001$, $d = 1.266$), while no significant difference was found between wearing a cloth mask or a surgical mask. The results for digit recall revealed a higher correct number of tasks without a mask compared with a cloth mask (Tukey's HSD: $p = 0.008$, $d = 0.952$). Compared with the correct number, the patterns for the correct rate were slightly different for number addition and visual search. For number addition, the results found the correct rate without wearing a mask is higher than either wearing a cloth mask (Tukey's HSD: $p = 0.039$, $d = 0.764$) or a surgical mask (Tukey's HSD: $p <$

0.001, d = 1.169), while no significant differences were found between wearing a cloth mask or a surgical mask (Tukey's HSD: p = 0.385, d = 0.375). For visual search, no significant difference was found among the distributions of correct rates among the three mask-wearing scenarios.

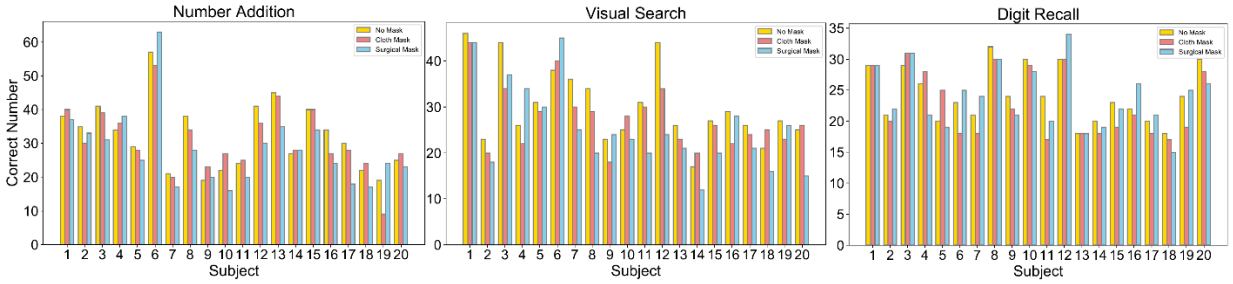

Fig. 4.15. Correct number of different subjects

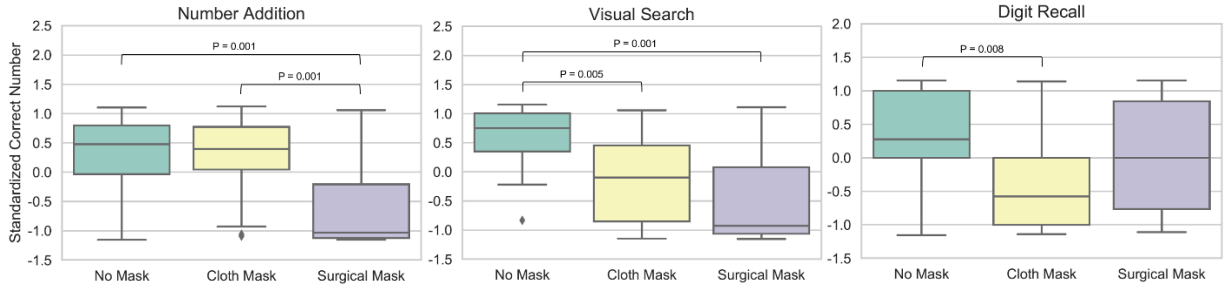

Fig. 4.16 Standardized correct number across all subjects

Table 4.6. Statistical analysis for the standardized correct number of tasks across all subjects (corresponding to Fig. 4.16)

	Pair	Mean Difference	Effect Size	p-value
Number Addition	CM & NM	0.009	0.014	0.900
	CM & SM	0.864	1.018	<0.001
	NM & SM	0.873	1.028	<0.001
Visual Search	CM & NM	0.726	1.001	0.005
	CM & SM	0.357	0.464	0.249
	NM & SM	1.083	1.266	<0.001
Digit Recall	CM & NM	0.720	0.952	0.008
	CM & SM	0.446	0.569	0.142
	NM & SM	0.274	0.370	0.471

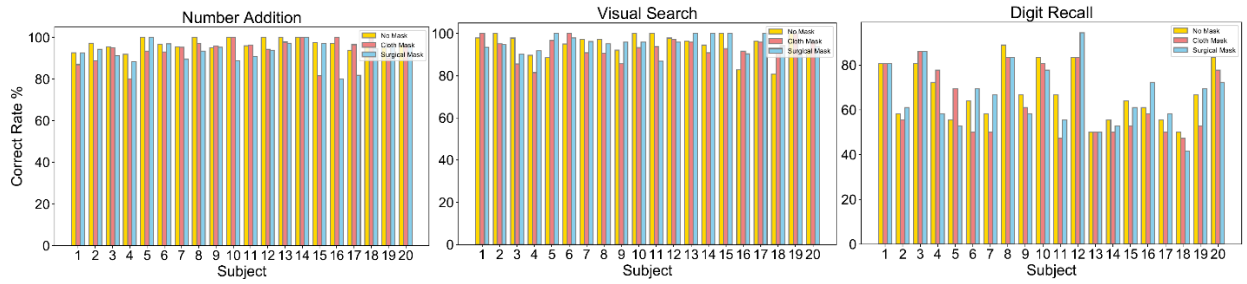

Fig. 4.17. Correct rate of different subjects

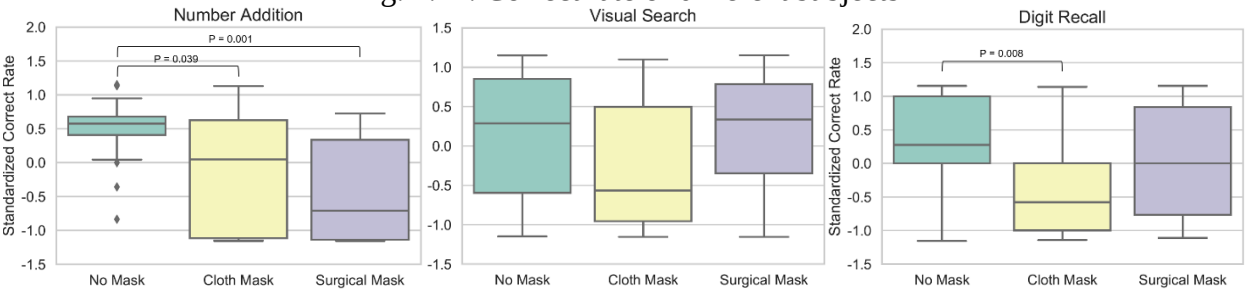

Fig. 4.18. Standardized correct rate across all subjects

Table 4.7. Statistical analysis for standardized correct rate across all subjects (corresponding to Fig. 4.18)

	Pair	Mean Difference	Effect Size	p-value
Number Addition	CM & NM	0.576	0.764	0.039
	CM & SM	0.305	0.375	0.385
	NM & SM	0.881	1.169	<0.001
Visual Search	CM & NM	0.359	0.434	0.355
	CM & SM	0.388	0.479	0.300
	NM & SM	0.029	0.036	0.900
Digit Recall	CM & NM	0.720	0.952	0.008
	CM & SM	0.446	0.569	0.142
	NM & SM	0.274	0.370	0.471

4.4.6 Investigating the effect of gender on physiological responses and task performance

The results revealed the importance of individual differences. Therefore, this study also explored potential reasons behind the variations. The physiological responses and the task performance were further divided into two groups based on the gender of the subjects. Table 4.8 shows the detailed results of the comparison. The average values of FAI, MW, SCL, HR, correct number, and correct rate for different genders were calculated and compared. In addition, the independent two-sample

t-test was performed to further evaluate whether there existed significant differences for each type of physiological response or task performance. The results revealed that no significant difference was found for the MW, SCL, and correct rate. However, the HR for females was statistically higher (Tukey's HSD: $p = 0.032$, $d = 0.306$). Moreover, the correct number of tasks for females was also statistically higher (Tukey's HSD: $p < 0.001$, $d = 0.534$). In contrast, the FAI of females was statistically lower (Tukey's HSD: p = 0.0.066, d = 0.315).

Table 4.8. Statistical analysis of the potential effect of gender

	Gender	Mean	Effect Size	p-value
FAI	Female	0.065	0.315	0.066
	Male	0.255		
MW	Female	2.331	0.162	0.349
	Male	2.093		
SCL	Female	2.510	0.084	0.572
	Male	2.781		
HR	Female	80.218	0.306	0.032
	Male	77.193		
Correct Number	Female	29.864	0.534	<0.001
	Male	24.899		
Correct Rate	Female	85.478	0.084	0.614
	Male	84.274		

4.5 Discussion

In general, there were nonnegligible effects of wearing a mask on work engagement and HR when each individual was considered in isolation. However, the effects varied a lot across individuals, and no one-size-fits-all pattern was found to conclude the effects. The personalized pattern of the effects indicated that people might have different feelings regarding wearing a mask during the pandemic. For example, some might feel safer with a mask and then be more engaged in the tasks, while others might be seriously affected by the worsening air quality in the breathing zone and thereby were not able to concentrate on the tasks they were performing. Moreover, some subjects might be more sensitive to wearing a mask than others. To support the current results, the

importance of personal characteristics was also confirmed in previous studies. For example, the individual differences in EEG responses to cognitive workload were confirmed by Matthews et al. [56]. The effects of thermal [23, 209] and lighting [57, 210] conditions on occupants' physiological and psychological data were also proven to vary across different individuals.

Regarding the MW and task performance, while the personal difference cannot be neglected, it was revealed that there existed general patterns to describe the effect of wearing a mask. Supported by brain waves and SCL, general patterns regarding the MW were found. Although there were slight differences between the results from brain waves and SCL, a general pattern revealed that wearing a mask could potentially reduce the MW of subjects. The possible reason behind this phenomenon might be that people felt more nervous and kept alert in the office during the pandemic period. In contrast, wearing a mask might make them feel safer and thus reduce the intensity of brain activities, thereby reducing their MW. The results showed that the number of correct responses to the cognitive tasks was in general higher without wearing a mask in most of the scenarios, and the type of mask also slightly affected the results. The number of correct responses to number addition and digit recall tasks might be related to the MW, as the higher MW was associated with more mental effort and thereby resulting in relatively higher outputs of the cognitive tasks. As for the correct rate, the results were consistent with the MW indicated by the brain waves, suggesting that a higher correct rate might be associated with a higher MW. To explore the potential reasons behind the individual differences, the results were compared as per gender, which suggested a significant difference between females and males regarding the FAI, HR, and the correct number of tasks. The results could provide a valuable reference for experimental design and data analysis of future studies.

It is worth noting that there are some limitations in this study. For example, to avoid fatigue, each task was set for 10 minutes. It will be interesting to investigate the effect of longer periods on the performance of the subjects especially fatigue will become another factor to measure. However, the results from this study can be used as departure points for future work where the duration of the experiment or difficulty of tasks is varied. In addition, the subjects in this study were all university graduate students, while a more diversified group of people can also be considered in the future. Moreover, the experimental environment might lead to additional tension among the subjects, and the differences in physiological responses in and out of the environmental environment could be future investigated in our future work.

4.6 Conclusions

This chapter investigates the effect of wearing a mask on physiological responses and the performance of individuals who work in office-like indoor environments. The work engagement, MW, SCL, HR, and task performance are measured and collected. Based on the results from brain waves and SCL (considered as an indicator of the MW), although the results vary across different individuals, wearing a mask can in general lower the MW of the subjects while they are performing cognitive tasks. Overall, the results of task performance (correct number and correct rate) are highly correlated to the measured MW, indicating that higher task performance is associated with a higher MW. However, in most of the scenarios, no significant difference is found between the cloth mask and the surgical mask. Similar to MW and task performance, the values of work engagement and HR are significant differences among different mask-wearing scenarios, the patterns vary across individuals. However, there is no one-size-fits-all pattern to conclude the effect of wearing a mask on work engagement and HR. For example, for some subjects, wearing a mask may reduce their work engagement while others may be more engaged with a mask.

One main contribution of this chapter is that the proposed method could be used to investigate the effect of wearing masks on occupants directly through physiological sensing. The results provide a deep understanding of how people's physiological responses and task performance may change if they are required to wear a mask as was the case during the pandemic period. The findings from this study could be valuable for those who need to wear a mask while working or policymakers looking to determine the optimal number of individuals required to work in person in the office on a daily basis.

Chapter 5 Measurement and Prediction of Work Engagement Under Different Indoor Lighting Conditions Using Physiological Sensing

5.1 Introduction

An inadequate indoor environment may cause health issues and thereby affect the creativity and productivity of the occupants and might lead to sickness and absenteeism [211]. In the current business environment, the employee is a key asset to the success of the organizations [25], and higher productivity of the employees is even worth extra cost [212, 213]. Work engagement commonly defined as the "positive, fulfilling, work-related state characterized by vigor, dedication, and absorption" [20] in the task being performed, is one of the most important factors that directly relate to employee performance [214] and has a significant positive effect on employee productivity [24, 26, 215, 216].

Work engagement is commonly estimated using indirect methods such as questionnaires and experiments [20, 153, 217-220]. For example, a 9-item questionnaire [217] is commonly used to collect feedback from people to evaluate their engagement. Also, experiments are designed to ask people to recall information after a period to assess their engagement during those moments [153, 220]. However, both of these approaches rely on extra feedback (i.e., questionnaires and experimental results) from human subjects to make the estimations, which are not the ground truth indicators measured from the brain. Moreover, they are not practical enough as they are not able to provide real-time measurements.

As indicated in related studies, positive feelings, engagement, and motivation are typically associated with a higher alpha power in the right frontal cortex when compared to alpha power

measured in the left frontal cortex [183, 185-187, 221]. The FAI, often measured as alpha power in the right relative to the alpha power in the left cortex, is used in this study as an indicator of work engagement [177-184]. Electroencephalogram (EEG) is used to measure the brain activities of the subjects, thereby calculating the engagement in a direct way by processing the related brain waves. In addition, previous studies have measured human brain waves under different lighting conditions. Several of them have shown that lighting levels could somehow affect brain activity [222-226], including the frontal region [227]. However, the correlation between the indoor lighting level and the occupants' ground truth engagement level has not been well studied. A better understanding of this correlation can help improve the occupants' indoor experience. Our research uses an EEG headset to measure the brain activity of the occupants while they are performing cognitive tasks under different indoor lighting levels. Based on the measured brain waves, the effect of indoor lighting level on calculated FAI is investigated.

Although our study uses EEG to establish this correlation, asking occupants to wear an EEG headset may not be practical in daily life. Any slight movements of the head may lead to a lot of noises on the EEG signal [164-166], rendering that the EEG device is not suitable to measure brain waves when the occupants always need to move their heads. Therefore, we also investigate approaches to predict the occupants' ground truth engagement from some easily measurable physiological indicators such as GSR, HR, and ST. Thus, the objectives of this chapter are: (1) To investigate the effect of the indoor lighting level on occupants' ground truth work engagement based on EEG data; (2) To investigate the possibility of predicting the engagement level using lighting level and easily measurable physiological data as predictors. The results of this study can help with the control of the indoor environments, thereby making the occupants feel more engaged

during their working time. Besides, the approach of predicting the occupant's engagement can be used as a practical tool to monitor the occupants' engagement in the future.

To achieve the objectives, an experiment that includes 12 subjects is performed in a controlled lab environment where the lighting level is the only changeable environmental parameter. The subjects are asked to perform three computer-based cognitive tasks (with the consistent backlight of the monitor) while their physiological data is being recorded. The FAIs of the subjects are calculated using the collected EEG data, and the corresponding relationship between engagement and lighting level is analyzed. In addition, Random Forest (RF) and Artificial Neural Network (ANN) are used to build personalized work engagement prediction models.

5.2 Related Work

Previous studies regarding the effect of lighting conditions on the performance of office workers have been comprehensively reviewed. In addition, related work regarding the assessment of work engagement was summarized, followed by a review of the evaluation of workers using physiological data. Based on the literature review, research gaps in previous studies were identified.

5.2.1 Investigation of lighting effect on the performance of office workers

As an important aspect of the indoor environment, the correlation between lighting conditions and occupants' satisfaction and productivity was investigated in many studies. Veitch et al. [228] confirmed a general conclusion that occupants witnessed improved reading performance when they believed the lighting level was being controlled, regardless of the lamp type. More detailed effects of the lighting were later investigated. For example, the effect of different lighting types was investigated by Knez and Hygge [229], who suggested that compared with warm-white, cool-white lighting would impair the long-term memory of the occupants. In

addition, an experiment conducted in a school suggested that full-spectrum fluorescent lamps with ultraviolet could improve the attendance and achievement of the students, while opposite results were found under the high-pressure sodium vapor lamps [230]. Hwang and Kim [231] applied questionnaires and self-report to investigate the effect of lighting on visual comfort and the eye health of the occupants. Glare, darkness, unqualified materials, and logical error of shade were found to be the cause of visual annoyance. Similarly, the visual response and mood of the occupants under different indoor lighting levels were studied by Lee et al. [232], where lower color temperatures were found not suitable for office space as they might cause sensations of glare and result in visual discomfort. Moreover, Knez and Kers [233] designed cognitive tasks to find the effect of indoor lighting, gender, and age on occupants' performance and mood. They found young people preferred warm white lighting, while the result was the opposite among older people.

Besides lighting types, the effect of lighting levels on human brain waves was also investigated in the literature. Smolder and De Kort [222, 223] compared the general theta band power of the brain wave under different lighting levels when the subjects were performing Psychomotor Vigilance Test and Necker Cube Pattern. The results indicated that higher illuminance helped improve the measured performance as well as subjective feelings of alertness and vitality. A similar experiment was conducted by Mangkuto et al. [234], but they used a jigsaw puzzle as the task. The results revealed that the average of beta waves in the primary visual cortex increased when the subjects were performing the task and an average illuminance of 1000 lux further increased the beta waves. To find the boundary illuminance for comfortable lighting conditions, Kakitsuba [225, 235] conducted an experiment to draw the correlation of brain waves with different lighting levels. The result showed there was a difference between light-emitting diode (LED) and fluorescent lamps. In addition, Min et al. [226] also studied the effect of different

lighting levels on the same cognitive task using EEG and found that a bright condition resulted in a longer reaction than a dark one with similar task performance. A more specific investigation of brain waves was conducted by Medithe and Nelakuditi [227], who measured the frontal region activity of the subjects during the experiment. An increment in the frontal region frequency was found when occupants performed mental activities and frontal brain activity was altered under low luminance conditions. Furthermore, Chang et al. [224] showed a correlation between the magnitude of the altering response and historical lighting exposure by comparing the EEG delta/theta activity. The results concluded that the illuminance history would affect the magnitude and duration of the alerting effect of light. The related studies regarding the lighting effect confirmed the importance of indoor lighting conditions for office workers. A proper lighting condition could positively affect their performance and indoor experience. Intrinsically, the brain activity of the occupants could be affected by the lighting conditions. However, none of these studies investigated the lighting effect on ground truth work engagement, which motivates this study.

5.2.2 Assessment of work engagement

Defined as the "positive, fulfilling, work-related state characterized by vigor, dedication, and absorption" [20], work engagement was assessed using questionnaires and experimental methods in previous studies. For example, Schaufeli et al. [217] developed a short questionnaire for the assessment of work engagement. The study constructed a database based on surveys of work engagement included in 27 studies across 10 different countries and developed a 9-item questionnaire (UWES-9). The factors considered in the developed questionnaire (UWES) included Vigor (VI), Dedication (DE), and Absorption (AB). The developed UWES questionnaire was examined and confirmed for use in both between-person and within-person comparisons [236].

Based on the initial idea of the work engagement scale, different questionnaires were used as the main approach for evaluating the work engagement of occupants in office buildings. McCunn and Gifford [237] applied questionnaires to evaluate the effect of green offices on employee engagement, and the results suggested that there was no positive effect of green design on employee engagement. In addition, Feige et al. [238] investigated the impact of sustainable buildings on work engagement using questionnaires and indicated that work engagement was correlated with the comfort levels of the occupants. However, to obtain the score to represent work engagement, people are required to fill up different questionnaires. Therefore, using questionnaires to obtain work engagement is time-consuming and may not be accurate enough as they are highly subjective.

Apart from questionnaires, work engagement was also assessed by designed experiments. Astolfi et al. [153] conducted an experiment to investigate the correlation between human brain waves and their engagement, in which the subjects were exposed to a documentary that contained clips related to international brands, and they were asked to recall the clips after 10 days. The engagement of the subjects was thus evaluated based on their performance. Similarly, to evaluate the efficacy of commercial advertisements, the engagement of the subjects was assessed based on their performance of recalling the commercial video clips in the experiment conducted by Vecchiato et al. [220]. Although the experimental methods for evaluating work engagement are objective, they are obviously not practical as extra experiments are required. To summarize, both questionnaires and experiments have their limitations in providing accurate and timely results, thus a more direct and reliable approach that can provide real-time ground truth work engagement is required.

5.2.3 Indoor occupant assessment using physiological data

Physiological data has been widely used to assess office workers and EEG was also applied to investigate the effect of the indoor thermal environment. For example, Choi et al. [145] studied the effect of indoor air temperature on occupants' attention represented by the average EEG power value, the results showed that the best attention was achieved when Predicted Mean Vote (PMV) values were slightly positive. Shan and Yang [239] tried three algorithms including linear discriminant analysis (LDA), Naïve Bayes (NB) classifier, and K-nearest neighbor (KNN) to classify the real-time thermal comfort states of occupants based on EEG data. The correlation between indoor thermal conditions and MW was also investigated. Wang et al. [23] applied EEG to obtain the ground truth of the MW in different thermal environments, they calculated the ratio of average frontal theta power and average parietal alpha power as an index of the MW. The MW values of the subjects were then collected while they were performing the designed cognitive tasks. As a result, higher values of MW were found in slightly warm environments for most of the subjects. Similarly, Kimura et al. [139] assigned working memory and learning tasks to the subjects and collected their brain waves using EEG headsets. The MW of the subjects under different room temperatures was calculated and compared. Although a slightly different index of the MW was used, the conclusion of this study was aligned with the one from Wang et al. [23].

Apart from brain waves, a variety of physiological parameters were also used in previous studies as indicators of human physiological responses. Zheng et al. [240] proposed an evaluation method for human physiological states based on five physiological parameters including HR, ST, rectal temperature, systolic pressure, and sweat rate. Also, EEG signal, SCL, HR, and tympanum temperature were measured and their values under different indoor temperatures were compared in the study conducted by Kimura et al. [139]. Similarly, Wu et al. [148] applied HR, ST, as well

as systolic and diastolic blood pressure to investigate the effect of long-term indoor thermal history. In addition, the effect of the wooden indoor environment was studied by Zhang et al. [241] based on blood pressure, electrocardiogram, electro-dermal activity, and ST. Moreover, Yeom et al. [193] used HR as the indicator to confirm the existence of significant physiological response differences in the indoor environment and immersive virtual environment. These previous studies confirmed the feasibility of using physiological parameters (e.g., EEG signal, GSR signal, HR, and ST) as the indicators of human physiological responses, which supports the fundamental idea of using related equipment in this study. However, none of the previous studies used appropriate physiological indicators to represent the ground truth work engagement of the occupants. Also, the correlation between GSR, HR, ST, and EEG signals was not well studied.

5.3 Research Methodology and Results

In this study, a comprehensive framework was developed to investigate the effect of lighting level on occupants' work engagement using EEG. In addition, a method for predicting this engagement using other physiological data was established, as shown in Fig. 5.1. The lighting level was used as the only environmental variable. Brain waves of the subjects were measured using an EEG to calculate the ground truth work engagement under three tasks: (1) number addition, (2) visual search, and (3) digit recall. FAI was then calculated as the indication of engagement based on the raw EEG data. The FAIs were divided into several levels with each level associated with an EV. At the same time, other physiological data of the subjects, including GSR signal, HR, and ST, were collected. After synchronizing the data collected from different sensors, machine learning (ML) techniques were used to explore if easily measurable physiological data and lighting levels could serve as predictors of occupants' EVs. More details of the methodology are described in the following sections.

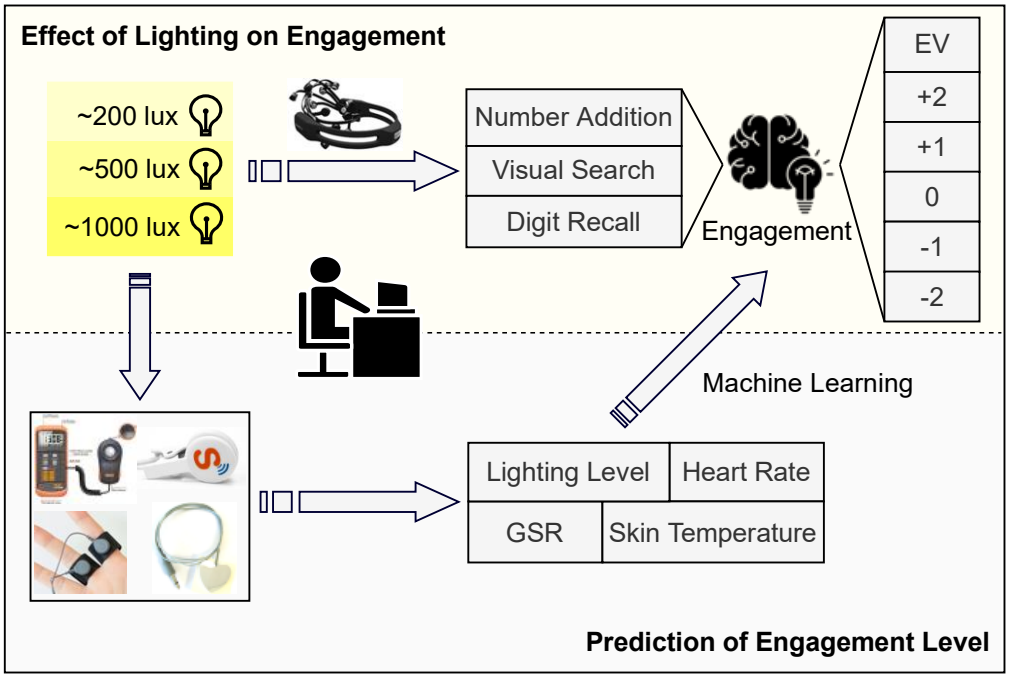

Fig. 5.1. Framework for measurement and prediction of work engagement under different lighting levels

5.3.1 Experimental design

Each subject participated in a three-day data collection experiment where EEG signal, GSR signal, HR, and ST data were collected while he/she was performing three different cognitive tasks under different lighting levels. The experiment was conducted in the Sustainable and Intelligent Civil Infrastructure Systems (SICIS) Laboratory at the University of Michigan. The lab was in the basement of the GG Brown building and did not have any windows, thus there was no access to natural ventilation and daylight in the lab. This allowed us to fully control the indoor environment with the existing air conditioning and lighting systems. Fig. 5.2 shows the setup of the experiment. The experiment was designed to reflect real-world scenarios. As in a real office environment, people normally use a computer with a constant backlight to conduct their daily work. At the same time, the lighting conditions of the environment are changeable through a light switch with a dimmer or other building automation system devices. The effect of the backlight from the monitor

on the workplace was measured using a lighting sensor. The results showed that without extra light sources, the illuminance produced by the backlight of the monitor was less than 200 lux at a very close point to the computer in the working area. Given the range of lighting illuminance levels tested in this chapter, the monitor backlight was assumed to have a limited effect on the performance of the occupants or the measurements of their engagement level when the surrounding environment lighting conditions were changed. In addition, the backlight of the computer monitor was maintained at the same level during all sessions of the experiment with the lighting level in the room designed to be the only changeable environmental parameter. Similar experiment designs could be found in previous studies [222, 223, 226] to support our method, which also applied computer monitors with consistent backlight to investigate the effect of indoor lighting conditions on subjects.

In this experiment, the lighting levels were controlled by the central lighting system with two auxiliary portable lamps as shown in Fig. 5.2, which allowed a flexible control of the lighting level. The consistency of lighting levels surrounding the subjects was ensured by a lighting sensor in the room. Illuminances of 200 lux, 500 lux, and 1000 lux, with a light color of 5000 K, were selected in our study, representing the suggested levels for performing basic work, normal office work, and normal drawing work, respectively [242]. The selection of lighting level in each session was randomized.

Apart from lighting levels, other environmental settings were also maintained the same during all sessions of the experiment. For example, the ambient room temperature was maintained at 24 ± 0.2 °C as recommended by ASHRAE [12]. During the experiment, a desktop was used by the subjects who were well-equipped with an EEG headset and other portable sensors. The subjects only need to focus on the computer screen and try to concentrate on the designed tasks. The

experiment protocol was reviewed and approved by the Institutional Review Board at the University of Michigan.

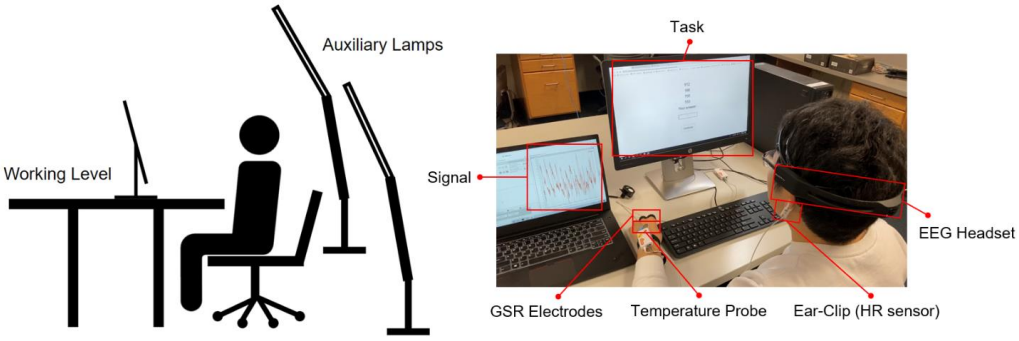

Fig. 5.2. Experimental Setup

5.3.1.1 Subjects

12 subjects who were identified as both physically and mentally healthy participated in the experiment from October to November 2020. All of them were graduate students at the University of Michigan between the age of 20 and 30. Each subject received a monetary reward upon completion of the experiment. To ensure the accuracy and reliability of the experiment data, the subjects were asked to follow these guidelines: (1) Ensure enough sleep at night and try to wake up at the same time during the three-day experiment; (2) take no foods or drinks that may cause excitement (e.g., coffee, alcohol, and tobacco) during the experiment period; (3) keep their hair dry and clean before showing up to the experiment; (4) wear the same or similar clothes and shoes throughout the experiment. In addition, the specific time slot for each subject was ensured to be the time without any class before. At the beginning of the experiment, each subject was assigned a unique ID as a reference for his/her data, without using any other personally identifiable information during the data collection and analysis process. All experiments followed COVID-19 public health recommendations to ensure the safety of the research staff and the subjects.

5.3.1.2 Experimental procedures and time setting

Details of the experimental procedures for each session are shown in Fig. 5.3. Before starting the experiment, each subject was given 30 min to settle down and relax, at the same time, a short introduction (less than 5 min) of the task rules was provided. In order to avoid the unexpected effect of fatigue, primary studies were conducted to investigate the reasonable time duration for cognitive tasks. It was found that the engagement level of the subjects was highly likely to decrease after performing the tasks for a long period, and thus 10 min was chosen to be the experiment time for each task. In addition, 10 min of rest time was given to the subjects, which allowed them to recover from the last task and start the new task with a fresh mind. The reliability of the experiment was also ensured by checking the consistency of results in the same subjects. A preliminary study repeated the experiment three times on two of the subjects. This revealed that the effect of lighting level on the same subjects for the same tasks was in general consistent.

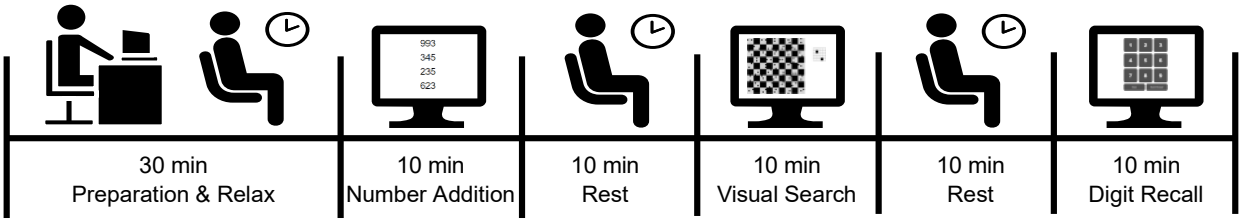

Fig. 5.3. Experimental procedures for each session

5.3.1.3 Design of cognitive tasks

The design of the cognitive tasks is identical to Section 4.3.1.2 as shown in Fig. 5.4

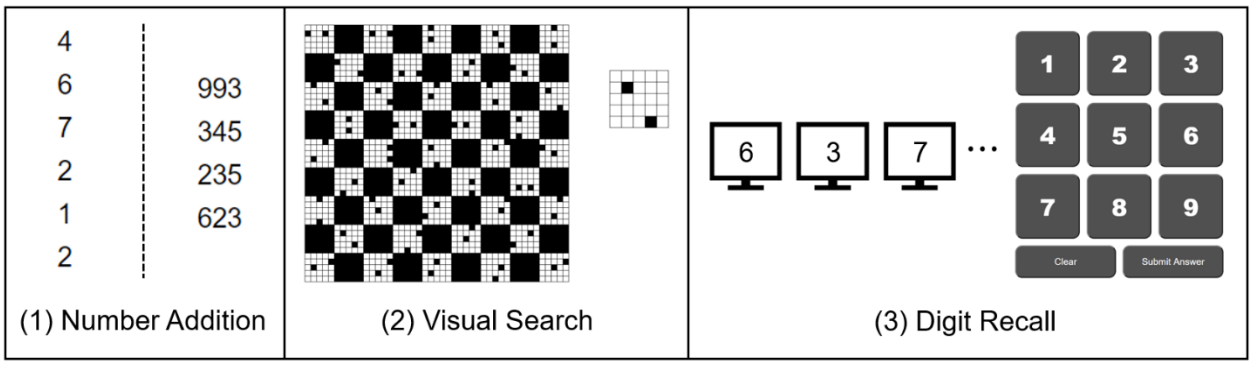

Fig. 5.4. The cognitive tasks

5.3.2 EEG data processing for engagement

5.3.2.1 Calculation of engagement level (FAI)

Previous studies have investigated and summarized the response of FAI (i.e., alpha power in the right relative to the left cortex) to different external situations. Harmon-Jones and Gable [185] conducted a comprehensive review of research that measured frontal asymmetry in response to manipulated situations related to motivation and emotion. They concluded that higher FAI was associated with higher approach motivation. A similar conclusion was also made by Davidson and Schaffer [186, 187] that higher FAI indicates positive feelings, motivation, and engagement. These responses were aligned with the definition of engagement [20]. Therefore, FAI is reasonably used as an indicator of the ground truth engagement of the human subjects in this study. The mathematical representation of FAI is shown in Eq. (5.1) [177, 178]. F3 and F4 indicate the signal from two specific electrodes in the headset and their positions are shown in Fig. 5.5.

$$FAI = ln\left(\frac{Alpha\ power\ of\ F4}{Alpha\ power\ of\ F3}\right) \tag{5.1}$$

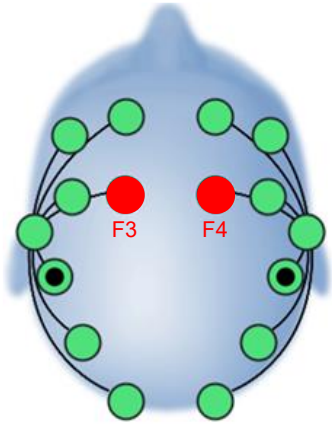

Fig. 5.5. Locations of F3 and F4 electrodes

5.3.2.2 Direct measurement of brain waves

In this study, the ground truth subjects' engagement level was directly measured using the EEG headset. EEG is a technique for monitoring brain activity by placing electrodes on the scalp surface [23, 170]. The activation of the neurons in the brain can induce voltage changes, and these voltage changes generate electric potential which can be detected by proper electrodes and thereby be recorded. Brain activities and subjects' cognitive states can be reflected by capturing the activities of the central nervous system using EEG [163]. Emotiv EPOC+, a low-cost EEG headset as shown in Fig. 5.2 was used in this study. It includes 14 channels and allows for quick setup without gels or pastes. The data sampling frequency of Emotiv EPOC+ was set to 128 Hz. Brain activity signals with reasonable quality can be captured and uploaded in real-time through Bluetooth to ordinary PCs, Macs, or smartphones [243].

5.3.2.3 EEG data processing

In total, 12 datasets were retained after the experiment. The datasets collected from different sensors were initially stored in separate files. On average, there were more than 75,000 rows for each file as the data sampling frequency was 128 Hz and all the raw datasets should be pre-processed. The data collected for the EEG was in form of floating-point values with

approximately 4200 μV of DC offset from each channel. Nevertheless, the raw data normally contains artifacts from various sources [164-166]. Therefore, a denoise process was required to remove the artifacts in the collected data. Denoise methods for EEG signals have been widely investigated in previous studies [170-174]. For example, Delorme and Makeig [171] developed a toolbox named EEGLAB to help with the process and denoise of EEG data, which contains built-in functions such as independent component analysis (ICA) and frequency analysis.

Fig. 5.6 summarizes the EEG data processing procedures used in previous studies. The DC offset should first be removed, followed by the denoise process. In general, the noises of EEG data contain both extrinsic artifacts and intrinsic artifacts. Extrinsic artifact removal can be conducted using the band-pass filter, which maintained the frequency of the data between 0.5 Hz and 65 Hz [167]. Eye blinking, vertical eye movement, and muscular movement were defined as intrinsic artifacts [168, 169] and require more effort to deal with. A common way to perform the removal of the intrinsic artifacts is to conduct an independent component analysis (ICA) and remove the artifact components. In this study, EEGLAB was used as the main tool for removing the artifacts of EEG data. All potential artifact components were identified and those with high possibilities of being noises were removed manually. With the clean data, Fast Fourier Transform (FFT) was applied to compute the band power within different frequency ranges. There are mainly five frequency bands including Delta (1−4 Hz), Theta (4−8 Hz), Alpha (8−12 Hz), Beta (12−25 Hz), and Gamma (>25 Hz) [23, 175, 176]. In addition, to conduct an ANOVA analysis for the dataset of each subject as well as perform machine learning (ML) for prediction models, the original 128 Hz raw data was pre-processed to obtain data points with a specific time window. According to the related studies, a reasonable time window range is between 2 and 8 seconds [182, 203]. In this study, the three most common time windows 2, 4, and 8 seconds were tested in a preliminary study,

and 8 seconds gave ML models the highest prediction accuracy. Therefore, the 8 seconds time window was selected. However, it is important to note that the length of the time window is a flexible parameter that can be changed based on the implementation.

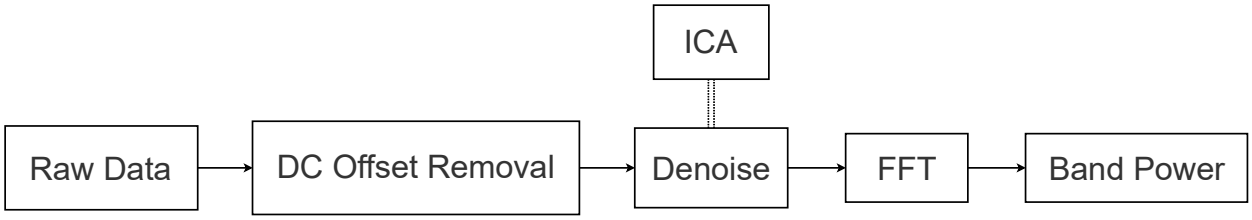

Fig. 5.6. EEG raw data processing procedures

5.3.2.4 The effect of lighting level on FAI

Based on the pre-defined time window, the FAIs of each task in each section were calculated. The mean and standard deviation of the FAIs under different lighting levels were calculated and compared. Repeated measure ANOVA was applied to conduct a statistical analysis of the results, a p-value of 0.05 was used as the threshold to determine whether there were significant differences between different categories. The differences between specific pairs of the datasets were further analyzed by the post hoc test. The results of FAIs for different tasks under three different lighting levels are listed in Table 5.1 to Table 5.3 and plotted in Fig. 5.7. Based on the range of results, the range of the plot was determined to be from -2 to 2 for FAIs, and the values beyond the range were considered to be an outlier, as shown in Eq. (5.2). Based on the analysis from ANOVA and post hoc test, the FAIs were found easily affected by the lighting level for most of the subjects. However, it was hard to conclude that there was a general pattern to suggest a better lighting level to fit all occupants. Also, the pattern among different lighting levels was slightly affected by the types of tasks. For example, subjects 5, 6, and 9 were more engaged with the environment of high illuminance (1000 lux), while subjects 3 and 7 were more engaged with relatively lower lighting levels (200 lux or 500 lux). Although the types of tasks might also

affect the results, personal patterns were still maintained in many cases. Subject 12 maintained a similar pattern of FAIs under different lighting levels among all types of cognitive tasks, which might indicate that his/her engagement was not sensitive to the types of tasks being performed. Similarly, subjects 1, 3, 5, 7, 8, 9, and 10 were found to have a similar pattern of results for at least two types of cognitive tasks. The inconsistent results might be caused by the different mental efforts that they need to exert for different tasks. In addition, for several subjects such as subjects 1, 2, and 11, no significant difference in the values of FAI was found under different lighting levels as their engagement levels were relatively stable regardless of the lighting levels. A possible reason for this phenomenon might be that they were not sensitive to the lighting level of the surrounding environment while performing the computer-based tasks. Overall, it could be seen from the results that the effect of lighting levels varies a lot on different individuals.

$$FAI_i = \begin{cases} FAI_i, & -2 \le FAI_i \le 2 \\ outlier, & otherwise \end{cases} \tag{5.2}$$

Table 5.1. Comparison of FAI of number addition task under different lighting levels

Subject	Statistic	200lux	500lux	1000lux	Difference ($p < 0.05$)
1	Mean	0.207	0.336	−0.153	200lux & 1000lux
	S.D.	0.450	0.331	0.262	500lux & 1000lux
2	Mean	−0.103	0.049	0.219	200lux & 1000lux
	S.D.	0.454	0.388	0.456	
3	Mean	0.093	0.585	−0.095	All pairs
	S.D.	0.361	0.341	0.527	
4	Mean	0.392	−0.532	−0.160	All pairs
	S.D.	0.367	0.409	0.377	
5	Mean	−0.106	0.081	−1.020	All pairs
	S.D.	0.360	0.145	0.231	
6	Mean	−1.880	0.150	0.341	All pairs
	S.D.	0.507	0.309	0.664	
7	Mean	0.409	0.419	−0.745	200lux & 1000lux
	S.D.	0.326	0.585	0.385	500lux & 1000lux
8	Mean	−1.065	−0.505	−1.555	All pairs
	S.D.	0.438	0.397	0.367	
9	Mean	0.220	0.242	0.535	200lux & 1000lux
	S.D.	0.325	0.433	0.413	500lux & 1000lux

10	Mean	−0.252	−0.075	0.383	All pairs
	S.D.	0.460	1.466	0.433	
11	Mean	0.108	0.591	0.135	200lux & 500lux
	S.D.	0.290	0.338	0.426	500lux & 1000lux
12	Mean	0.093	−0.662	−0.154	All pairs
	S.D.	0.442	0.332	0.441	

Table 5.2. Comparison of FAI of visual search task under different lighting levels

Subject	**Statistic**	**200lux**	**500lux**	**1000lux**	**Difference (p < 0.05)**
1	Mean	0.428	0.107	−0.032	200lux & 500lux
	S.D.	0.351	0.343	0.339	200lux & 1000lux
2	Mean	0.022	0.016	−0.034	N/A
	S.D.	0.313	0.431	0.330	
3	Mean	0.103	0.493	−3.914	All pairs
	S.D.	0.509	0.399	0.469	
4	Mean	−1.754	−0.352	−2.269	All pairs
	S.D.	0.368	0.281	0.485	
5	Mean	−0.371	−0.423	−0.009	200lux & 1000lux
	S.D.	0.445	0.300	0.318	500lux & 1000lux
6	Mean	0.126	2.759	0.227	200lux & 500lux
	S.D.	0.438	0.495	0.570	500lux & 1000lux
7	Mean	−0.578	0.815	0.244	All pairs
	S.D.	0.287	0.538	0.264	
8	Mean	−0.048	−0.222	−0.454	All pairs
	S.D.	0.495	0.284	0.297	
9	Mean	−1.658	−0.563	1.153	All pairs
	S.D.	0.217	0.470	0.782	
10	Mean	2.826	0.344	−0.112	All pairs
	S.D.	0.591	0.427	0.405	
11	Mean	0.294	0.390	0.368	N/A
	S.D.	0.402	0.400	0.277	
12	Mean	0.502	−0.506	−0.504	All pairs
	S.D.	0.367	0.343	0.664	

Table 5.3. Comparison of FAI of digit recall task under different lighting levels

Subject	Statistic	200lux	500lux	1000lux	Difference ($p < 0.05$)
1	Mean	0.066	0.004	0.076	N/A
	S.D.	0.389	0.239	0.288	
2	Mean	0.571	0.010	−0.321	All pairs
	S.D.	0.250	0.414	0.284	
3	Mean	0.217	−0.441	−0.068	All pairs
	S.D.	0.370	0.376	0.530	
4	Mean	−0.116	0.572	0.256	All pairs
	S.D.	0.366	0.377	0.456	
5	Mean	−0.210	−0.753	0.116	All pairs
	S.D.	0.363	0.345	0.285	
6	Mean	−0.366	0.761	−0.365	200lux & 500lux
	S.D.	0.457	0.492	0.457	500lux & 1000lux
7	Mean	−0.100	0.263	−0.711	All pairs
	S.D.	0.385	0.284	0.356	
8	Mean	0.218	0.117	0.298	500lux & 1000lux
	S.D.	0.426	0.445	0.415	
9	Mean	0.177	−0.171	0.881	All pairs
	S.D.	0.401	0.434	0.559	
10	Mean	−0.684	−0.170	2.160	All pairs
	S.D.	0.600	0.567	0.527	
11	Mean	0.168	0.114	0.235	500lux & 1000lux
	S.D.	0.329	0.290	0.348	
12	Mean	−0.172	−0.519	−0.238	200lux & 500lux
	S.D.	0.325	0.327	0.436	500lux & 1000lux

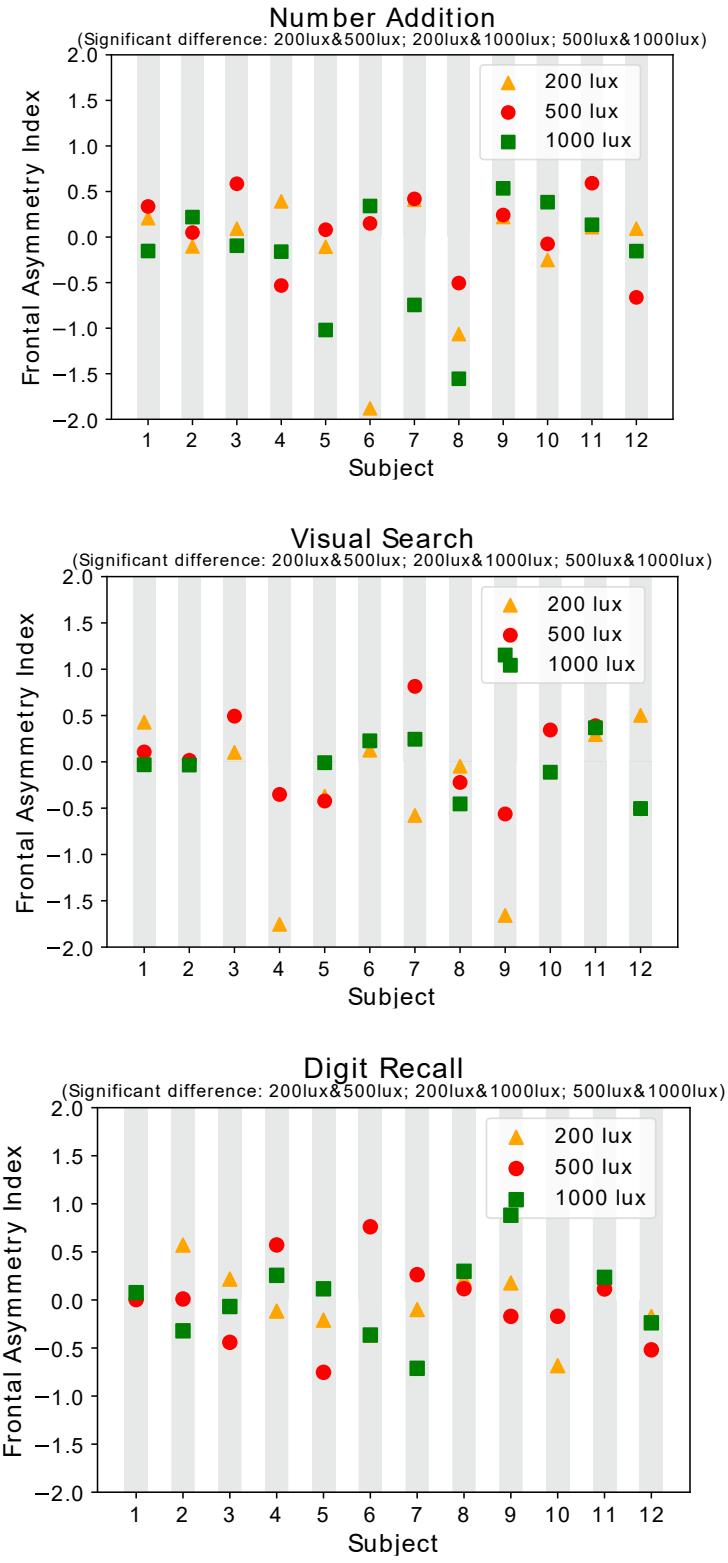

Fig. 5.7. FAI under different lighting levels

5.3.3 Prediction of EV using easily measurable physiological data and lighting level

Although the brain waves of people can be directly measured and processed to obtain the FAI as an indicator of work engagement, EEG headsets may not be practical enough in a real office environment. For example, wearing a headset may cause discomfort (e.g., headache) to the subjects while they are performing tasks. In addition, data collection from the EEG headsets requires the subjects to stay still to avoid intensive artifacts. Therefore, this study explores the feasibility of using other easily measurable physiological parameters (i.e., GSR, HR, and ST) to predict engagement levels. The details of this effort are described in the following sections.

5.3.3.1 Self-defined engagement vote (EV)

The raw values of FAI calculated using Eq. (5.1) are continuous numbers, which may not be straightforward for people to understand and cannot represent the relative engagement levels. A more systematic way to represent the engagement of the occupants can be very helpful. Appropriate representative discrete values can be used to indicate different engagement levels of people. Therefore, this study proposed a new indication system for work engagement. The general idea of the approach was to divide the FAI values into different levels, and each level should be represented by a discrete number (e.g., -1, 0, and 1) named "engagement vote" (EV). As the required resolution (number of engagement levels) of the indication system may vary with its application, different scales of the system can be developed. For example, when people only want to know the rough engagement level, a lower resolution should be applied, and vice versa. This study proposed 3-scale and 5-scale systems as examples. For a 3-scale case, the FAI values were divided into three levels as shown in Fig. 5.8 (a), the votes for the three levels were -1, 0, and 1, representing engagement levels of low, neutral, and high, respectively. For the 5-scale case, the FAI values were divided into five levels as shown in Fig. 5.8 (b), the votes for the five levels were

−2, −1, 0, 1, and 2, representing engagement levels of very low, low, neutral, high, and very high, respectively.

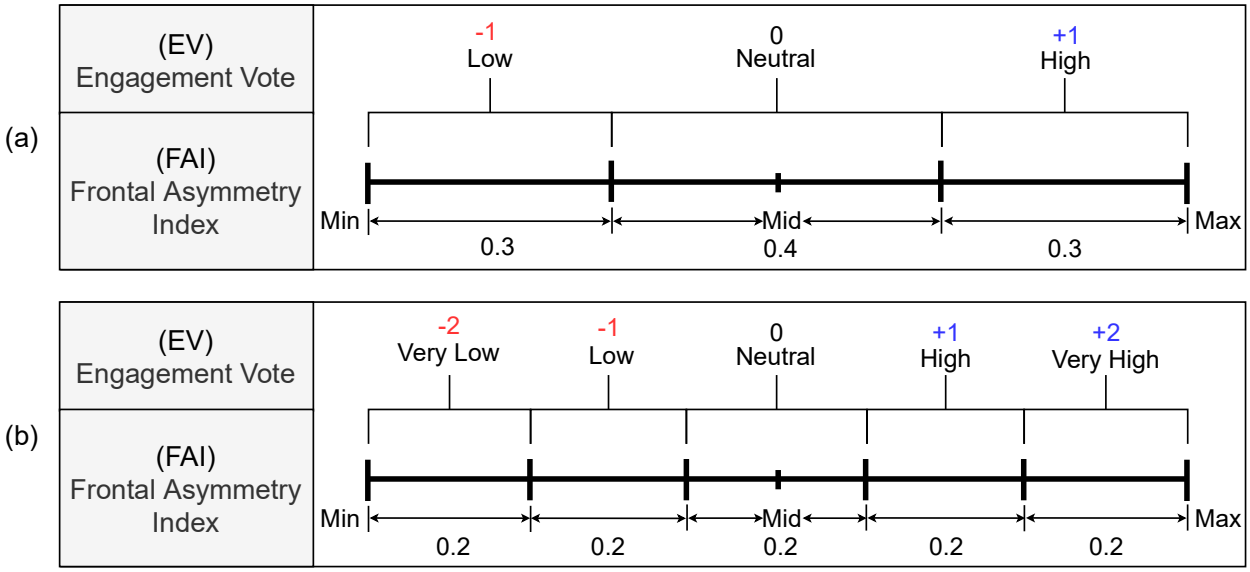

Fig. 5.8. Indication system of work engagement for (a) 3-scale and (b) 5-scale

5.3.3.2 Choice of physiological data

Previous studies have confirmed that changes in GSR signal can reflect the general changes in autonomic arousal [140], and manipulation of GSR may influence central neural activity [191, 192], which indicates that GSR is correlated to brain activity. The general components of the GSR signal are shown in Fig. 5.9. The slow changes in the GSR signal are reflected by the tonic component while the phasic component reveals stimulus-related changes. The tonic component is also called the SCL, and it is generally considered the background level of activity. A primary study for monitoring the GSR signals was also conducted in a nursing school, aimed to monitor the changes in GSR signals for the nurses when they were taking care of the patients. The results showed that the general tendency of the skin conductance was well represented by the tonic component and the phasic component was sensitive to external (e.g., hand movements) or psychological stimuli (sudden screaming coming from the patients), which were aligned with

previous studies [141, 195]. Therefore, to avoid the possible effects of any stimulus, the tonic component of the GSR signal was used to represent the skin state in this study.

The usage of GSR as an accessory to the EEG headset was confirmed previously [139], HR and ST have also been widely used in previous studies as factors to predict the physiological conditions of the occupants [36, 69, 198]. In this study, the hypothesis for HR is that it may affect the engagement of the occupants because it is correlated with emotional well-being [199, 201]. ST may significantly affect the thermal comfort of the occupants, and different comfort levels may lead to variations in human brain activity [23, 139]. Therefore, tonic components of the GSR signal, HR, and ST were measured and synchronized during the experiment, which was later used to predict the EV.

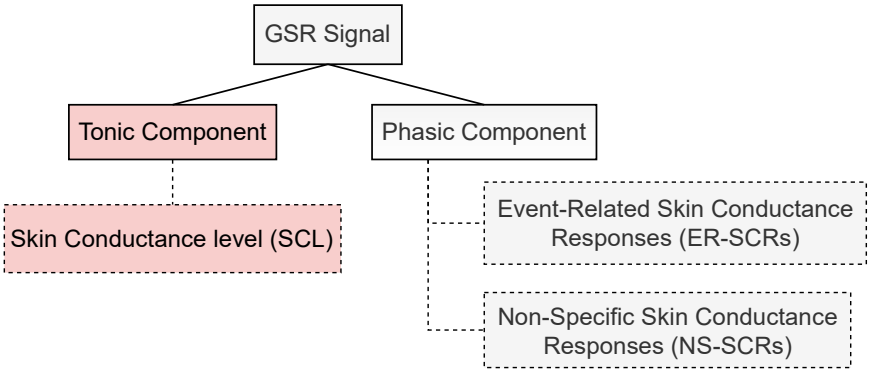

Fig. 5.9. Components of GSR signal

5.3.3.3 Collection of physiological data

As shown in Fig. 5.2, Shimmer3 GSR+ Unit was used to collect the GSR signals during the experiment. An optical Pulse Ear-Clip and a Skin Surface Temperature Probe were used to collect the HR and ST of the subjects, respectively. To ensure the quality of the collected data and minimize the possible data loss when collecting the GSR signal and ST, the electrodes were attached to the subjects as securely as possible to the unused hand of the subjects. The Pulse Ear-

Clip was attached to one of the ears of the subjects. As the subjects were told to keep their head still while wearing the EEG headset, the quality of the HR data was also ensured.

5.3.3.4 Prediction of EV using machine learning techniques

As highly correlated input features may affect the performance of the ML model, any duplicated correlated features should be removed before performing the training for classification [244, 245]. The input data can be checked by a correlation matrix constructed using principal component analysis (PCA) [246]. The formula to support the correlation matrix is shown in Eq. (5.3) [247], an example of the correlation matrix of the features from this study was computed as shown in Fig. 5.10, where LTG represents the lighting level. In this study, no significant correlations were found in the input features, thus all the measured physiological data (e.g., GSR signal, HR, and ST) and lighting level were included in the input dataset.

$$r_{jk} = \frac{\sum_{i=1}^{n}(X_{ij} - \bar{X}_j)(X_{ik} - \bar{X}_k)}{\sqrt{\sum_{i=1}^{n}(X_{ij} - \bar{X}_j)^2}\sqrt{\sum_{i=1}^{n}(X_{ij} - \bar{X}_k)^2}} \qquad (5.3)$$

Where $\bar{X}_j$ and $\bar{X}_k$ denote the sample mean of j and k-th variables.

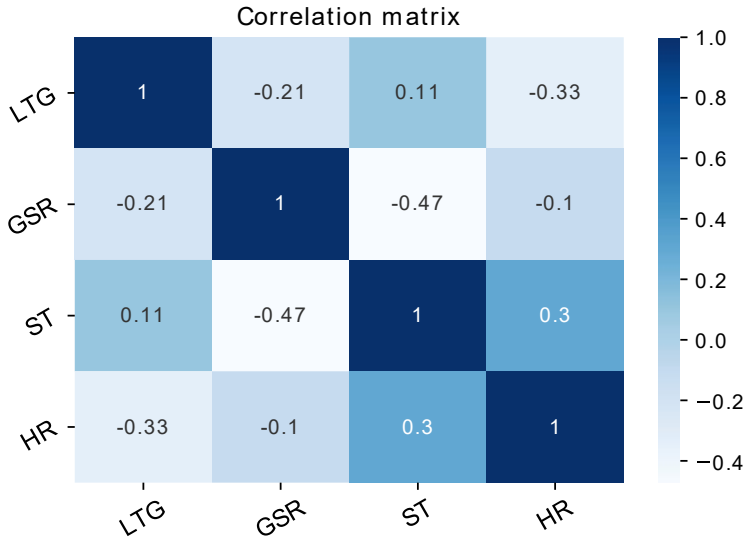

Fig. 5.10. Example of a correlation matrix (subject 10)

Fig. 5.11 shows the framework to conduct the ML analysis. Regarding the accuracy of the different traditional ML algorithms, RF was proven to have the highest accuracy in similar studies [5]. Therefore, RF was chosen to be the baseline ML algorithm for classification in this study. In addition, a basic ANN was chosen to be another ML algorithm for data training. The purpose of using an ANN was to compare its performance with traditional ML (i.e., RF) and see whether it could potentially improve the accuracy, as ANN was also proven successful in signal-processing problems [248]. In this study, the designed ANN contains three hidden layers, the first layer contains 4 neurons, while the second and third layers contain 8 neutrons. SoftMax Activation and Categorical Cross-Entropy Loss as shown in Eq. (5.4) were set for ANN.

$$L = \frac{1}{N}\sum_{i} -logP(Y = k|X = x_i) = \frac{1}{N}\sum_{i} -log\left(\frac{e^{s_i}}{\sum_j e^{s_j}}\right) \tag{5.4}$$

5.3.3.5 Data training process

After collecting the denoised data, the dataset was built for each potential occupant as shown in Fig. 5.11. With a total of 12 files from different lighting levels and tasks, the total duration of the dataset was around 120 min for each occupant. Based on the time window of 8 seconds, EV and its corresponding physiological data were paired. However, the first five epochs were dropped to avoid any possible errors caused by the calibration of the sensors. In addition, due to the occasional bad signals of the Ear-Clip, outliers of HRs were found in the raw data, thus an upper bound threshold of the HRs (i.e., 120 BPM) was set to filter out the potential errors in HR signals. Similarly, as the reading of the HR would be close to 0 when there was a bad connection, a lower bound threshold of 30 was set for the HR to avoid any data loss due to bad connections. The average HR that excluded the invalid timestamps was calculated to be the final training data, and if any of the invalid periods was longer than 8 seconds, the entire epoch was dropped. For the

training process, 70% of randomly selected data was used as the training dataset and the rest 30% of the data was used as the test dataset.

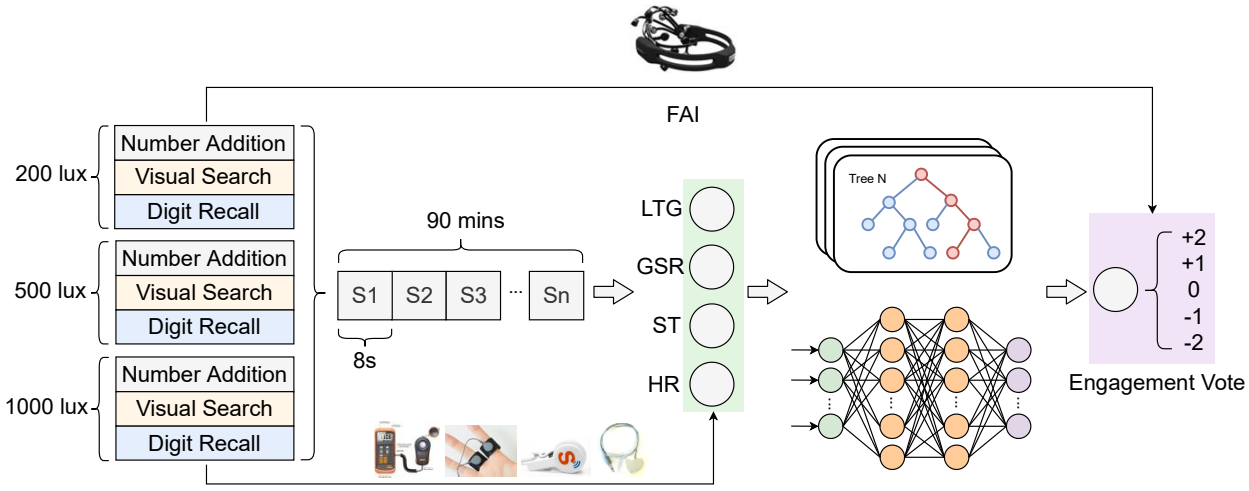

Fig. 5.11. Classification of EV using ML

5.3.3.6 The performance of EV classification

The overall accuracies of the classification and the confusion matrix for each class were obtained and compared. The overall accuracy was indicated by the fraction of the predictions our model got right. The confusion matrix was used to describe the performance of the ML models with respect to different classes. The accuracies of RF and ANN for each subject are listed and compared to give a more comprehensive understanding of the possible results as different algorithms might be suitable for specific characteristics of the datasets. In general, it was found that although ANN was able to give slightly higher accuracies for a few subjects, RF outperforms ANN in most of the cases. The purpose of this study was to investigate the possibility of predicting engagement levels using easily measurable physiological data and environmental parameters (i.e., lighting level in this study). Therefore, in the following comparison, we mainly focus on the final accuracies because it is reasonable to always choose a model with higher accuracy.

Table 4 shows the overall accuracies of the classification for both the 3-scale and 5-scale cases. The average classification accuracy for the 3-scale case was around 83.3%. For all of the subjects, the overall classification accuracy could reach up to more than 70%, and 4 of which were higher than 90%. Among all the subjects, the highest classification accuracy of a specific subject could reach 97.5% (Subject 6) using RF, while the lowest one could still achieve an accuracy of 72.3% (Subject 5). For the 5-scale case, the classification accuracy was 62.2% on average. The final accuracies for more than half of the subjects were higher than 60%, and 2 of them were higher than 70%. The highest classification accuracy was found in Subject 6, which reached 74.1%, while the lowest accuracy among all the subjects was found in Subject 12, which was only 48.3%. The final classification accuracies vary across subjects, possible reasons could be individual differences or errors during the data collection and analysis.

Table 5.4. Overall classification accuracies

Subject	**3-scale EV**			**5-scale EV**		
	RF (%)	**ANN (%)**	**Final (%)**	**RF (%)**	**ANN (%)**	**Final (%)**
1	91.3	91.8	91.8	56.3	63.4	63.4
2	85.9	87.0	87.0	57.8	51.0	57.8
3	90.8	81.6	90.8	70.6	54.0	70.6
4	77.2	71.4	77.2	69.8	50.8	69.8
5	72.3	71.3	72.3	57.9	47.2	57.9
6	97.5	81.7	97.5	74.1	61.9	74.1
7	79.3	63.6	79.3	57.1	52.2	57.1
8	74.1	73.0	74.1	51.3	48.1	51.3
9	84.1	79.1	84.1	67.0	51.1	67.0
10	72.9	61.3	72.9	64.1	57.5	64.1
11	93.3	93.8	93.8	55.9	65.1	65.1
12	78.3	77.8	78.3	46.1	48.3	48.3
Avg.	83.1	77.8	**83.3**	60.7	54.2	**62.2**

Table 5.5 and Table 5.6 show the average normalized confusion matrix [249] of the subjects to describe the performance of classification for 3-scale and 5-scale cases, respectively. Each row of the matrix represents the chance to give the predicted instances, while the left column represents the actual instances. Taking the first row of Table 5.6 as an example, the actual instance

was −2, the chance for the ML model to predict it as −2 was 62%, while the chances for it to give the prediction as −1, 0, 1, and 2 were 31.5%, 5.6%, 0.9%, and 0%, respectively. Similar to the first row of Table 5.6, the results described in all rows of both Table 5.5 and Table 5.6 gave a similar pattern that the highest possibilities were always associated with the actual instance. The closer the predicted EV is to the actual one, the higher possibility it would be predicted. For example, when the actual EV of the subject was 0 in Table 5.6, there would be up to a 68.4% chance for the ML model to give a correct prediction. For other possible predicted results, it was most likely the model would predict it as −1 (17.3 %) or 1 (13.2 %). In contrast, there was almost no chance for the model to predict the EV as −2 (0.8%) or 2 (0.3%). Therefore, the confusion matrix further confirmed the feasibility of the ML model.

Table 5.5. Normalized confusion matrix for 3-scale classification

EV	−1	0	1
−1	60.0	39.0	1.0
0	4.2	91.6	4.2
1	1.2	30.0	68.8

Table 5.6. Normalized confusion matrix for 5-scale classification

EV	−2	−1	0	1	2
−2	62.0	31.5	5.6	0.9	0.0
−1	7.0	57.0	32.8	3.2	0.0
0	0.8	17.3	68.4	13.2	0.3
1	0.8	4.4	28.5	59.3	7.0
2	0.0	1.3	8.3	38.8	51.6

5.4 Discussion

5.4.1 Insights from the pattern of engagement under different lighting levels

The results shown in Table 5.1 to Table 5.3 indicated that subjects' engagement might be affected by the lighting level when performing different tasks. However, as seen in Fig 7, no one-size-fits-all pattern on the effect of lighting level on engagement could be applied. One possible

explanation for the results might be the distinct personal sensitivities of lighting levels and different lighting preferences. Also, it was found that the lighting level had a less obvious effect on the engagement of some subjects, which indicates that environmental lighting level may not be a key factor in their engagement while they were performing computer-based tasks. In contrast, although the types of tasks also affect the results, for most of the subjects, the correlation between lighting condition and their engagement level remained the same for at least two types of tasks. The results revealed that the effect of indoor lighting level on occupants' engagement should be discussed individually. Therefore, the results emphasized that rather than following a general design standard, personalized models were more crucial and should be investigated. The rationality of the findings could be supported by previous studies [23, 56] that indicated the responses of the human brain activities to environmental changes varies across different individuals. In addition, the results aligned with conclusions from the studies regarding the personal preferences of indoor lighting conditions of different individuals [210, 250, 251]. For example, Despenic et al. [250] collected the lighting preference and control behavior of office workers, and the results showed that the lighting preference varied across different individuals. Furthermore, Newsham et al. [252] found that personal lighting conditions offered significant improvement in mood, environmental satisfaction, satisfaction with performance, and self-assessed productivity.

5.4.2 Classification of engagement levels using easily measurable physiological data and lighting level

Because the results regarding the effects of lighting conditions vary from person to person, it was reasonable to train a personalized prediction model for each subject. Based on the results in section 5.3.3.6, although the final accuracies vary from person to person, acceptable results were achieved using GSR signal, HR, ST, and lighting level to estimate the rough engagement levels of

any subjects. The results revealed that different physiological data from humans might be correlated with those from the brain, and the effect of lighting levels on engagement in the former part of this study also played a role in the prediction model. Two scales of the indication system for FAI were investigated, which could provide different resolutions of the prediction models. A higher resolution sacrifices a noticeable amount of prediction accuracy. On average, the prediction accuracy for a 3-scale case was more than 20% higher than a 5-scale one. In general, combined with the results analyzed from the confusion matrix, the ML models were considered feasible enough. Therefore, it can be concluded that it is possible to conduct a rough estimation of occupants' engagement levels using easily measurable physiological data and certain types of environmental parameters. Since the EEG headset may not be practical in some real-life scenarios, this study opens the possibility of using more practical physiological sensors to estimate human brain activities.

5.4.3 Limitations and future work

One of the main limitations of this study is that due to the complexity and sensitivity of brain waves, it is hard to eliminate all the possible factors that may induce errors. For example, human brain activities may be affected by their lifestyles and working environment. Therefore, we asked the subjects to maintain a regular schedule of working and sleeping during the experiment periods, and the place and time slots for the experiment were fixed for the subjects during all sessions. However, there may still be some uncontrollable factors that can affect the results, such as the moods of the subjects. In addition, using a computer to perform office work is the most common scenario in the real world. Our study aimed to maintain the same environment, and the cognitive tasks were designed to be computer-based. Since the backlight of the monitor may affect subjects' perception of the lighting levels, the findings from the current experiment might not be

guaranteed under the scenario when no computer is used. Furthermore, the objective of this chapter is to establish the approach for the measurement of work engagement using physiological data and investigate how the indoor lighting level may affect the work engagement of different individuals. The results can help with the design of the indoor lighting system to improve the overall productivity of the occupants. In our future research, we may consider conducting more repeated experiments on the same subjects to obtain more insights regarding inner subject patterns.

5.5 Conclusions

This chapter presents a novel method to investigate the effect of lighting level on occupants' ground truth work engagement using EEG. The subjects' brain waves are measured using a low-cost, wireless EEG headset while they are performing cognitive tasks under three typical lighting levels. The FAI is then calculated as an initial indicator of work engagement. In the meanwhile, Shimmer GSR+ Unit, Optical Pulse Ear-Clip, and Skin Surface Temperature Probe are applied to record the GSR, HR, and ST of the subjects, respectively. The FAIs of the subjects under different scenarios are compared and analyzed. The results indicate that the effect of lighting level on work engagement varies across different subjects. However, for most of the subjects, the correlations between the lighting level and their engagement level follow similar patterns for at least some cognitive tasks. The results highlight the importance of obtaining personalized models for occupants' engagement rather than following a general design standard. Therefore, this chapter also investigates the possibility of using easily measurable physiological parameters (i.e., GSR signal, HR, and ST) and lighting level as predictors of engagement level. To perform the classification of the engagement level, a new indication system for subjects' engagement is proposed, which assigns continuous FAIs to discrete numbers (EVs). The two most typical ML algorithms (i.e., RF and ANN) are used and compared. Also, in order to adapt to different demands,

two scales of the indication system for FAI are tested. The results reveal that RF outperforms ANN in most of the cases, and the final classification accuracies are 83.3% for the 3-scale case and 62.2% for the 5-scale case on average.

The main contributions from this chapter include: First, the proposed method can be used to study the work engagement of occupants in a direct way instead of estimating from questionnaires or experiments. Second, the effect of lighting level on work engagement is analyzed and discussed. Third, this chapter has proposed a new indication system for the FAI to indicate the engagement level of people. Based on the indication system, ML models with acceptable performances are built to estimate work engagement using easily measurable physiological data and lighting levels. The results thus open a new possibility of using more portable and practical devices to estimate human brain activities.

Chapter 6 A Case Study of DID-Based Framework by Integrating the Prediction Models for Thermal Comfort and Work Engagement

6.1 Introduction

To provide a better understanding of the proposed methods, a case study is used to showcase the capabilities of the DID framework. A schematic diagram of the case study is shown in Fig. 6.1. The thermal comfort metric (i.e., Thermal sensation) is selected as the example of human comfort as it is ranked as one of the most important factors that affect the occupants' satisfaction in buildings [253, 254]. Based on the thermal comfort prediction models, the recommendation system is used to pick suitable rooms for the subjects. After the occupants are assigned to the rooms, the real-time physiological data is used to make a dynamic estimation of thermal sensation thus providing further recommendations regarding the settings of the indoor thermal conditions. In order to demonstrate the scalability of this framework, another example where it is applied can be to determine the lighting level that helps support occupants' work engagement. In this case, recommendations regarding indoor lighting levels can also be given. More details are described in the following sections.

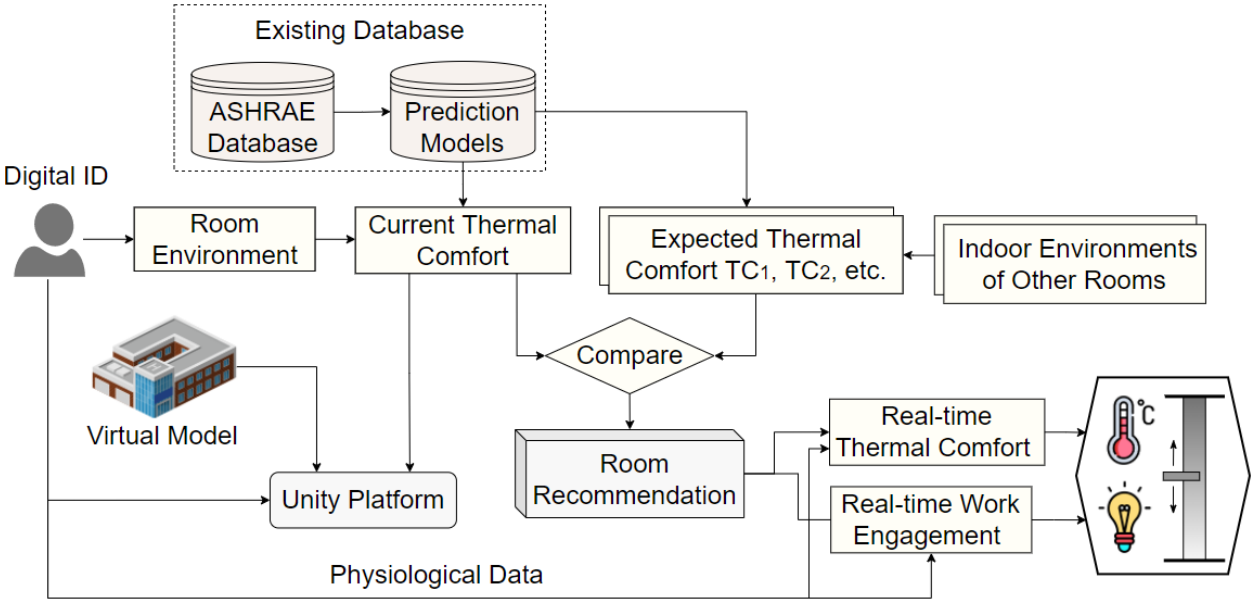

Fig. 6.1. The framework of the case study

Three rooms (Fig. 6.2) in the GG Brown Building at the University of Michigan are used as the scenes to demonstrate the proposed system, all the rooms are student labs. Fig. 6.3 shows the floor layout of the basement of GGB, and the locations of these rooms are highlighted. The areas of rooms 1006, 1140, and 1105 are around 40, 30, and 75 square meters, respectively. These rooms do not have any windows, thus there is no natural ventilation, and the indoor environments are fully controlled by the central heating, ventilation, and air conditioning (HVAC) system through thermostats, which allows the occupants to directly control the indoor temperature. Corresponding environment sensors (i.e., COZIR) are selected and installed in the three rooms to obtain real-time temperature and humidity data.

Fig. 6.2. Example rooms (1006, 1140, and 1105)

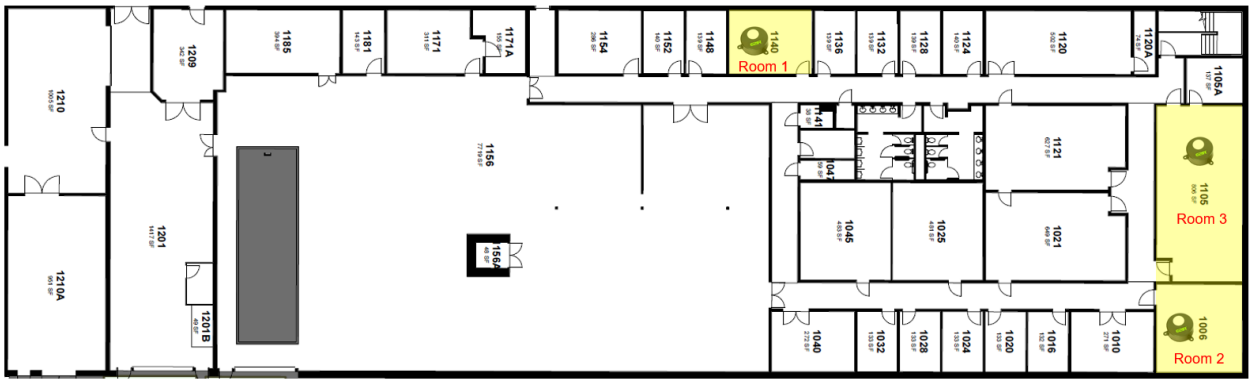

Fig. 6.3. The layout of the GGB basement

6.2 Digital ID of the Subjects

6.2.1 Existing database for new occupants

For new occupants (group #2) without existing personal thermal comfort models, general prediction models are required. ASHRAE Global Thermal Comfort Database II is a public thermal comfort database that contains 107,583 datasets, and it allows end-users to only export the data

with specific parameters through a web-based tool [15]. Because it is open source and contains a large number of datasets, it is used as an example public database to establish the general thermal comfort models for new occupants. The datasets are carefully selected with meaningful static parameters by referring to the previous studies [69, 106]. According to the previous study [103], thermal sensation is a subjective thermal metric that is most widely used. Therefore, although thermal sensation might not always equal thermal comfort [255], it is used as an example to illustrate the prediction models. However, it is worth noting that although the thermal sensation is used as an illustrative example, the method is fully scalable and can be applied to other thermal comfort metrics (e.g., thermal satisfaction and thermal preference). In the real world, the system might not use only one single thermal metric but incorporate different thermal comfort metrics into the building systems. In order to obtain as many data points as possible, rather than using the web tool, the original full database is downloaded and manually filtered. The retained datasets include thermal sensation, age, gender, occupant height, occupant weight, cloth insulation, air temperature, relative humidity, and air velocity, and remove all the datasets that miss any of these parameters. In addition, as the office or educational buildings are the main focus, the datasets for residential buildings are excluded. The details of the final datasets are summarized in Table 6.1.

Table 6.1. Details of the filtered dataset

Count	8574
Age range	18 ~ 68
Gender	Male/Female
Height (cm)	120 ~ 203
Weight (kg)	34 ~ 130
Clothing Level (Clo)	0.08 ~ 2.14
Air Temperature (°C)	13.4 ~ 40.5
Relative Humidity (%)	15.2 ~ 88.8

Regarding the machine learning algorithms for the demonstration, Random Forest (RF) is proven to have the highest accuracy in relevant studies [5], thus it is chosen to test the training

strategy in this section. Fig. 6.4 shows the machine learning process of the demonstration. Based on the previous study [69], human profile data including gender, age, height weight, clothing level, room temperature, and relative humidity are taken as the input features of the model. In addition, since the cooling/heating strategy (categorized by air-conditioned, mixed-mode, and naturally ventilated) can also affect thermal sensation [256], it is also included as one of the input features. The thermal sensation ranges from −3 to 3 [12] are encoded as the outputs.

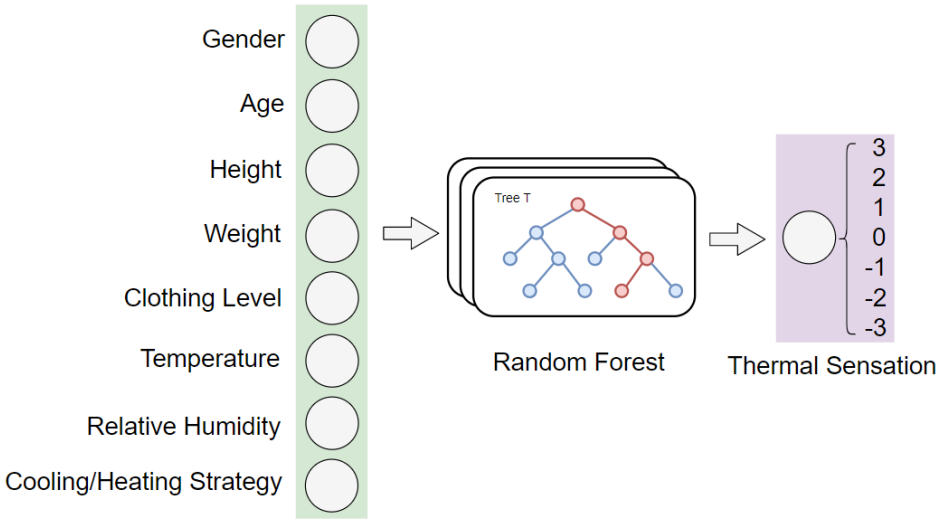

Fig. 6.4. Machine learning for thermal sensation

To show the accuracies of the prediction models, the proposed hypothesis proposed is validated. Therefore, a systematic comparison of different data training strategies is developed as shown in Fig. 6.5. Category C refers to any categories of human profiles based on their age, gender, height, and weight. n samples (30%) from category C are randomly selected as the test set. In this case, for a dataset that contains N data points in total, the training set in case 1 is the whole dataset minus the selected test set (N−n), while case 2 used the rest of the dataset (m) in category C as the training set. Case 3, on the other hand, used the same amount (m) of randomly sampled data from case 1 as the training data. In this case, three cases used different training sets to establish prediction models while the test set is the same, which provided a fair comparison strategy.

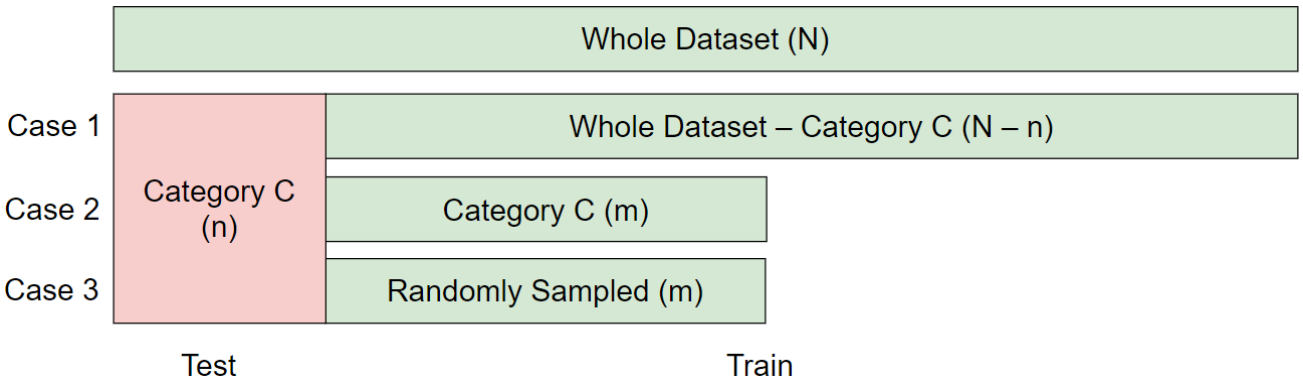

Fig. 6.5. Different data training strategies

Based on the comparison strategies, 6 example categories of human profiles are selected and the detail for each category is shown in Table 6.2. To ensure the reliability of the prediction models, the categories with less than 100 data points are excluded. Referring to Fig. 6.5, for category 1, n is 93 (30% of 310) and m is 217 (70% of 310). The hyper-parameters of the random forest are set as follows: the number of estimators is set to be 100, the maximum tree depth is set to expand until all leaves are pure or until all leaves contain less than the minimum number of samples required to split an internal node (i.e., 2). The minimum number of samples required to be at a left node is set to be 4 and the number of features for the best split is set to be "auto". The results are computed 100 times with a randomly selected test set each time. The accuracy is indicated by the fraction of the predictions our model gets right. The results of the training and test accuracies for the three cases are summarized in Table 6.2. The training accuracies indicate that there is no significant overfitting in the prediction models. In addition, the corresponding confusion matrices for the three cases are shown in Table 6.3, which further support the feasibility of the prediction models. Although more data points are associated with thermal sensations of -1, 0, and 1, the prediction accuracies for other values are also reasonable. In addition, even when the models fail to give the correct prediction, the predicted values are still close to the actual ones. Take the

thermal sensation of 0 as an example, even if the predicted values are not 0, they will most likely be predicted as −1 or 1.

Table 6.2. Results of the comparison of the data training strategies

Category	Age	Gender	Height (cm)	Weight (kg)	Count	Case 1		Case 2		Case 3	
						Train	Test	Train	Test	Train	Test
1	20~30	Male	160~170	50~70	310	0.814	0.615	0.809	0.555	0.790	0.433
2	20~30	Male	170~180	60~80	665	0.813	0.594	0.793	0.593	0.792	0.433
3	30~40	Male	170~180	60~80	285	0.814	0.610	0.770	0.574	0.770	0.489
4	20~30	Female	150~160	40~60	705	0.813	0.669	0.808	0.671	0.785	0.463
5	20~30	Female	160~170	50~70	1146	0.813	0.687	0.807	0.690	0.783	0.496
6	30~40	Female	160~170	50~70	292	0.813	0.693	0.804	0.683	0.769	0.545
Average						0.813	**0.645**	0.799	**0.627**	0.782	**0.477**

Table 6.3. Confusion matrices for the three cases

Case 1		Predicted						
		−3	−2	−1	0	1	2	3
	−3	0.19	0.19	0.00	0.00	0.00	0.00	0.00
	−2	0.10	2.03	1.83	0.77	0.48	0.00	0.00
	−1	0.00	0.77	16.59	5.40	3.18	0.00	0.00
Actual	0	0.00	0.00	4.24	22.76	2.80	0.19	0.00
	1	0.00	0.00	3.47	4.53	16.68	1.25	0.00
	2	0.00	0.00	0.39	0.48	2.03	6.46	0.68
	3	0.00	0.00	0.00	0.00	0.68	0.87	0.96
Case 2		Predicted						
		−3	−2	−1	0	1	2	3
	−3	0.30	0.30	0.10	0.00	0.00	0.00	0.00
	−2	0.10	2.08	1.69	0.89	0.79	0.00	0.00
	−1	0.00	0.79	15.97	6.15	3.77	0.10	0.00
Actual	0	0.00	0.10	4.27	22.22	3.97	0.30	0.00
	1	0.00	0.00	3.97	4.17	12.10	2.58	0.20
	2	0.00	0.00	0.69	0.69	3.08	5.65	0.40
	3	0.00	0.00	0.10	0.00	0.79	0.79	0.89
Case 3		Predicted						
		−3	−2	−1	0	1	2	3
	−3	0.22	0.11	0.11	0.11	0.00	0.00	0.00
	−2	0.00	2.21	1.65	1.21	0.44	0.00	0.00
	−1	0.00	0.44	14.77	7.28	4.85	0.33	0.00
Actual	0	0.00	0.00	5.73	18.08	4.41	0.55	0.00
	1	0.00	0.00	5.40	5.62	11.47	2.32	0.11
	2	0.00	0.00	0.55	1.32	4.52	3.20	0.33
	3	0.00	0.00	0.00	0.00	0.55	0.88	1.21

Regarding the data collection and training strategy in the initial guess for the new occupants, it can be observed that case 1 and case 2 achieve almost identical prediction accuracies without significant difference ($p > 0.05$), with the fact that case 1 has more than 10 times larger datasets compared with case 2. On the other hand, the prediction accuracies from case 3 are significantly lower compared to case 1 and case 2 ($p<0.05$), with more than 0.15 lower average accuracy. The reason is that the dataset in case 3 covers all categories of the human profiles but only has the same sizes of datasets as case 2. The results can provide valuable insights regarding the establishment of the database as well as the data training plan. At the initial stage of establishing the DID database, it is suggested that the collection of the training dataset should be maintained within a category of occupants that fits the usage of the buildings. In this way, higher prediction accuracies can be achieved with a much smaller dataset, referring to the accuracy comparison between case 2 and case 3. In addition, if there already exists a large dataset across all the categories of human profiles, the prediction models can be trained using either the whole dataset or the dataset within target categories, as they can provide similar performance, referring to the comparison between case 1 and case 2. Furthermore, assuming the database will be updated with more data samples within specific categories, the performance of using the categorized dataset to train the model may outperform the whole dataset, as their dataset size will get closer, referring to the tendency of prediction accuracy from case 1 to case 3 compared to case 2. It can be seen that once the sizes of the dataset are similar, the prediction model obtained by the categorized dataset can have much higher accuracy.

The results prove that the hypothesis is correct, and the selected public database (ASHRAE Global Thermal Comfort Database II) can help with the establishment of prediction models with

acceptable accuracies. Therefore, the baseline prediction models obtained here are used for the initial guess of the new occupants (group #2) in this case study.

6.2.2 Personal database for existing occupants

For the occupants with an existing prediction model (group #1), personal thermal sensation models are used. In addition to the database for the room recommendation, the example database for real-time monitoring of the occupants' states is also included. Fig.6.6 shows an example dataset, the left one shows the personal thermal sensation based on the indoor temperature and humidity, and the middle one shows the thermal sensation based on physiological responses (e.g., SCL, HR, and ST) of the subject, the right one is for the prediction of work engagement based on indoor lighting level and physiological responses of the subject. The prediction models for work engagement can be used to make recommendations for lighting levels. Note that the human static parameters (e.g., age, gender, height, and weight) are not needed for the personal thermal sensation models as the data for each model come from one single occupant.

For the thermal sensation database used in the room recommendation, the data are collected from the experiments in our previous studies [36, 57, 67]. People are asked to report their thermal sensation (from -3 to 3) under different indoor environments, and the random forest (RF) algorithm is used to establish a thermal sensation prediction model based on the indoor environment (e.g., temperature and relativity humidity). Therefore, given the indoor temperature and relative humidity, the models can estimate the thermal sensation of occupants. On average, the prediction accuracy of the models from our example datasets is 79.4% using RF.

Room Temp	Humidity	TC_EV
20	36.6	-1
17.9	55.3	-3
15.3	53.2	-3
29.4	46.8	3
15	32.1	-3
28.3	29.9	2
16.8	39.7	-3
16.5	56.6	-3
32	46.8	3
29.6	35	3
29.2	33.4	2
28.2	31.3	1
29.5	46.8	2
23.8	53.2	0
13.5	47.2	-3
31.2	55.3	3
18.1	30	-3
29.3	47.2	2
21.2	55.2	-1
22	42.6	-1
20.8	49	-1
25.6	42.6	0
17.9	47.2	-2
28.5	37.2	2
25.9	42.5	1
22.1	47.4	-1
28.8	22.3	2
27.5	43.2	1

Skin Conductance	Heart Rate	Skin Temp	TC_PHY
0.292460317	56.4577098	29.2505313	-2
0.449192821	53.4132757	29.4353257	-2
0.432888986	55.3580443	33.041612	0
0.389399142	55.4267165	34.0122227	1
0.257795677	59.3632791	29.0832424	-2
0.250172397	61.9034627	29.1450057	-2
0.350139444	56.1964813	34.1332221	1
0.456654803	58.9315602	29.1662701	-2
0.391406163	54.3063236	32.7634419	0
0.284680597	55.8233849	28.932524	-2
0.271645715	56.7525828	29.135024	-2
0.257598651	59.6234844	29.1364742	-2
0.391336788	55.4191704	33.8932475	1
0.433809246	55.0436309	29.4747531	-2
0.399149808	55.9636932	33.8699053	1
0.454631479	57.1741638	29.223824	-2
0.252355284	56.9778185	29.1001834	-2
0.419220363	56.562519	33.7037563	1
0.442370477	55.539859	33.0759168	0
0.361974137	57.3676851	32.9766013	0
0.430650599	58.5996499	33.6459379	1
0.362414322	55.9472857	33.9999314	1
0.406461941	58.8667689	33.0612919	0
0.326695874	56.0108938	29.4569293	-2
0.360345904	57.5870749	33.7234833	2
0.420017136	54.7853457	33.041797	0
0.245263764	56.4494764	29.1716108	-2
0.367777361	56.7900395	34.049367	1

Lighting Level	Skin Conductance	Skin Temp	Heart Rate	Engagement
200	0.279176986	33.4255069	74.3830586	0
200	0.287174631	32.92335339	66.8263683	0
500	1.157017462	30.44195509	69.0793774	0
500	0.550005116	30.97578856	75.5309995	0
500	1.054047081	30.29731151	63.6401602	-1
1000	0.609844149	31.58552033	76.7030619	-1
1000	1.028192727	32.36726903	66.432231	0
1000	0.329496025	32.88669994	72.2049056	0
200	0.28971029	32.91944757	63.0538732	-1
1000	0.315555104	32.89671395	69.6257618	0
1000	0.595781822	31.85521834	71.3503616	0
200	0.275759831	32.94396791	64.9811874	0
500	0.552036939	30.89144779	67.6713965	0
200	0.290060634	34.06448472	79.0497788	1
200	0.293855017	34.09970424	87.6784532	0
200	0.189905147	32.76376207	74.2810896	2
1000	1.053404061	32.33254067	73.9124066	0
200	0.285714286	33.46083545	70.8799433	0
500	1.006666077	30.53898048	68.1524302	-1
500	0.775350517	30.80182352	68.9777701	0
200	0.287574404	34.05247466	75.6950136	0
500	0.773631317	30.81859876	69.0352614	0
500	0.782813974	30.85215132	67.7009144	0
1000	0.77615787	32.35406102	66.348323	-1
500	1.15005524	30.4623416	66.9378832	-1
500	1.155308234	30.33409703	64.8425667	0
200	0.316467387	34.35036884	78.1873202	-2
500	1.076536311	30.32552396	68.7818927	-1

Fig. 6.6. Example of the dataset for existing DID database

6.3 The Room Recommendation Strategy

The recommendation strategy follows the approach described in Section 2.1.5. In this case study, the thermal sensation is the only index that needs to be considered. The indoor thermal environments of the three example rooms are measured using the COZIR sensors. As an illustrative example, the parameters in Table 6.4 are some random initial settings, and based on these initial indoor conditions, the implementation of the framework regarding the room recommendation is demonstrated. Here, ids 1 to 6 are used to indicate the people in group #1 and ids 7 to 12 for people in group #2. At first, the occupants are randomly assigned to different rooms by assuming that they have no information regarding the room conditions. Then the prediction models mentioned in previous sections are used and the CSI for each room is computed. The scores of different rooms and recommendations regarding the best-fit rooms for each occupant are shown in Table 6.5. According to the results, for most of the occupants (1, 2, 3, 4, 5, 6, 9, 10, and 11), there is at least one room that is expected to give the most suitable (score of 1) indoor environments. In this case,

the recommendations regarding the best-fit rooms are given to these occupants. For example, occupant 1 is suggested to go to room 2, occupant 2 is suggested to stay in room 1, and so on.

However, not every occupant can have a room with the optimal thermal environment for them. In this case, the occupants will be suggested to a relatively more suitable room and the room setting will be changed to minimize discomfort. The strategy for modifying the room settings is explained in the next section. Therefore, the rooms with the highest Room CSI are chosen. Fig. 6.7 shows the comparison of the Room CSI before and after applying our recommendations, which shows the potential improvement of the occupants' thermal sensation. Note for this section, people in both group #1 and group #2 have databases to support the recommendation system, the only difference is that people in group #1 use the personal database while those in group #2 use the public database.

Table 6.4. The indoor environments of different rooms

	Room Temperature (°C)	**Relative Humidity (%)**
Room 1	23.8	53.2
Room 2	20.7	61.1
Room 3	18.2	67.3

Table 6.5. Scores of different rooms for each occupant

Occupant	**1**	**2**	**3**	**4**	**5**	**6**	**7**	**8**	**9**	**10**	**11**	**12**
Thermal Sensation												
Room 1	1	0	1	1	1	0	−1	−1	0	2	1	−1
Room 2	0	−1	0	0	0	−1	−1	−2	0	1	1	−1
Room 3	−1	−2	−1	0	−1	−2	−2	−3	−2	0	0	−2
Room Score Index												
Room 1	0.67	1	0.67	0.67	0.67	1	0.67	0.67	1	0.33	0.67	0.67
Room 2	1	0.67	1	1	1	0.67	0.67	0.33	1	0.67	0.67	0.67
Room 3	0.67	0.33	0.67	1	0.67	0.33	0.33	0	0.33	1	1	0.33
Room Assignment												
Original	1	3	3	2	1	3	1	3	1	1	2	3
Recommended	2	1	2	2&3	2	1	1&2	1	1&2	3	3	1&2

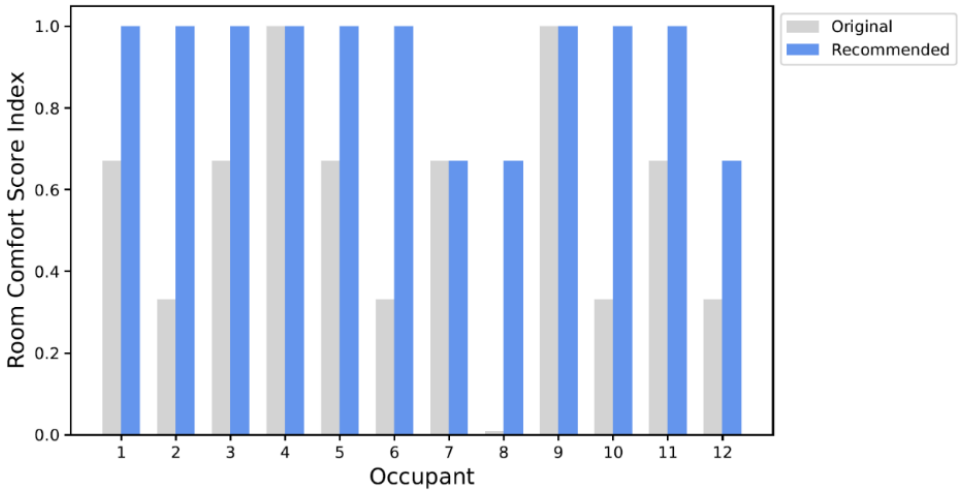

Fig. 6.7. Room Score Index comparison

6.4 Real-Time Visualization in Unity

Unity is used to develop a real-time visualization platform because it is compatible with BIM models and allows a real-time update of the human models. A BIM model is generated and imported into Unity for the virtual environment. The building model is the GGB Building as shown in Fig. 6.8. COZIR sensors are connected to the computer and the environmental data are read and saved in local .csv files. A C# script is generated in Unity to read the imported data in .csv files. It can be seen that the indoor environmental parameters (i.e., temperature and humidity) can be visualized explicitly, and there are two buttons to display or hide the texts of sensing data. In addition, two human models are created to demonstrate the different occupants can be represented, and distinct rendering colors are assigned to them based on the estimated thermal preferences. In this example, blue indicates that the occupant is feeling cool or cold (with the thermal sensation of -3, -2, and -1), and prefer a warmer environment, while red means the occupant feels warm or hot (with the thermal sensation of 1, 2, and 3) and prefers a cooler environment, green implies a neutral feeling of the occupant. Once the corresponding occupants change their locations (e.g., shift to another room), the new thermal comfort preferences will be given based on the new environmental parameters. Similarly, two buttons for displaying and hiding the occupant models

are given, and in this way, the user can have better control of the visualization interface. In general, the platform can provide real-time information about the indoor environment and occupants' comfort levels.

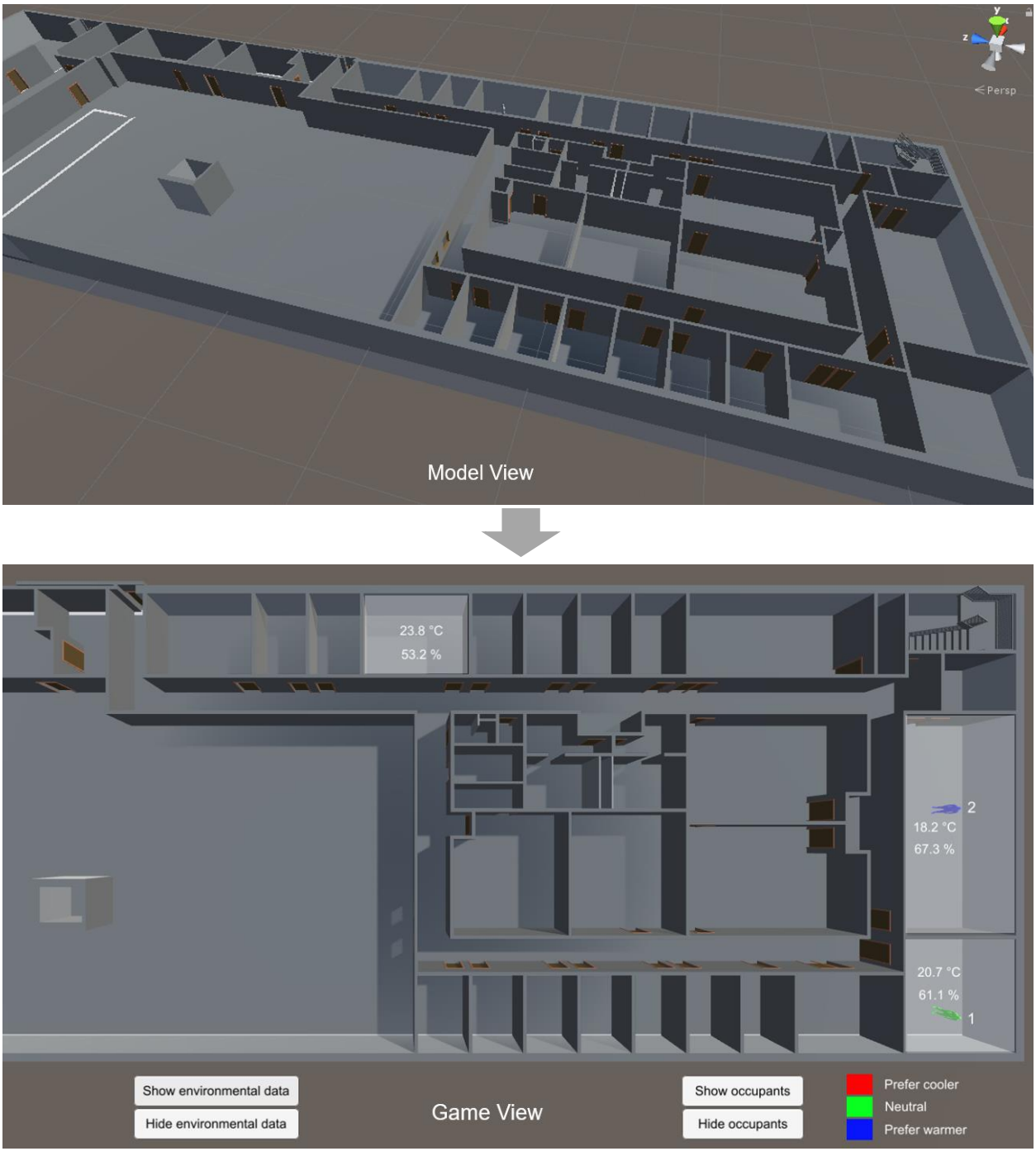

Fig. 6.8. Developed real-time visualization platform based on Unity

6.5 Discussion

In general, a case study is used to demonstrate the proposed framework and how the DID could be incorporated. Different personal databases are used to demonstrate occupants with different profiles (group #1). The scenarios when people are new occupants (group #2) are also illustrated. Various types of database and prediction models are incorporated into our framework. An explicit example is given to show how these databases are used and how the systems make use of them to provide recommendations and feedback. The results show that compared to the randomly assigned rooms, the recommended rooms can provide better thermal environments for the occupants.

It is worth noting that the proposed framework is generic, and any other types of building information or technologies can be implemented. Although the case study used specific human parameters and prediction models as examples, the framework can fit any other occupant-related parameters or state (e.g., lighting comfort, sound comfort, and odor comfort). The only difference will be the input parameters. In addition, after comparing the capabilities of different platforms, a real-time visualization platform based on Unity is developed. The functionalities of the developed platform are also extendable, and the case study intends to provide an example of the capabilities of the platform as well as the key functionalities. The interfaces can be re-designed based on the requirement of the projects or personal preferences. By integrating the real-time sensing data and the predicted values, the developed platform can provide real-time information for both the overview of the indoor environment and the occupants' state, which can be valuable references for the building managers. With the help of the proposed framework, unnecessary space conditioning when the room is unoccupied or over-conditioning can be reduced. As a result, the indoor experience of the occupants as well as the energy efficiency of the building can be improved.

There are several advantages of the proposed framework. Compared with the occupant-centric environmental control framework in previous studies [5, 70], our framework focuses not only on thermal comfort models but also on the overall indoor experience of the occupants based on the concept of DID and CSI. The concept of CSI can incorporate different indoor comfort indexes of the occupants and allow the systems to estimate occupants' overall indoor experience. In addition, rather than only proposing a concept, the framework is validated using a detailed example to demonstrate the mechanism of the systems. The case study contains two different types of prediction models (e.g., thermal sensation and work engagement) to show the scalability of the framework. In the case study, the ASHRAE Global Thermal Comfort Database II is used as a publicly available dataset for pre-training the model, which guarantees the reproducibility of the results. Furthermore, a visualization platform that serves as an auxiliary tool for the building control systems is also developed and demonstrated.

It is also worth acknowledging some limitations of this study. To allow the system to work based on individual preferences, the DID database contains some private information about the occupants, thus people may concern about their privacy. Therefore, data security needs to be ensured in a real-world implementation. In addition, to implement the framework, the buildings need to be equipped with a number of sensors and preferably with a building automation system (BAS). Furthermore, this study provides a general idea of the framework with several example methods. The framework is scalable and allows different technologies and algorithms to be incorporated, while the detailed discussion of optimization algorithms is not in the scope of this chapter. For example, the recommendation strategy does not discuss the maximum capacity of the rooms and the conflict perceptions of different occupants.

6.6 Conclusions

This chapter proposes a novel concept of DID for human-centric monitoring and control of the indoor environment, which provides valuable insights into next-generation smart buildings. The concept of DID is defined and explicitly explained. Based on the DID, the interaction between different systems in the framework is presented, and possible approaches and algorithms for specific systems are discussed. A case study using the scene of the GGB building at the University of Michigan is presented to demonstrate the framework. Two groups of occupants are used to demonstrate how the DID, in different scenarios, can be adopted into the framework to provide recommendations for room allocation and indoor environment control. As thermal sensation is used as the target index to recommend the rooms, the results show an improvement in the thermal sensation of the occupants if they follow the recommendations compared with randomly assigned rooms. Different types of database and prediction models are used during the process to demonstrate the scalability of the framework. Example feedback for the building systems is also demonstrated based on previous results. Furthermore, a Unity-based platform that enables the real-time visualization of indoor environmental parameters and occupants' states is developed. In general, DID-based indoor environment monitoring and control allows efficient human-centric management of the indoor environment. It is scalable and considered a valuable framework for future smart buildings.

Chapter 7 A Systematic Analysis of Physiological Responses as Indicators of Driver Takeover Readiness in Conditionally Automated Driving

7.1 Introduction

The adoption of Autonomous Vehicles (AVs) is expected to curb traffic congestion, reduce the stress and fatigue of drivers, and improve driving safety [71, 257]. Even though the ideal goal of AVs is to achieve full automation, current AV designs require humans to still play an important role in the driving functions. This is mainly because the current or near future AV designs do not have the reliable relevant technologies [17, 18] to make them fully autonomous and allow complete disengagement of the driver (e.g., insufficient accuracies of computer vision systems [258]). As a result, the current automation systems in vehicles are mostly categorized as "Level 2 Partial Automation", which only provides some driving assistance such as lane centering and adaptive cruise control thus the drivers must always stay alert and prepare for resuming full control of the vehicle [72]. Fatal accidents might be caused if the driver fails to take over control in time such as in the Tesla crash that happened in California [73].

As the technologies of AVs move forward, "Level 3: Conditional Automation" defined by the Society of Automotive Engineers (SAE), the vehicle systems are supposed to manage all driving functions under certain conditions and the drivers are required to take over the control only if a request or alert is issued by the car (as shown in Fig. 7.1). For example, when there are construction zones [259] or unfamiliar situations (e.g., obstacles) in front of the lane [260], the drivers may need to perform the takeover immediately.

At the same time, instead of always focusing on the roadway, the drivers are given some freedom in performing secondary tasks such as using their cell phones or other devices, watching videos, and reading. Engagement in these activities will thus further complicate the timely takeover of the vehicles and in some cases result in suboptimal takeover quality [261]. This highlights the importance of interactions between the driver and the vehicle aiming at understanding the driver's readiness to take over at any time and reminding the driver in a timely manner when the takeover should be done. A key step to achieving this end is to build a system that measures drivers' states and that can be used subsequently to estimate takeover readiness [262, 263].

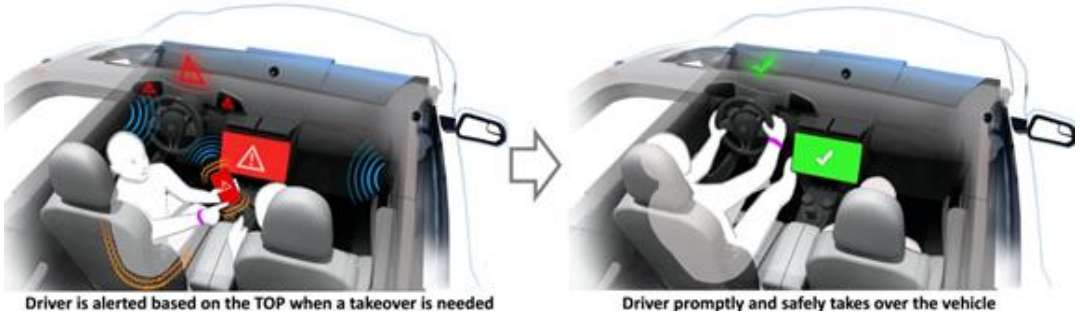

Fig. 7.1. Conditional automation (SAE Level 3): eyes-off but mind-on

To achieve this, a comprehensive understanding of the human states, while they are driving or waiting for the takeover, is the key [264, 265]. A good understanding of human states can provide important information regarding what are good input features for estimating the takeover readiness and TOP and how they should be used. One way to understand in real-time the driver states is to monitor their physiological responses [266, 267]. For example, existing research has tried to adopt physiological sensors to monitor drivers' ST [268], HR [269], and GSR [270] while they are performing driving tasks. Existing studies reveal that these types of physiological data have the potential to be adopted to bridge the interaction between the driver and the vehicle. In addition, some of these physiological responses are used as features for establishing the prediction models for the TOP of the drivers [262, 263]. A detailed review of existing literature reveals that

some important indicators of human mental states such as MW and work engagement are not well explored in driving situations. More importantly, there is a lack of systematic analysis of changes in different physiological responses before and during takeover periods which allows people to compare and evaluate the values of different physiological data. These raise two important research questions: whether there is a specific pattern regarding the changes in physiological responses prior to and during the takeover periods? And which types of commonly used physiological data have the potential to be applied as the input features for estimating takeover readiness?

To address the research gaps and incorporate a reliable human-vehicle interaction system in conditional automation, two steps of research are needed: (1) understand the correlation between the drivers' physiological data and takeover activities, and (2) build reliable prediction models for takeover readiness. The scope of this study is to systematically investigate the physiological responses of the drivers under conditional automation.

To achieve this, an experiment is designed using a driving simulator. Different takeover scenarios (i.e., two traffic densities and three takeover events) are incorporated to diversify the driving simulation. The vehicle data and the physiological responses of the subjects are collected while they are performing the driving simulation (both before and during a takeover event). In addition, the subjects are asked to perform secondary tasks while they are waiting for the takeover scenarios. Besides the SCL and HR, brain signals are incorporated in this study to calculate the Frontal Asymmetry Index (FAI) (as an indicator of engagement) and Mental Workload (MW) of the subjects. The collected physiological data are then analyzed and compared with respect to different takeover scenarios, takeover readiness, and individuals. Details of the experimental design can be found in the methodology section. The main objectives of this study include: (1)

systematically understand the changes in physiological responses (i.e., SCL, MW, FAI, and HR) prior to and during the takeover activities across all the subjects; (2) compare the sensitivities of physiological responses during the takeover activities as references to determine good factors for estimating takeover readiness; (3) explore the correlation between physiological data, takeover scenario, and indicators of takeover readiness; and (4) explore the individual differences of the physiological responses and provide the suggestions regarding applying them in prediction models for takeover readiness.

7.2 Related Work

Existing literature that confirms the feasibility of using physiological data for the evaluation of the physical or psychological states of the drivers is reviewed. In addition, relevant studies regarding the application of physiological data in estimating driving-related parameters are summarized. Based on the literature, the research gaps are identified.

7.2.1 Application of physiological data to evaluate the states of the drivers

Several studies have tried to adopt physiological data to help understand and evaluate the psychological and physiological states of drivers. For example, Pakdamanian et al. [265] conducted a preliminary study of the correlation between physiological data and takeover requests at Level 3 driving automation, which incorporated brain signals, GSR, and Photoplethysmography (PPG) to compare the effect of visual and auditory alerts on startle of the drivers. The results suggested that a combination of visual and auditory alerts led to a shorter takeover time with greater engagement than indicated by EEG and PPG results. Similarly, Du et al. [264] investigated the effect of takeover design on GSR and HR responses at Level 3 driving automation. The results showed that a 4 s lead time (the time interval after the alerts and prior to the takeover events) of the takeover resulted in larger maximum and mean values of the phasic component of GSR

compared with a 7 s lead time, while the high traffic density tended to increase the acceleration of HR. In addition, Kim et al. [259] compared the effect of different types of alerts for takeover requests and the lead time on the speed of drivers' waking up, which used GSR and HR as the physiological indicators of the drivers. The results showed higher increases in GSR with a short lead time. Similarly, the GSR and HR were adopted in the experiment of trust on autonomous driving under different weather conditions conducted by Sheng et al. [271]. The results showed that the number of peaks in the GSR signal was sensitive to the effect of weather. Moreover, some physiological data was applied to indicate the mental load and stress of the drivers. For example, the GSR signal was used as the stress indicator in an automated driving experiment conducted [272], which showed that attention-aware takeover requests could help reduce the stress level of the drivers. To evaluate the workload and stress level of the drivers in conditionally automated driving, the GSR and electrocardiogram (ECG) of the subjects were monitored in the studies by Meteier et al. [273], which confirmed that these physiological signals could well indicate the mental state of the drivers.

7.2.2 Using physiological data as input features of driving-related prediction models

Rather than being used as indicators, some of the physiological responses were used as the input features to build the prediction models for the drivers' states such as their mental states and takeover performance (TOP). For example, a classifier was developed by Singh et al. [274] as a tool to evaluate the stress level (i.e., relaxed, moderate, and stressed) of automotive drivers using the GSR and PPG. Different types of neural network architectures were tested and compared, and the results showed that the Layer Recurrent Neural Network could give the optimal precision of the prediction at 89.23%. Mårtensson et al. [275], on the other hand, used the information extracted from EEG, ECG, and electrooculography (EOG) as the input features to help classify sleepiness

(i.e., alert or sleep based on the Karolinska sleepiness scale) of the drivers. The results revealed that the random forest algorithm could be used to build a robust classifier with an accuracy of 94.1%. In addition, Du et al. [19] incorporated the physiological data including HR, GSR, and eye movement as the input features to predict the TOP performance based on several machine learning models. Overall prediction accuracy of 84.3% was achieved using the random forest classifier. Similarly, a deep neural network named DeepTake was established by Pakdamanian [260] to estimate the takeover-relevant indicators during automated driving. In addition to vehicle-related features, the model incorporated the GSR and HR as the input features. The final prediction accuracies for the classification of the defined takeover quality, time, and intention were 83%, 93%, and 96% respectively. Furthermore, to help with the improvement of driving safety, Li et al. [276] incorporated eye movement information and Heart Rate Variability to estimate the driving risks during lane-changing activities. The study applied a hidden Markov model as the model for the learning process and overall accuracy of 90.67% was achieved.

7.2.3 Research gaps

Despite many previous studies, there is a lack of systematic analysis of different physiological responses associated with takeover behaviors. For example, it is still not clear which types of physiological data are more sensitive to takeover behaviors and what are the differences in their changes during the takeover periods. The comprehensive comparison of different types of data during the takeover could provide valuable information to help in selecting the physiological data in TOP-relevant studies. In addition, the importance of mental states such as Mental Workload (MW) and engagement was emphasized by many researchers as they could affect the decision-making [277-279] and productivity [280, 281] of people thus affecting the efficiency and safety of driving activities [282, 283]. However, they have not been well studied in relevant to conditional

automation in previous studies. Moreover, it has been addressed that the above-mentioned physiological data could vary a lot across individuals even when they are doing similar tasks in the same environments, [23, 56, 57]. However, the findings in previous studies are generalized results from a certain group of people, which ignored the important role of individual differences.

7.3 Research Methodology

In this study, an experiment was designed to systematically analyze and compare the effects of driving takeover behaviors on a variety of human physiological responses. To simulate the conditional automation, subjects were recruited to handle the driving takeover scenarios using a driving simulator while their physiological signals including brain signals, GSR, and HR were collected. Each subject was asked to perform 18 different takeover scenarios with different combinations of secondary tasks, takeover events, and traffic densities. The results of the physiological data were then analyzed and compared. Details regarding the experimental design and data collection can be found in the following sections.

7.3.1 Experimental design for the driving scenarios

The simulation of the driving scenarios was developed based on the Unity game engine. It contains both manual driving (MD) and automated driving (AD). The MD allows the subjects to practice driving in the simulator while the AD was used for the experiment. The subjects can freely press the gas and brake pedals, but there would be no response when the vehicle was in AD mode. During the AD mode, the speed of the vehicle was maintained at 70 mph (113 km/h) which is the general speed limit on most highways. The subjects were asked to wait for the takeover alert while the vehicle was driving by itself. To simulate the possible distractions during real autonomous driving, three different secondary tasks were assigned to the subjects prior to each takeover alert: (1) observing, (2) 1-back task, and (3) 2-back task. For the observing task, the subjects were

allowed to observe the road or the surrounding environment without doing additional tasks. For the 1-back task, there were visual patterns that showed and disappeared on the screen, the subjects needed to recall whether the current pattern was the same as the one step earlier. Similarly, the 2-back task required the subjects to recall the pattern two steps earlier. Therefore, the 2-back task is considered a difficult version of the 1-back task. The stimulus used in this experiment was the position of a box at a 3×3 grid as shown in Fig. 7.2. For the scenarios with 1-back and 2-back tasks, subjects were instructed to engage in the secondary task during AD mode.

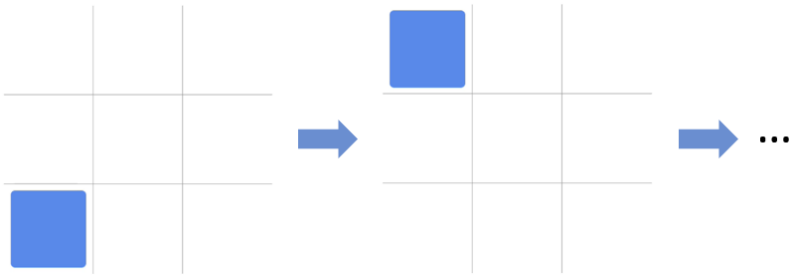

Fig. 7.2. N-back task

Whenever there was a takeover request, the subject would hear an alert with a sound (a BI at 85 dB which lasted for one second) and a visual stimulus (red panel) as shown in Fig. 7.3. The alert was issued 7 seconds prior to the takeover scenarios. The mode of the vehicle would be shifted from AD to MD with the alerts, thus the subjects were expected to stop the secondary task immediately and try to manually control the vehicle to avoid any potential collisions or accidents. To simulate different traffic conditions, the takeover simulation contained two different traffic densities and three takeover events. A low traffic density scenario contains 40 vehicles per mile while a high traffic density scenario has 80 vehicles per mile. The three takeover events include (1) an obstacle in front of the lane, (2) a police car on the right side, and (3) a fake alert as shown in Table 7.1 and Fig. 7.4. Considering all the possible combinations of the secondary tasks and simulation designs, there were 18 different scenarios (3 secondary tasks × 3 takeover events × 2

traffic densities) in total. The vehicle would be reset to AD once the subjects successfully completed the takeover behaviors and followed by the next round of the takeover. If the takeover activities failed, the takeover periods would stop and wait for the research staff to manually start the next takeover simulation. After each simulation, the most commonly used indicators of the takeover readiness including maximum acceleration [276, 284], time to collision (TTC) [19, 285], and reaction time (time between the alert and the start of the takeover) [260, 264] were recorded.

Fig. 7.3. Visual alert for the takeover

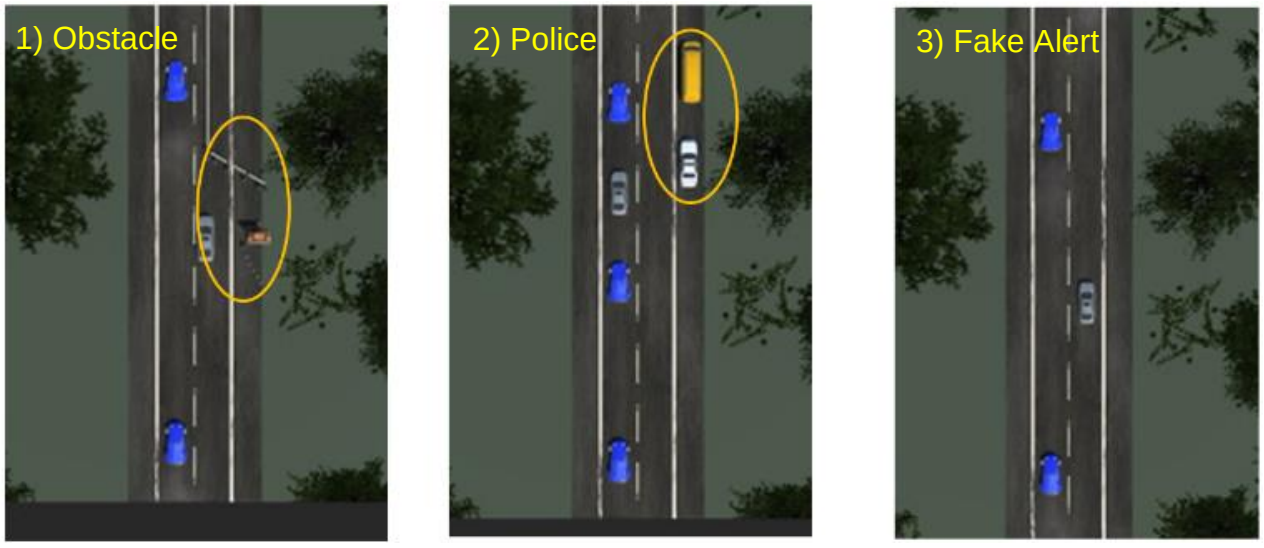

Fig. 7.4. Three designed takeover events (from the top view)

Table 7.1. Experiment scenarios and descriptions

Category	Description
Secondary Task	Observing
	1-back task
	2-back task
Takeover Event	Obstacles in front of the car
	Police by side
	Fake alert
Traffic Density	Low
	High

After the simulation of the conditional automation was developed using the Unity game engine, a driving simulator named ProSimu T5 Pro (as shown in Fig. 7.5) was used to incorporate the program. The simulator was equipped with three Samsung 55'' 4K QLED HDR Monitors to display the driving scenarios. Gas and brake pedals were provided to simulate the real driving experience. The subjects were allowed to adjust the seat, steering wheel, and pedals to maintain their own preferred driving postures.

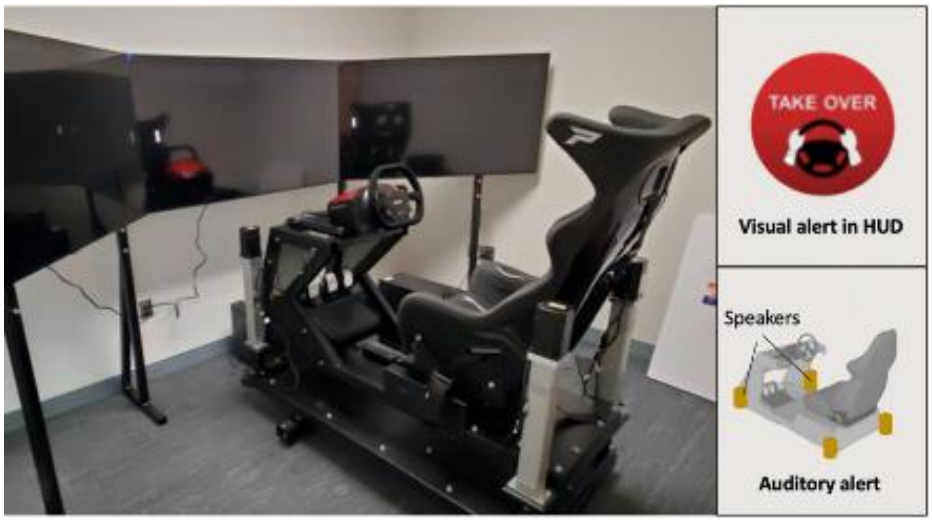

Fig. 7.5. ProSimu T5 Pro driving simulator

7.3.2 Timeline of the experiment

The detailed experimental timeline is shown in Fig. 7.6. After the subjects arrived at the experimental lab, they were given around 20 min to relax and get used to the indoor environment

while the research staff provided detailed instructions for the experiment. The setup of the devices lasted for around 10 min, followed by a 9 min manual driving which allowed the subjects to practice the driving simulation. During the manual driving, each subject experienced the three different types of takeover events under low traffic density with the alerts before each takeover scenario. The AD mode of the vehicle started right after the manual driving scenarios. The letters "L" and "H" in Fig. 7.6 indicate low and high traffic densities, and the letters "A", "B", and "C" refer to three different secondary tasks (observing, 1-back, and 2-back, respectively), and the numbers "1", "2", and "3" represent three takeover events (an obstacle in front of the lane, a police car on the side, and fake alert, respectively). Each subject was asked to complete the takeover of all 18 scenarios with each of them lasting for around 3 min. To avoid learning curves, the sequence of the scenarios was randomized. A 10 min break was given after 9 scenarios to allow the subjects to get rid of the equipment and get refreshed. The re-setup after the rest lasted for about 5 min. Overall, the total experimental time (including the preparation, rest, and re-setup period) for each subject was around 88 min.

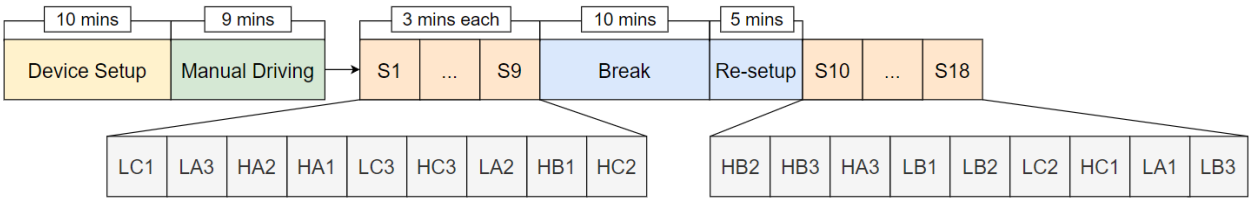

Fig. 7.6. Experimental timeline

7.3.3 Subjects and equipment

The recruitment of the subjects was conducted among all the graduate students and employees who were working at Clemson University International Center for Automotive Research (CU-ICAR). Twenty subjects (18 males and 2 females) aged between 23 to 39 were recruited to participate in the study. Subjects were physically and psychologically healthy. In

addition, all subjects were confirmed to have valid driving licenses. A pilot study was first conducted in July 2021 to validate the experimental design and ensure the functionalities of the equipment. The experiment was then conducted from January to February 2022. To respect the health concerns of the subjects during COVID, all the subjects were allowed to wear a mask. Each subject would receive compensation upon completion of the experiments. The subjects were allowed to withdraw from the experiment at any time.

7.3.4 Collection of physiological data

Previous studies have shown that GSR signal and HR were good indicators to evaluate the mental or physiological states of the drivers [264, 286] and could be potential input features for predicting their TOP [19]. For example, in an experiment conducted by Pakdamanian et al. [260], the GSR signals and HR (PPG signal) was applied to reflect the workload of the driver during the takeover activities and were used as the input features to predict the takeover quality of the subjects. The results showed promising accuracies for predicting the takeover intention and time. In addition to GSR and HR, this study also calculated human mental states including MW and FAI using brain signals as these have been shown to affect people's decision-making [277-279] and productivity [280, 281] and thereby might have a significant effect on the driving activities [282, 283]. Previous studies have tried to use the raw brain signals to calculate MW [287-289] and FAI [57, 289]. A preliminary study has demonstrated the feasibility of using brain signals collected by EEG during driving takeover-relevant events [265]. Therefore, the GSR signal, HR, and brain signals of the subjects were selected and recorded during the experiment.

Fig. 7.7 shows the positions of the physiological sensors. The raw data of GSR and HR collected from the sensors could be directly used in the result analysis after straightforward pre-processes such as separating the components (e.g., tonic and phasic components in GSR) and

cleaning (e.g., removing the outliers). However, sophisticated analyses were required to obtain the MW and FAI from the raw brain signals collected by the EEG headset. Details regarding the methods used to analyze the collected physiological data are described in the following sections.

Fig. 7.7. Physiological sensors during the experiment

7.3.4.1 Measurement of SCL

The GSR signal contains both tonic components and phasic components. The tonic component, most commonly measured as the SCL, usually changes slowly and is considered a background signal of the skin conditions and could be used to reflect sympathetic activities [141, 194, 195]. In several previous studies, SCL was applied in as an indicator of the MW [196, 197]. The phasic component is more event-related and could change rapidly, and thus it is often used to test the reaction of human responses to specific stimuli [141]. In this study, the SCL was used to represent the general responses of the skin states of the subjects. The Shimmer3 GSR+ Unit was used to record the GSR signals, which allowed real-time visualization of the data through the Bluetooth connection to the software named ConsensysPro. The sampling frequency of the GSR signal was 128 Hz. In general, the locations on the hands (i.e., palm or fingers) are commonly used for attaching the GSR electrodes in many previous studies [57, 259, 260, 265]. However, since the

subjects would need to hold on to the wheel during the takeover period, thus palm could not be used as the location for the collection of GSR signals. In addition, when the subjects put their hands on the wheel to control the vehicles, it might still cause some noise to the GSR signals collected from the fingers, thus another set of GSR electrodes that adhered to the shoulders (another common location) of the subjects was used to cross-validate the changes of the GSR signals (as shown in Fig. 7.7).

7.3.4.2 Measurement of MW and FAI based on EEG data

By placing the EEG headset electrodes at different locations on the surface of the scalp, the brain signals of the subjects can be recorded by capturing the voltage changes. In this study, a 14-channel EEG headset, Emotiv EPOC X (as shown in Fig. 7.7), was applied. It allows quick setup using saline solution. The real-time brain signals at different channels could be visualized by the Bluetooth connection on the computer. The sampling frequency of the headset was set to 128Hz. The raw data collected from the EEG headset was floating-point values with a DC offset of approximately 4200 μV. In addition, it contained a lot of noise which was categorized into extrinsic and intrinsic artifacts. The extrinsic artifacts were removed by a band-pass filter with a frequency from 0.5 Hz to 65 Hz [167]. The intrinsic artifacts were caused by the eye blinking and muscle movements of the subjects, which needed to be identified and removed manually. In this study, EEGLAB [171] was applied to help with the removal of the intrinsic artifacts.

After the removal of artifacts, the data collected from EEG was further processed to obtain the MW and FAI. At first, the band power of the denoised EEG data across different frequencies was obtained by applying the Fast Fourier Transform (FFT). The typical frequency bands usually include Delta (1-4 Hz), Theta (4-8 Hz), Alpha (8-12 Hz), Beta (12-25 Hz), and Gamma (>25 Hz)

[23, 175, 176]. The obtained band power was further utilized to compute the MW and FAI in this study.

Previous studies have shown that the frontal theta power of the human brain signal was typically higher while its parietal alpha power was lower when people had higher MW [188-190]. For the 14-channel EEG headset used in this study, F3 and F4 provide the brain signals for the frontal lobe while P7 and P8 provided the Brain Signals in the parietal lobe. Eq. (7.1) [23] was applied to calculate the index of the MW as it computes the ratio of the theta power from the frontal part to alpha power from the parietal part. The locations of the corresponding channels on a 14-channel EED headset can be found in Fig. 4.6.

$$Mental\ Workload\ Index = \frac{F3\ theta\ power + F4\ theta\ power}{P7\ alpha\ power + P8\ alpha\ power} \tag{7.1}$$

Similarly, the correlation between the band power from different channels and human engagement was investigated. The FAI was one of the most commonly used indicators for engagement and motivation. In several previous studies, a positive correlation between FAI and engagement was found [20, 186, 187] (a higher FAI indicated a higher level of engagement). The FAI can be calculated based on the alpha power from the left and right lobe as shown in Eq. (7.2) [177, 178]. In this study, the FAI is used as the indicator of the drivers' engagement.

$$Frontal\ Asymmetry\ Index = ln\left(\frac{alpha\ power\ of\ F4}{alpha\ power\ of\ F3}\right) \tag{7.2}$$

7.3.4.3 Measurement of HR

As shown in Fig. 7.7, the Optical Pulse Ear-Clip was used to collect the PPG of the subjects which were further converted to HR. Due to the occasional bad quality of the raw data, the algorithm that converted the PPG signal to HR might fail, which resulted in the readings of HR at either 0 or some arbitrary larger number (e.g., >150 bpm). Therefore, in addition to making sure

of a stable attachment of the ear clip, a filter that removed the HR results below 30 bpm and above 150 bpm was used to clean up the data. The sampling frequency of the HR was identical to the EEG headset and SCL at 128 Hz.

7.4 Results

With the data collected from the physiological sensors, the results were further processed and analyzed. Pre-processes analysis was conducted to synchronize the raw data from different equipment. The raw data from brain signals were used to calculate the indicators of MW and FAI. The changes in physiological responses of the drivers during the takeover periods (i.e., from -5 s to 10 s) were plotted to show the potential effects of the takeover behaviors. In addition, the average values of the physiological data were analyzed with statistical methods. The data was plotted per different individuals as the references for further utilization of the data. Details of the data analysis methods and results are described in the following sections.

7.4.1 Data analysis

Due to the occasional equipment issues and data corruption during the experiment, 315 out of 360 sets (one for each takeover activity) of data were retained for analysis. All the collected data was initially stored in CSV. files with a frequency of 128 Hz. A time window of 1 s was applied to pre-process the raw data. As mentioned in the introduction, one of the objectives of this study is to conduct a systematic investigation of the changes in physiological responses during the takeover activities, the values of the pre-processed data were plotted along with time. By observing the recorded data, most of the takeover activities were finished within 10 s starting from the alerts, while only a small proportion of the takeover periods lasted for less than 10 s. Therefore, 10 s after the alert was chosen as the ending time of the plots to ensure the data within the plot range was all coming from the takeover periods. In addition, it was important to distinguish the changes before

and during the takeover periods to help evaluate takeover readiness. Therefore, the time range from −5 to 0 s ("−" indicates prior to the takeover scenario) was added as a reference. For example, an increase in the physiological data during the takeover periods might be less meaningful if it just maintained its tendency before a takeover alert. In this case, the time range of the plots was −5 to 10 s added as a reference (as shown in Fig. 7.8). Similar types of plots could be found in some related studies [259, 264, 290]. The results corresponding to different scenario designs (i.e., secondary task, takeover event, and traffic density) were processed separately and compared. Since the changes in the physiological data could be very small compared with the original values, only the differences in values (Δ) were plotted. The differences in values were calculated based on the values at time 0 (when the takeover alerts happen).

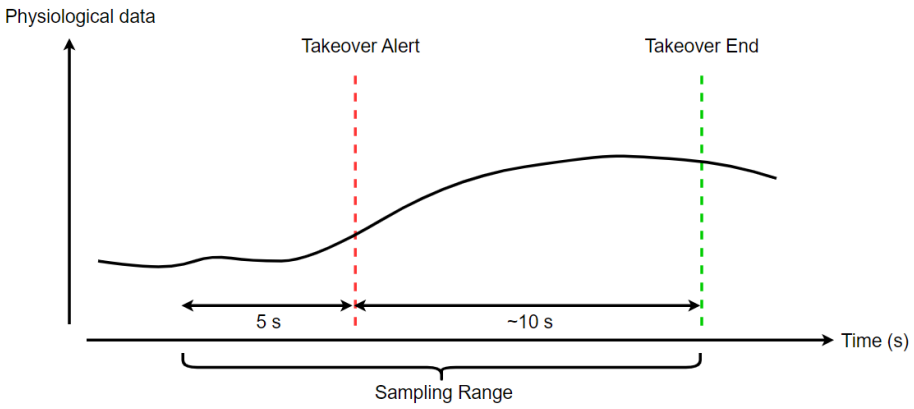

Fig. 7.8. The time window for the plots

In addition to the plots showing the changes in the physiological responses, the average values of the physiological data (i.e., SCL, MW, FAI, and HR) with respect to different takeover scenarios were compared. The ranges of the physiological data for the different subjects were plotted to show the differences across individuals. In these two parts, the Shapiro-Wilkinson test [206] was applied to test the normality of the datasets, and the p-value was less than 0.05, which revealed that the data does not follow a normal distribution. Therefore, a non-parametric test

alternative to the ANOVA was used in this study. To compare the results associated with low and high traffic densities, the Wilcoxon signed-rank test [291] was applied. Since the results from different secondary tasks and takeover events have three groups of data, the Friedman test [292] followed by a Nemenyi post hoc test [293] was conducted. The p-values of 0.001, 0.01, and 0.05 were used as three thresholds to determine the significance of data in different groups. The Cliff's Delta [294] was applied to express the differences in the data.

7.4.2 The effect of takeover activities with respect to secondary tasks

7.4.2.1 Changes in the physiological responses during the takeover periods

As shown in Fig. 7.9, except for the FAI, the values of all types of physiological data increased during the takeover period. Although the general pattern of the changes in the SCL collected from two different locations of the human body (i.e., shoulders and fingers) were similar, the amplitudes of the changes were not identical. Compared with the data collected from the shoulders of the subjects, the changes in SCL were more significant in the data from the fingers. To be specific, the peak differences of the SCL collected from fingers could reach more than 0.4 μS, which was more than 10 times the amplitudes from the backs (less than 0.03 μS). Based on the results, the SCL collected from the shoulders increased more significantly in the scenarios when the subjects were performing 2-back tasks.

In general, the MW of the subject increased after the alerts and gradually dropped back, while no obvious differences between the tendencies with respect to different secondary tasks. Similar to SCL and MW, the values of HR rapidly increased after the alerts. However, it suddenly dropped back to the values that were close to the prior takeover periods after it peaked at around 6s. The secondary tasks prior to the takeover behaviors did not affect the tendencies of the changes in HR. Different from other physiological data, the FAI of the subjects did not increase after the

alerts. Instead, for the scenarios when the subjects were performing 1-back and 2-back prior to the takeover, the FAI slightly decreased after the takeover alerts, while the FAI for the observing scenario did not change during the takeover period. It revealed that the secondary tasks chosen for this study slightly affected the pattern of changes in FAI during the takeover periods.

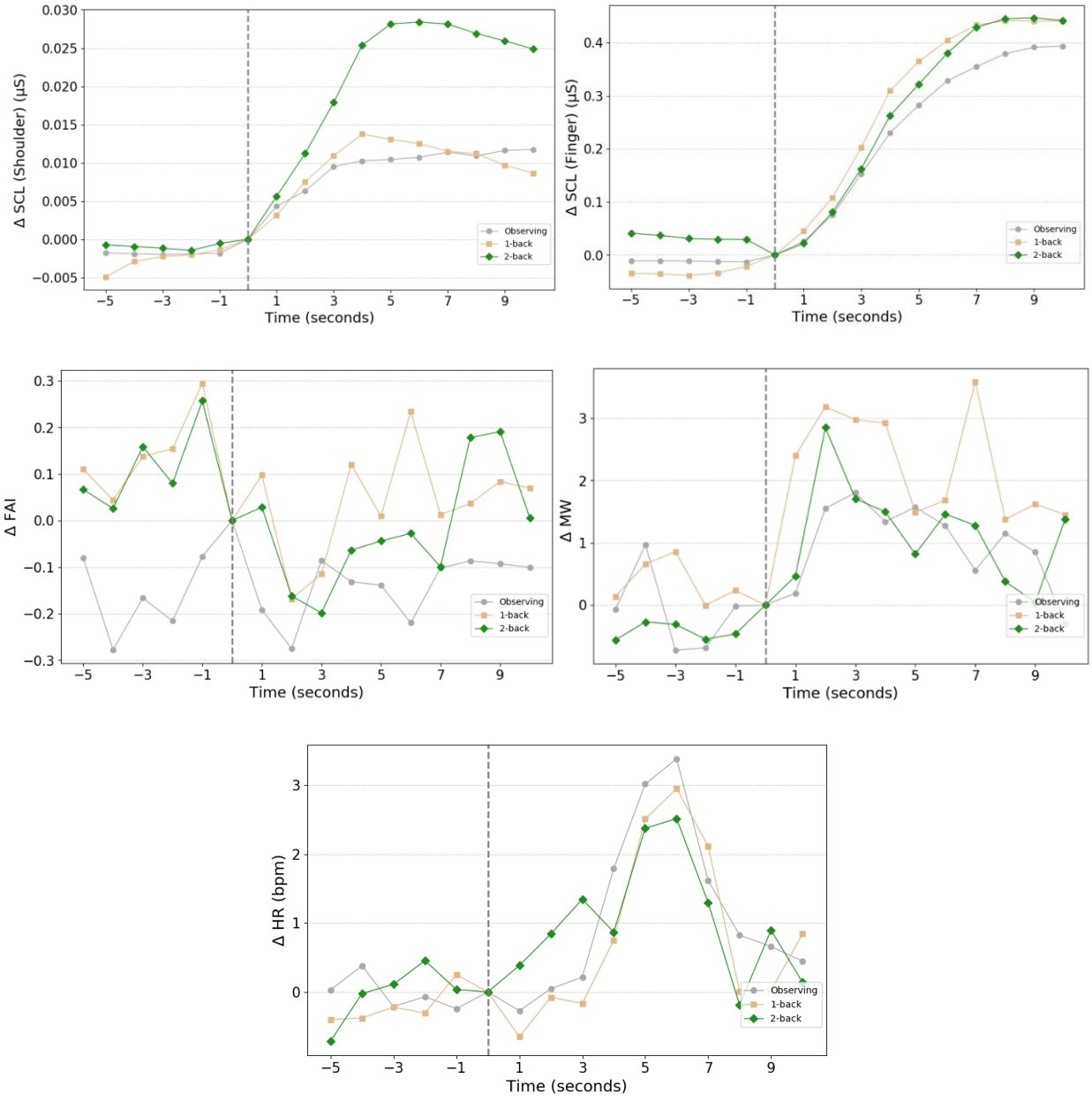

Fig. 7.9. Changes in the physiological during takeover behaviors with respect to the secondary tasks

7.4.2.2 Effect of a secondary task on average physiological data during the takeover periods

The mean and standard deviation of the physiological data during the takeover periods are summarized in Table 7.2. The differences in the specific physiological data concerning the secondary tasks are plotted in Fig. 7.10. The average FAI of the subjects associated with the observing task is higher than the 1-back task (Nemenyi: $p = 0.046$, Cliff's Delta = 0.06) and 2-back task (Nemenyi: $p = 0.002$, Cliff's Delta = 0.08). In contrast, the MW of the subjects associated with 2-back is higher than the observing task (Nemenyi: $p <= 0.033$, Cliff's Delta = 0.04) and 1-back task (Nemenyi: $p = 0.04$, Cliff's Delta = 0.06). In addition, the HR of the subjects associated with the observing task is lower than the 1-back task (Nemenyi: $p < 0.001$, Cliff's Delta = -0.156) and 2-back task (Nemenyi: $p < 0.001$, Cliff's Delta = -0.17). As for the SCL collected from the fingers, it indicated that the 1-back task led to a higher average value compared with the observing task (Nemenyi: $p < 0.001$, Cliff's Delta = 0.04) and 2-back task (Nemenyi: $p < 0.001$, Cliff's Delta = 0.05). The statistical analysis showed no differences in the average values of other physiological data concerning the secondary tasks.

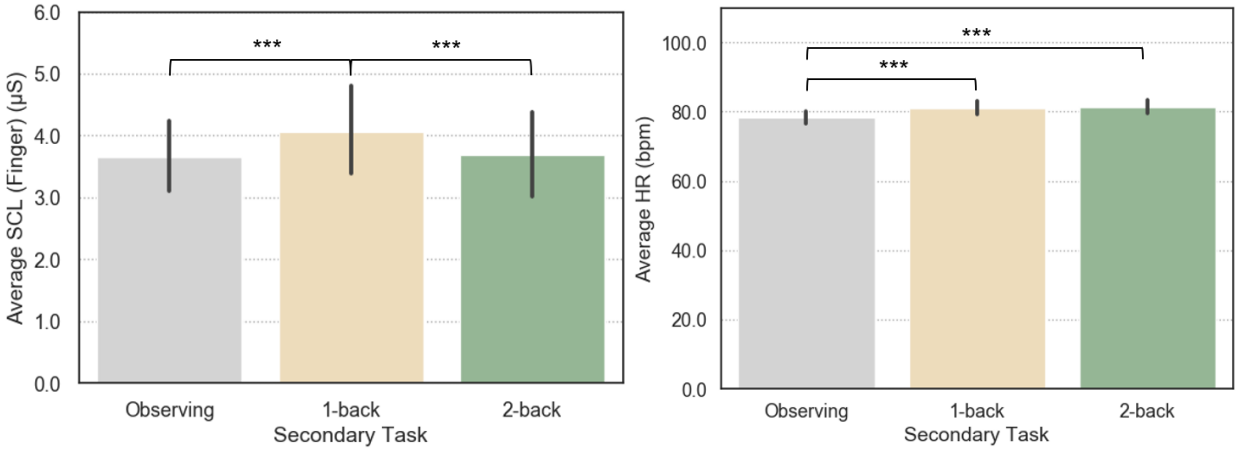

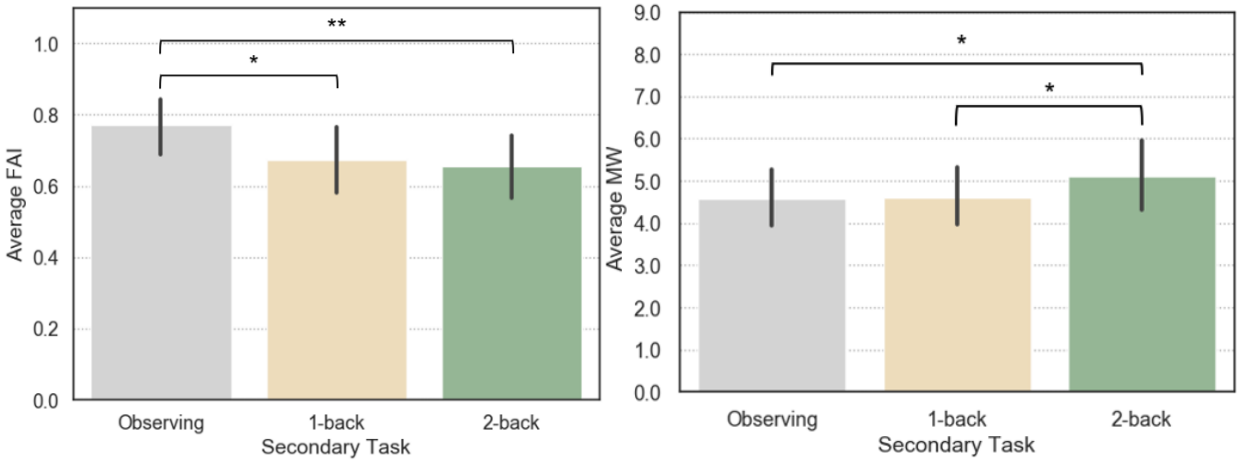

Fig. 7.10. Differences in physiological data with respect to the secondary task. The following indication is used for all the figures: *The difference is significant with p-value < 0.05; ** The difference is significant with p-value <0.01; The difference is significant with p-value <0.001.

Table 7.2. Mean and standard deviation of physiological data with respect to different secondary tasks before the takeover requests

	Observing		**1-back**		**2-back**	
	Mean	S.D.	Mean	S.D.	Mean	S.D.
SCL (Shoulder) (µS)	3.926	0.004	3.784	0.004	3.804	0.01
SCL (Finger) (µS)	3.661	0.144	4.07	0.163	3.688	0.169
FAI	0.77	0.072	0.674	0.105	0.654	0.116
MW	4.584	0.673	4.616	1.002	5.1	0.807
HR (bpm)	78.35	1.195	81.073	1.166	81.413	0.85

7.4.3 The effect of takeover activities with respect to takeover events

7.4.3.1 Changes in the physiological responses during the takeover periods

As shown in Fig. 7.11, the differences in the patterns in the changes in the physiological data could be observed in the SCL concerning the takeover events. From the SCL collected from either the shoulders or the fingers of the subjects, it could be seen that the peaks and slop of the changes during takeover event 3 (i.e., fake alert) were slower than the other two takeover events. In addition, the FAI slightly decreased after the takeover alerts during all three takeover events. The overall pattern of the changes in all the physiological data was similar and identical to the observation from Section 7.4.2.1. The SCL, MW, and HR increased with similar patterns

regardless of the takeover events, which indicates that the takeover events would not cause obvious effects regarding their changes.

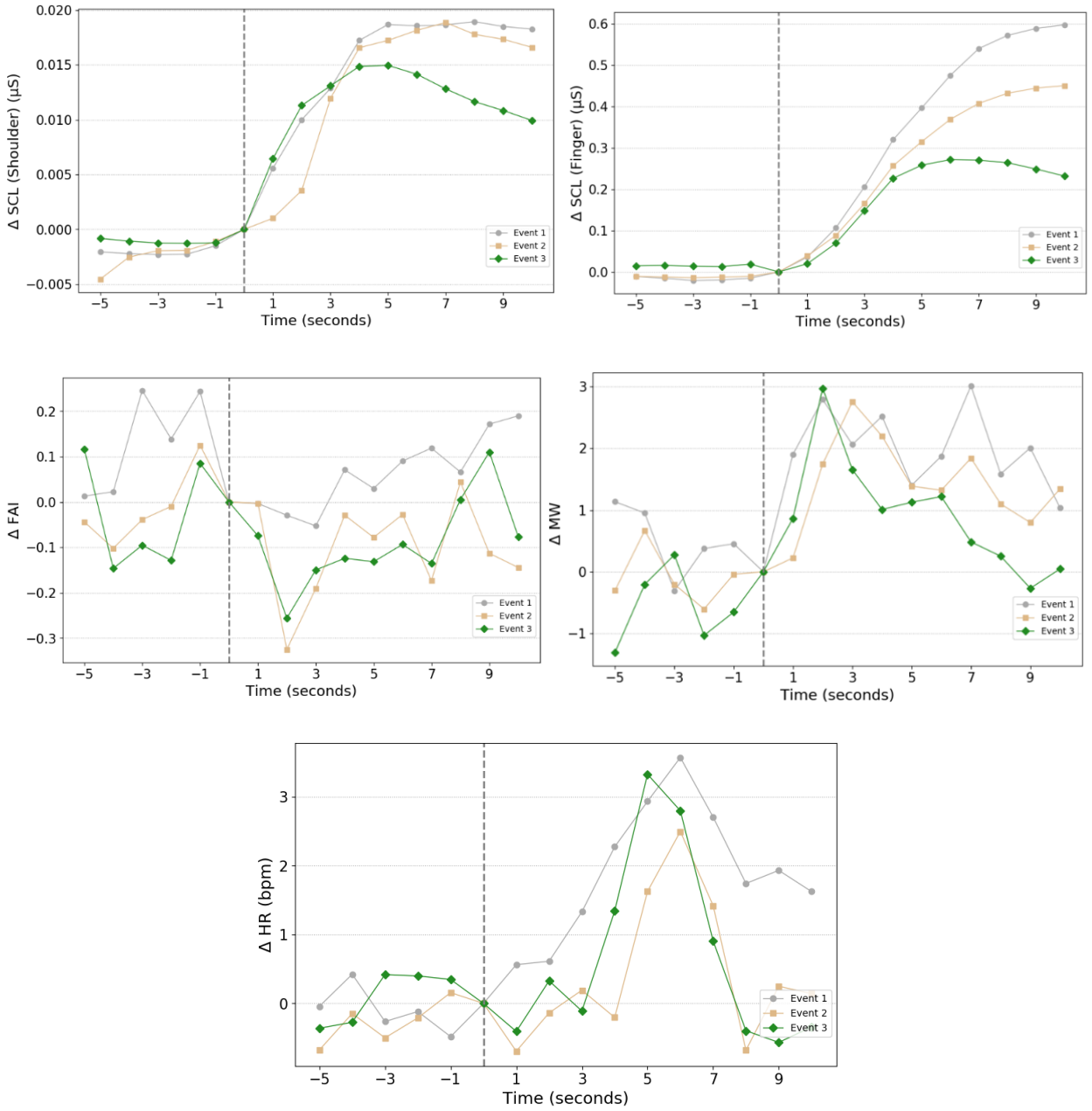

Fig. 7.11. Changes in the physiological during takeover behaviors with respect to takeover events

7.4.3.2 Effect of takeover events on average physiological responses during the takeover periods

The mean and standard deviation of physiological data concerning different takeover events is summarized in Table 7.3. Based on the statistical analysis, as shown in Fig. 7.12, the overall HR of the subjects was affected by the takeover events. The average HR of the subjects associated with event 1 was higher than event 2 (Nemenyi: $p = 0.02$, Cliff's Delta = 0.03) and event 3 (Nemenyi: $p < 0.001$, Cliff's Delta = 0.08). However, there were no significant differences in the average values of other physiological data concerning the takeover events.

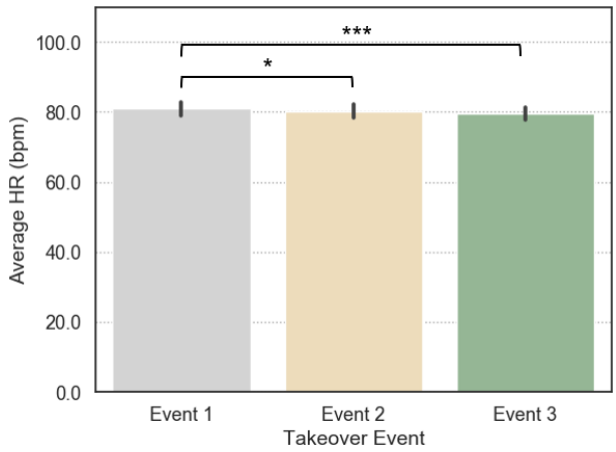

Fig. 7.12. Differences in physiological data with respect to takeover events

Table 7.3. Mean and standard deviation of physiological data with respect to different takeover events

	Event1		**Event2**		**Event3**	
	Mean	**S.D.**	**Mean**	**S.D.**	**Mean**	**S.D.**
SCL (Shoulder) (µS)	3.79	0.006	3.823	0.007	3.907	0.004
SCL (Finger) (µS)	3.794	0.218	3.812	0.162	3.808	0.1
FAI	0.725	0.076	0.674	0.103	0.706	0.092
MW	4.782	0.804	4.8	0.771	4.699	0.879
HR (bpm)	81	1.071	80.227	0.951	79.488	1.282

7.4.4 The effect of takeover activities with respect to traffic densities

7.4.4.1 Changes in the physiological responses during the takeover periods

The overall patterns of the physiological responses during the takeover periods remained the same when plotted as per different traffic densities as indicated in Fig. 7.13. Except for FAI, the values of all types of physiological data increased regardless of the traffic densities of the simulation. For example, the peak amplitudes and the slopes of the changes were almost identical in low traffic densities or high traffic densities for most of the physiological data, which indicated that the traffic densities were not a major factor that might have the pattern of these physiological responses of the subjects while they were taking over the control of the vehicle. The FAI decreased during the takeover periods in both traffic densities. However, the difference values of the FAI under high traffic density were slightly higher than the low traffic density.

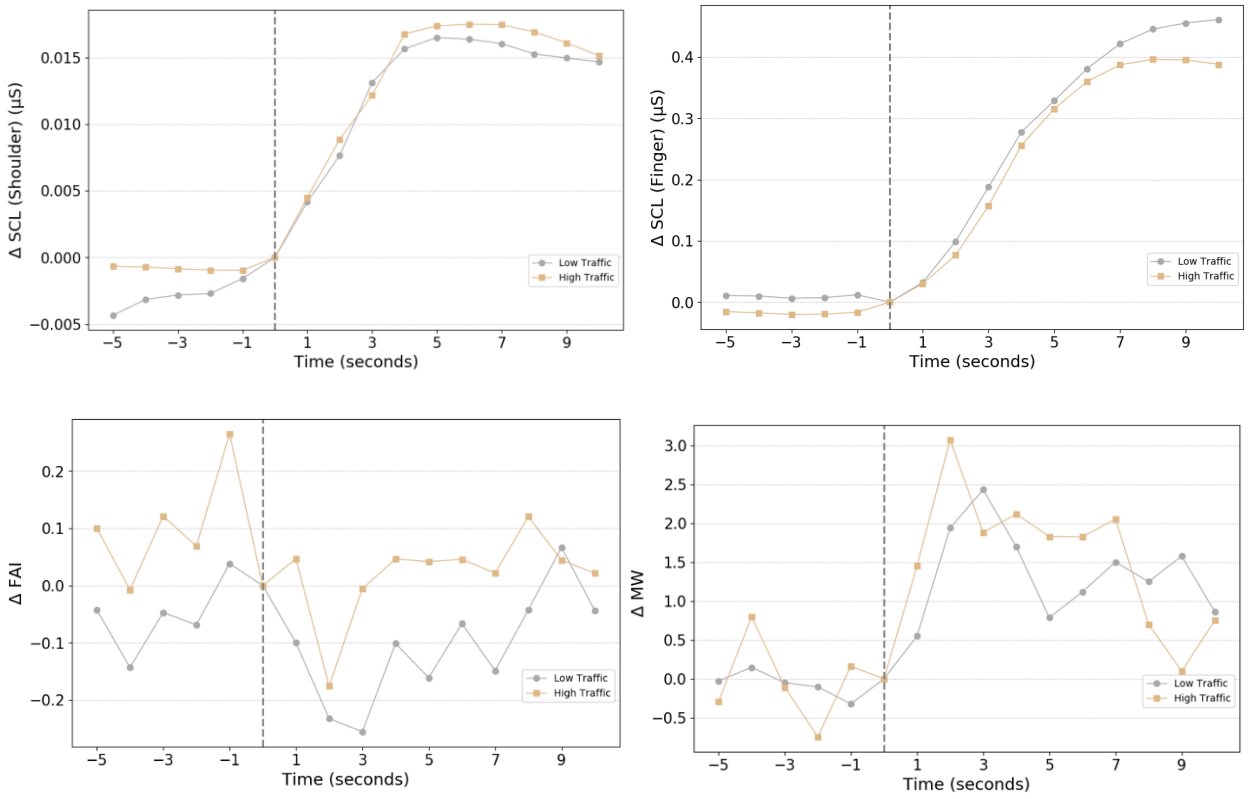

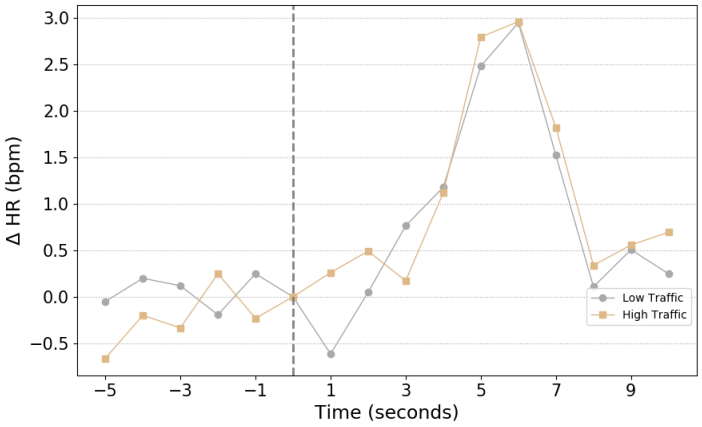

Fig. 7.13. Changes in the physiological during takeover behaviors with respect to traffic densities

7.4.4.2 Effect of traffic density on average physiological responses during the takeover periods

The Mean and standard deviation of physiological data concerning different traffic densities are summarized in Table 7.4. Although the traffic densities did not affect the pattern of the physiological responses during the takeover period, they did affect the average values of specific physiological data such as MW. As shown in Fig. 7.14, the average MW of the subjects was higher in high traffic density scenarios than which in low traffic density scenarios (Wilcoxon signed-rank: $p = 0.045$, Cliff's Delta = 0.03). However, for other physiological responses including FAI, their average values in high traffic density and low traffic density are not significantly different.

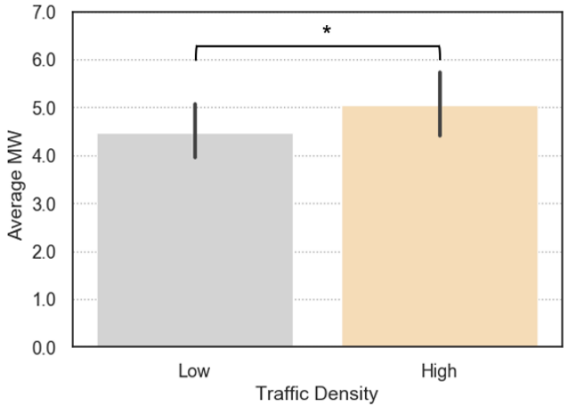

Fig. 7.14. Differences in physiological data with respect to traffic densities

Table 7.4. Mean and standard deviation of physiological data with respect to different traffic densities

	Low Traffic Density		High Traffic Density	
	Mean	**S.D.**	**Mean**	**S.D.**
SCL (Shoulder) (μS)	3.806	0.005	3.874	0.006
SCL (Finger) (μS)	3.853	0.166	3.757	0.15
FAI	0.708	0.092	0.695	0.069
MW	4.478	0.652	5.046	0.899
HR (bpm)	80.143	1.069	80.332	0.992

7.4.5 Correlation between the physiological data, takeover scenario, and takeover readiness

The corresponding correlation matrix between the physiological data, takeover scenarios, and takeover readiness indicators was created as shown in Fig. 7.15. Due to the better heat dissipation and sweat evaporation on fingers compared with the shoulder (covered by clothes), the SCL from fingers was used here. It can be seen that compared with other features, the takeover event played a slightly more important role in the maximum acceleration (Max Acc) and TTC of the vehicle, while the SCL was the second most relevant feature to the maximum acceleration. In addition, the reaction time is more relevant to the SCL and HR rather than other physiological data. Despite these, there was no specific physiological data or takeover scenario that dominate the takeover readiness. Thus, it is suggested that all the features should be integrated to make a more accurate prediction of the takeover readiness.

Fig. 7.15. Correlation matrix between the physiological data, takeover scenario, and vehicle data

7.4.6 Role of the individual differences

It can be seen from the previous sections that although there were significant differences in the average values of some types of physiological data based on statistical analysis, the results from Cliff's Delta were overall small. Since Cliff's Delta is fundamentally based on the probability of a value selected from one group that is larger than one selected from another group, personal differences in the physiological data might be the reason for the low values of Cliff's Delta [295]. Therefore, the distribution of the physiological data during the takeover periods with respect to different subjects was plotted. As shown in Fig. 7.16, the ranges of all the physiological data varied a lot across different individuals (with all the Nemenyi p-value <0.05), indicating that the specific physiological data of one subject could be much higher or lower than which of another subject. In

addition, it is obvious that the physiological responses of some subjects were more sensitive than others. For example, the MW of subjects 3, 4, 8, 10, and 19 is more stable than others. It can be seen that the ranges of the SCL collected from the shoulders were very small per each subject, which indicated that SCL from the shoulder was relatively stable physiological data.

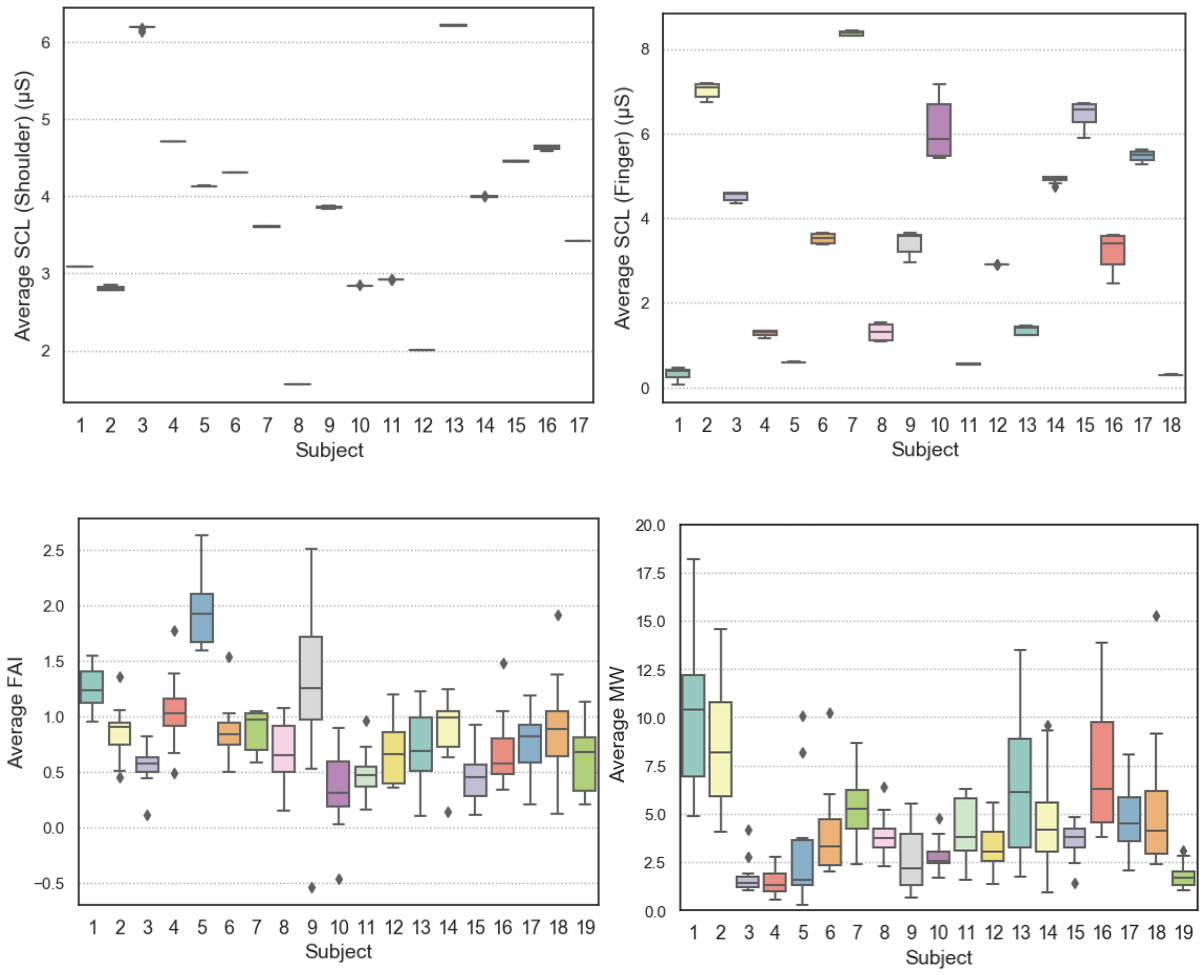

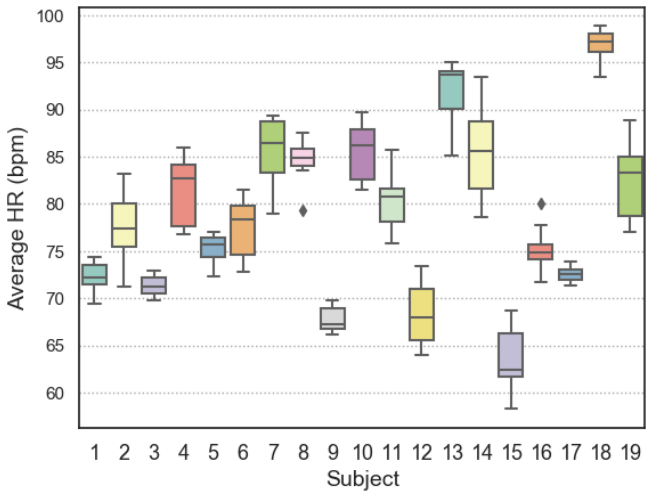

Fig. 7.16. Distribution of physiological data as per different subjects (the data from specific subjects is removed due to data corruption)

7.5 Discussion

7.5.1 Changes in physiological data

For all types of physiological indicators except FAI, increases were observed during the takeover periods compared with relatively stable values prior to the takeover alerts. The increases in the SCL signal reflected more intensive activities of the sympathetic nervous systems of the subjects, which indicated a strong correlation between the autonomic arousal [140] of the subjects and the takeover behaviors. Therefore, SCL could be a good feature for future research relevant to TOP. Although the pattern of changes in SCL collected from the shoulders and fingers were similar, their sensitivities varied a lot. The SCL collected from fingers was more than ten times more sensitive than those collected from the shoulders, which might be caused by the intensive movement or the exposure of the hands during the experiments. Similarly, the HR of the subjects increased rapidly after the alerts for the takeover. However, it dropped very rapidly to its normal level, which indicated that the effect of the takeover behaviors on HR was more instantaneous compared with other physiological data. Therefore, the values of HR before the takeover alerts might be less meaningful for indicating the human states during the takeover periods. Overall,

even focuses were different, the increasing pattern of the SCL and HR was consistent with the findings in the previous study conducted by Kim et al. [259], who compared the effect of the takeover requests with different lead times and alert types (i.e., visual and audio). The general pattern of MW was also slightly different from either SCL or HR, which increased rapidly at first but gradually decreased. The pattern indicated the MW of the subjects would increase fast when they realized that they need to take over the vehicles, while the subjects gradually relaxed as the takeover periods went on. In contrast to all other physiological responses, the FAI of the subjects, specifically during the scenarios with 1-back and 2-back tasks, slightly decreased right after the alerts of the takeover request. The results indicated that the subjects were engaged in the secondary task before the takeover periods, which distracted their attention from the driving activities. In this case, they were not able to concentrate on the takeover activities immediately after hearing the alerts.

7.5.2 Effect of takeover scenarios

Overall, the takeover scenarios would not affect the patterns of the changes in these physiological responses. However, specific takeover designs might lead to slight differences in the slope or peak of the changes. Specifically, the 2-back task might cause a more rapid increase and higher peak in changes of SCL. In addition, the statistical analysis of the average values of physiological data indicated that specific takeover scenarios could affect the average level of the physiological data. For example, the secondary tasks prior to the takeover could affect the average value of FAI. The results indicated that the overall engagement of the subjects during the takeover periods was lower when they were doing a harder secondary task prior to the takeover. One possible reason for this phenomenon is that the subjects were more distracted when they were doing harder the secondary task, thus preventing them from concentrating on the takeover

activities. This is consistent with the findings of a slight decrease in the FAI after the alerts of takeover requests. In contrast, a harder secondary task prior to the takeover activities could result in a higher MW of the subject even during the takeover periods. Similarly, an easier secondary task could lead to lower HR of the subjects during the takeover periods. However, the increased difficulty of the secondary tasks might not continuously increase the SCL of the subjects. These findings revealed that harder secondary tasks could potentially lead to more intensive neural activities.

The results also showed that takeover events would not affect the overall levels of physiological responses of the subjects except the HR. It was found that the HR of the subjects were relatively lower with a fake alert in which they would notice that they did not need to do any extra work except maintain the speed of the vehicles. In contrast, when there was an obstacle in front of their lane, their HR was relatively higher. However, the differences in the HR during the three takeover events were small compared to the original values of the HR, indicating that the takeover events were not likely to cause noticeable tensions among the subjects. As per the traffic density, the results showed that a higher traffic density could potentially result in higher MW for the subjects, which revealed that more surrounding vehicles might make the subjects feel more stressed during the takeover periods.

7.5.3 Correlation between the physiological data, takeover scenario, and takeover readiness indicators

Although several features such as takeover event, SCL, and HR had slightly higher correlations with the specific indicators of takeover readiness, none of them were found to dominate the results. It might indicate that the takeover readiness should be estimated from a variety of different features instead of a few specific inputs. In addition, the higher correlations

were not identical for different indicators of takeover readiness. For example, the SCL and takeover event were more related to TTC while the SCL and HR were more related to reaction time. Therefore, it is suggested that a classifier that combined the results of different vehicle data might be a better indicator of takeover readiness.

7.5.4 Effect of personal differences and possible solutions

Although some general patterns regarding the effect of takeover behaviors on physiological responses were found, the personal traits could not be neglected [296]. As indicated in Section 7.4.6, the ranges of the physiological data could be significantly different from one to another. These differences could be caused by the physical characteristics of people such as their age, gender, height, weight, and lifestyles, or the psychological issues during the experiments. Therefore, when considering using the physiological data collected from different subjects as the input features of the learning models (e.g., deep learning), it is important to eliminate the individual differences. Pre-processes such as log transformation, normalization, and standardization could be applied to scale down the mixed data points and bring them to similar ranges. For example, a standardization of the data as shown in Eq. (7.3) [205] could be applied. The data processed using this method only reflects how many standard deviations (SD) a data point offsets from one's average value. The value of 1 indicates that the value is one SD larger than the average value of the dataset. When the average values are coming from one subject, the results only reflect the relative offset rather than the absolute values, thus eliminating the effects of differences in data ranges caused by individual differences.

$$Standarized(x_i) = \frac{x_i - \mu}{\sigma} \tag{7.3}$$

Where x_i refer to the values of the data in different scenarios while μ is the average value of the dataset, and σ represents its standard deviation.

After applying the transformation, the data points from different subjects would theoretically be clustered together, thus improving the feasibility of using them as the input features of learning models.

7.5.5 Limitations and future work

While the results have provided many insights regarding the potential physiological factors for TOP, there are some limitations in this study. First, although the driving simulator could provide driving experiences that were very close to real driving, it could be new to the subjects. Even though the subjects were given opportunities to get used to the simulation, the results might still be slightly different from a real driving scenario. However, the design and environment of the simulation were consistent for all subjects across all scenarios, the results could still provide valuable references based on the pair-to-pair comparisons. Second, to fairly compare the data collected in different takeover scenarios, the duration and time interval of different takeover scenarios were set to be identical. Nevertheless, the time interval between takeover scenarios and the total driving time in the real world might vary a lot with more randomness. Therefore, the long-term effect of the driving activities on the takeover and physiological responses of the drivers could be investigated in the future. Finally, more diverse groups of subjects with distinct driving experiences and age groups would be considered in the future for further understanding of the effect of individual differences. Based on these findings, we aim to explore the feasibility of building TOP models using different learning models in the future.

7.6 Conclusions

This study investigated the effects of takeover activities on the physiological responses of the drivers in conditional automation. To conduct the experiments, a driving simulation program based on Unity and a driving simulator was developed. Different takeover scenarios (e.g.,

secondary tasks, takeover events, and traffic densities) were incorporated to diversify the experimental design. During the experiments, the typical physiological data (i.e., SCL, MW, FAI, and HR) was collected from the subjects. The tendencies of the changes in different physiological data before and during the takeover periods were plotted and analyzed. The results revealed that the FAI (which represents the engagement of the drivers) slightly decreased during the takeover period when they were shifted from 1-back or 2-back tasks prior to the takeover. In contrast, the MW, SCL (from shoulder and finger), and HR increased after the alerts of the takeover requests. Compared with SCL and MW, the HR increased rapidly and dropped back fast. A common finding from data collected from the shoulder and finger showed that the SCL increased slower with a lower peak when the takeover alerts were fake. Except for the effect of takeover events on the SCL, the pattern of the changes in physiological data was not affected by the types of takeover events for other physiological responses. However, the analysis of the average values of physiological data during the takeover periods revealed some effects of the takeover events on the drivers. The harder secondary tasks prior to the takeover could lead to lower engagement of the drivers during the takeover periods, indicating that difficult secondary tasks could distract people from preparing for the takeover activities. In contrast, hard secondary tasks prior to the takeover could potentially increase the HR and MW of the drivers during the takeover periods. In addition, a higher traffic density could increase the MW of the drivers during the takeover periods. It was also shown that an easier takeover event could result in lower HR for the drivers. Furthermore, the correlation matrix between the physiological data, takeover scenarios, and takeover readiness indicators was discussed. Since personal characteristics might play an important role in the physiological responses, the differences in the physiological data across individuals were analyzed with corresponding suggestions for standardization.

The contributions of this study include: first, a systematic analysis of the potential values of physiological data on conditional automation was conducted, and the results of the changes in physiological responses during takeover periods provided valuable references to support future studies such as selecting the physiological input features to estimate the TOP of the drivers. Second, the effect of takeover scenarios on the overall values of physiological data was analyzed, which could provide additional information regarding the design of the driving simulation in similar studies. Third, the correlation between the physiological data, takeover scenario, and indicators of takeover readiness was analyzed which revealed that although the takeover event, SCL, and HR were slightly more related to maximum acceleration and reaction time, none of the features dominated the takeover readiness. Fourth, the analysis of individual differences emphasized the importance of personal characteristics and the necessity of standardization or normalization when considering using the physiological data from different people for the training of the TOP prediction models.

Chapter 8 Conclusions

8.1 Research Contributions

This research contributes to promoting the human well-being and sustainability of communities by integrating personal human data in the management and control of enclosed spaces such as buildings and AVs. The specific contributions of this research are as follows:

- The proposed Digital ID-based framework can provide sufficient support for human-centric indoor monitoring and management.
- The joint optimization algorithm is able to maximize the thermal comfort of occupants while achieving building energy savings.
- A physiological sensing method is proposed to help investigate the effects of indoor environments on the mental states of the occupants.
- The effects of wearing a mask on occupants' mental states are investigated. The results indicate wearing masks might reduce MW and productivity.
- The effects of lighting conditions on occupants' work engagement are investigated. The results vary across individuals, while they can be used to predict work engagement along with easily measurable physiological data.
- A visualization platform is developed for the real-time monitoring of the human states in buildings.
- A systematic analysis of the effects of driving takeover behaviors on the physiological responses of the drivers is conducted. The results indicate that driving the takeover might

cause increases in SCL, HR, MW, and secondary tasks prior to the takeover might reduce the takeover engagement.

- The possibility of using physiological data and takeover scenarios to predict takeover readiness is investigated. The results reveal that the physiological data and takeover scenarios have great potential to be used to estimate takeover readiness.

8.2 Future Research Directions

I have prepared myself with expertise in human-building interaction, construction engineering, data analytics, energy simulation, machine learning, and robotics. I envision several directions as my research agenda in the near future.

8.2.1 Multi-indoor environment qualities (IEQs)

As described in my proposed DID framework, the human indoor experience should take all the IEQs into consideration. Therefore, I will continue to enrich the ideas from my doctoral research by extending the indoor environmental parameters to the broader list that refers to WELL standards (e.g., air quality, acoustic, and odor). Eventually, a more comprehensive understanding of the effect of IEQ on human physiological responses and productivity could be achieved.

8.2.2 Robots-assisted human-infrastructure interaction

Incorporating robots in the building environment as assistants of the infrastructure and environment monitoring could be an interesting and promising research field. Although some tasks could already be done with the help of the sensors I proposed, many tasks still require human effort. For example, during the construction and early operation stage of the infrastructure projects, people usually need to conduct repeated work or dangerous work such as monitoring the IEQs of the sites. Allowing robots to do these tasks could make the process safer and more efficient [297-299]. Therefore, I will adopt the mobile robots in the indoor environment and establish the

interaction between the robots and humans to assist with data collection (e.g., environmental data and human feedback) and specific tasks (e.g., facility monitoring).

8.2.3 Application in the broader context

While my doctoral research focuses on the interaction between human and indoor environments (of buildings and vehicles), I will find broader impacts of my research in the generalized AEC industry. In particular, I hope to adopt the concept of DID into broader domains (e.g., city scale) through extended phases (planning, design, construction, maintenance, and demolition).

Bibliography

[1] K. Ahmad, M. Maabreh, M. Ghaly, K. Khan, J. Qadir, A. Al-Fuqaha, Developing future human-centered smart cities: Critical analysis of smart city security, Data management, and Ethical challenges, Computer Science Review 43 (2022) 100452.

[2] J. Leech, R. Burnett, W. Nelson, S. Aaron, M. Raizenne, Outdoor air pollution epidemiologic studies, American Journal of Respiration Critical Care Medicine 161(3) (2000) A308.

[3] C.J. Matz, D.M. Stieb, M. Egyed, O. Brion, M. Johnson, Evaluation of daily time spent in transportation and traffic-influenced microenvironments by urban Canadians, Air Quality, Atmosphere & Health 11(2) (2018) 209-220.

[4] T. Cheung, S. Schiavon, T. Parkinson, P. Li, G. Brager, Analysis of the accuracy on PMV – PPD model using the ASHRAE Global Thermal Comfort Database II, Building and Environment 153 (2019) 205-217.

[5] J. Kim, S. Schiavon, G. Brager, Personal comfort models – A new paradigm in thermal comfort for occupant-centric environmental control, Building and Environment 132 (2018) 114-124.

[6] W. Jung, F. Jazizadeh, Energy saving potentials of integrating personal thermal comfort models for control of building systems: Comprehensive quantification through combinatorial consideration of influential parameters, Applied Energy 268 (2020) 114882.

[7] J. Ngarambe, G.Y. Yun, M. Santamouris, The use of artificial intelligence (AI) methods in the prediction of thermal comfort in buildings: energy implications of AI-based thermal comfort controls, Energy and Buildings 211 (2020) 109807.

[8] S.-i. Tanabe, M. Haneda, N. Nishihara, Workplace productivity and individual thermal satisfaction, Building and Environment 91 (2015) 42-50.

[9] O.A. Seppänen, W. Fisk, Some Quantitative Relations between Indoor Environmental Quality and Work Performance or Health, HVAC&R Research 12(4) (2006) 957-973.

[10] T. Akimoto, S.-i. Tanabe, T. Yanai, M. Sasaki, Thermal comfort and productivity - Evaluation of workplace environment in a task conditioned office, Building and Environment 45(1) (2010) 45-50.

[11] M. Frontczak, S. Schiavon, J. Goins, E. Arens, H. Zhang, P. Wargocki, Quantitative relationships between occupant satisfaction and satisfaction aspects of indoor environmental quality and building design, 22(2) (2012) 119-131.

[12] ASHRAE, Standard 55-2017, Thermal Environmental Conditions for Human Occupancy, Atlanta USA, 2017.

[13] V.J.L. Gan, M. Deng, Y. Tan, W. Chen, J.C.P. Cheng, BIM-based framework to analyze the effect of natural ventilation on thermal comfort and energy performance in buildings, Energy Procedia 158 (2019) 3319-3324.

[14] T. Sood, P. Janssen, C. Miller, Spacematch: Using environmental preferences to match occupants to suitable activity-based workspaces, Frontiers in Built Environment 6 (2020) 113.

[15] V. Földváry Ličina, T. Cheung, H. Zhang, R. de Dear, T. Parkinson, E. Arens, C. Chun, S. et al., Development of the ASHRAE Global Thermal Comfort Database II, Building and Environment 142 (2018) 502-512.

[16] L. Pérez-Lombard, J. Ortiz, C. Pout, A review on buildings energy consumption information, Energy and Buildings 40(3) (2008) 394-398.

[17] J. Wu, Z. Huang, Z. Hu, C. Lv, Toward human-in-the-loop AI: Enhancing deep reinforcement learning via real-time human guidance for autonomous driving, Engineering (2022).

[18] L. Liu, S. Lu, R. Zhong, B. Wu, Y. Yao, Q. Zhang, W. Shi, Computing Systems for Autonomous Driving: State of the Art and Challenges, IEEE Internet of Things Journal 8(8) (2021) 6469-6486.

[19] N. Du, F. Zhou, E.M. Pulver, D.M. Tilbury, L.P. Robert, A.K. Pradhan, X.J. Yang, Predicting driver takeover performance in conditionally automated driving, Accident Analysis & Prevention 148 (2020) 105748.

[20] W.B. Schaufeli, M. Salanova, V. González-romá, A.B. Bakker, The Measurement of Engagement and Burnout: A Two Sample Confirmatory Factor Analytic Approach, Journal of Happiness Studies 3(1) (2002) 71-92.

[21] A.F. Kramer, Physiological metrics of mental workload: A review of recent progress, 1991.

[22] L. Kremer, M. Lipprandt, R. Röhrig, B. Breil, Examining Mental Workload Relating to Digital Health Technologies in Health Care: Systematic Review, J Med Internet Res 24(10) (2022) e40946.

[23] X. Wang, D. Li, C.C. Menassa, V.R. Kamat, Investigating the effect of indoor thermal environment on occupants' mental workload and task performance using electroencephalogram, Building and Environment 158 (2019) 120-132.

[24] J. Anitha, Determinants of employee engagement and their impact on employee performance, International Journal of Productivity and Performance Management 63(3) (2014) 308-323.

[25] V. Saxena, R. Srivastava, Impact of employee engagement on employee performance–Case of manufacturing sectors, International Journal of Management Research and Business Strategy 4(2) (2015) 139-174.

[26] J. Hanaysha, Improving employee productivity through work engagement: Evidence from higher education sector, Management Science Letters 6(1) (2016) 61-70.

[27] MIRVAC, The Super Experience - Designing for Talent in the Digital Workplace, 2019. https://cdn.worktechacademy.com/uploads/2019/09/WORKTECH-Academy-Mirvac-The-Super-Experience-White-Paper-2019.pdf?_ga=2.79728144.628437762.1577049988-1390632762.1577049988.

[28] Humanyze, Data to Design - Bringing the Right Intelligence to Redesigning the Workplace, 2018. https://cdn.worktechacademy.com/uploads/2018/12/WORKTECH-Academy-Humanyze-Data-to-Design-Report.pdf?_ga=2.40387493.628437762.1577049988-1390632762.1577049988.

[29] C. Huizenga, S. Abbaszadeh, L. Zagreus, E.A. Arens, Air quality and thermal comfort in office buildings: results of a large indoor environmental quality survey, Proceeding of Healthy Buildings, 2006, pp. 393-397.

[30] D.K. Milton, P.M. Clencross, M.D. Walters, Risk of sick leave associated with outdoor air supply rate, humidification, and occupant complaints, Indoor air 10 (2000) 212-221.

[31] P. Wargocki, D.P. Wyon, J. Sundell, G. Clausen, P.O.J.I.a. Fanger, The effects of outdoor air supply rate in an office on perceived air quality, sick building syndrome (SBS) symptoms and productivity, 10(4) (2000) 222-236.

[32] L. Lan, P. Wargocki, D.P. Wyon, Z. Lian, Effects of thermal discomfort in an office on perceived air quality, SBS symptoms, physiological responses, and human performance, Indoor Air 21(5) (2011) 376-390.

[33] S. Tang, D.R. Shelden, C.M. Eastman, P. Pishdad-Bozorgi, X. Gao, A review of building information modeling (BIM) and the internet of things (IoT) devices integration: Present status and future trends, Automation in Construction 101 (2019) 127-139.

[34] M.M. Rathore, A. Ahmad, A. Paul, S. Rho, Urban planning and building smart cities based on the Internet of Things using Big Data analytics, Computer Networks 101 (2016) 63-80.

[35] S. Zhan, A. Chong, B. Lasternas, Automated recognition and mapping of building management system (BMS) data points for building energy modeling (BEM), Building Simulation 14(1) (2021) 43-52.

[36] D. Li, C.C. Menassa, V.R. Kamat, Personalized human comfort in indoor building environments under diverse conditioning modes, Building and Environment 126 (2017) 304-317.

[37] B. Dong, V. Prakash, F. Feng, Z. O'Neill, A review of smart building sensing system for better indoor environment control, Energy and Buildings 199 (2019) 29-46.

[38] M. Deng, C.C. Menassa, V.R. Kamat, From BIM to digital twins: a systematic review of the evolution of intelligent building representations in the AEC-FM industry, Journal of Information Technology in Construction (ITcon) 26(5) (2021) 58-83.

[39] H.N. Rafsanjani, A. Ghahramani, Towards utilizing internet of things (IoT) devices for understanding individual occupants' energy usage of personal and shared appliances in office buildings, Journal of Building Engineering 27 (2020) 100948.

[40] F.A. Machado, C.G. Dezotti, R.C. Ruschel, The Interface Layer of a BIM-IoT Prototype for Energy Consumption Monitoring, in: I. Mutis, T. Hartmann (Eds.) Advances in Informatics and

Computing in Civil and Construction Engineering, Springer International Publishing, Cham, 2019, pp. 685-693.

[41] Z. Riaz, M. Arslan, F. Peña-Mora, Challenges in Data Management When Monitoring Confined Spaces Using BIM and Wireless Sensor Technology, Computing in Civil Engineering 20152015, pp. 123-130.

[42] K.-M. Chang, R.-J. Dzeng, Y.-J.J.A.s. Wu, An automated IoT visualization BIM platform for decision support in facilities management, 8(7) (2018) 1086.

[43] D. Pasini, Connecting BIM and IoT for addressing user awareness toward energy savings, Journal of Structural Integrity and Maintenance 3(4) (2018) 243-253.

[44] A. Ioannou, L. Itard, T. Agarwal, In-situ real time measurements of thermal comfort and comparison with the adaptive comfort theory in Dutch residential dwellings, Energy and Buildings 170 (2018) 229-241.

[45] D. Lee, G. Cha, S. Park, A study on data visualization of embedded sensors for building energy monitoring using BIM, International Journal of Precision Engineering and Manufacturing 17(6) (2016) 807-814.

[46] D. Pasini, S.M. Ventura, S. Rinaldi, P. Bellagente, A. Flammini, A.L.C. Ciribini, Exploiting Internet of Things and building information modeling framework for management of cognitive buildings, 2016 IEEE International Smart Cities Conference (ISC2), 2016, pp. 1-6.

[47] Y. Nakama, Y. Onishi, K. Iki, Development of building information management system with data collecting functions based on IoT technology, 33rd eCAADe Conference Proceedings, Vienna, Austria, 2015.

[48] M. Marzouk, A. Abdelaty, Monitoring thermal comfort in subways using building information modeling, Energy and Buildings 84 (2014) 252-257.

[49] Q. Lu, A.K. Parlikad, P. Woodall, G.D. Ranasinghe, J. Heaton, Developing a Dynamic Digital Twin at a Building Level: using Cambridge Campus as Case Study, International Conference on Smart Infrastructure and Construction 2019 (ICSIC), pp. 67-75.

[50] G.M. Revel, M. Arnesano, F. Pietroni, A Low-Cost Sensor for Real-Time Monitoring of Indoor Thermal Comfort for Ambient Assisted Living, in: S. Longhi, P. Siciliano, M. Germani, A. Monteriù (Eds.) Ambient Assisted Living, Springer International Publishing, Cham, 2014, pp. 3-12.

[51] K.-M. Chang, R.-J. Dzeng, Y.-J. Wu, An Automated IoT Visualization BIM Platform for Decision Support in Facilities Management, Appl. Sci 8, 1086 (2018).

[52] T.V. Tran, N.T. Dang, W.-Y. Chung, Battery-free smart-sensor system for real-time indoor air quality monitoring, Sensors and Actuators B: Chemical 248 (2017) 930-939.

[53] J. Kim, C. Chu, S. Shin, ISSAQ: An Integrated Sensing Systems for Real-Time Indoor Air Quality Monitoring, IEEE Sensors Journal 14(12) (2014) 4230-4244.

[54] S. Karjalainen, Gender differences in thermal comfort and use of thermostats in everyday thermal environments, Building and Environment 42(4) (2007) 1594-1603.

[55] G. Calis, M. Kuru, Statistical significance of gender and age on thermal comfort: a case study in Turkey, Thomas Telford Ltd, 2017, pp. 40-51.

[56] G. Matthews, L. Reinerman-Jones, J. Abich, A. Kustubayeva, Metrics for individual differences in EEG response to cognitive workload: Optimizing performance prediction, Personality and Individual Differences 118 (2017) 22-28.

[57] M. Deng, X. Wang, C.C. Menassa, Measurement and prediction of work engagement under different indoor lighting conditions using physiological sensing, Building and Environment 203 (2021) 108098.

[58] P.J. Stone, R. Luchetti, Your office is where you are, 63(2) (1985) 102-117.

[59] R. Appel-Meulenbroek, P. Groenen, I. Janssen, An end-user's perspective on activity-based office concepts, Journal of Corporate Real Estate 13(2) (2011) 122-135.

[60] H. Jahncke, D.M. Hallman, Objective measures of cognitive performance in activity based workplaces and traditional office types, Journal of Environmental Psychology 72 (2020) 101503.

[61] L. Arundell, B. Sudholz, M. Teychenne, J. Salmon, B. Hayward, G.N. Healy, A. Timperio, The Impact of Activity Based Working (ABW) on Workplace Activity, Eating Behaviours, Productivity, and Satisfaction, International Journal of Environmental Research and Public Health 15(5) (2018).

[62] L. Engelen, J. Chau, S. Young, M. Mackey, D. Jeyapalan, A. Bauman, Is activity-based working impacting health, work performance and perceptions? A systematic review, Building Research & Information 47(4) (2019) 468-479.

[63] M.S. Rahaman, H. Pare, J. Liono, F.D. Salim, Y. Ren, J. Chan, S. Kudo, T. Rawling, A. Sinickas, OccuSpace: Towards a Robust Occupancy Prediction System for Activity Based Workplace, 2019 IEEE International Conference on Pervasive Computing and Communications Workshops (PerCom Workshops), 2019, pp. 415-418.

[64] O.T. Masoso, L.J. Grobler, The dark side of occupants' behaviour on building energy use, Energy and Buildings 42(2) (2010) 173-177.

[65] M. Deng, B. Fu, C. Menassa, Room match: Achieving thermal comfort through smart space allocation and environmental control in buildings, Proceedings of the 2021 Winter Simulation Conference, 2021.

[66] K. Ho, H.W. Hirai, Y. Kuo, H.M. Meng, K.K.F. Tsoi, Indoor Air Monitoring Platform and Personal Health Reporting System: Big Data Analytics for Public Health Research, 2015 IEEE International Congress on Big Data, 2015, pp. 309-312.

[67] D. Li, C.C. Menassa, V.R. Kamat, Non-intrusive interpretation of human thermal comfort through analysis of facial infrared thermography, Energy and Buildings 176 (2018) 246-261.

[68] D. Li, C.C. Menassa, V.R. Kamat, Robust non-intrusive interpretation of occupant thermal comfort in built environments with low-cost networked thermal cameras, Applied Energy 251 (2019) 113336.

[69] G. Ma, Y. Liu, S. Shang, A building information model (BIM) and artificial neural network (ANN) based system for personal thermal comfort evaluation and energy efficient design of interior space, Sustainability 11(18) (2019) 4972.

[70] T. Yang, A. Bandyopadhyay, Z. O'Neill, J. Wen, B. Dong, From occupants to occupants: A review of the occupant information understanding for building HVAC occupant-centric control, Building Simulation 15(6) (2022) 913-932.

[71] T. Litman, Autonomous vehicle implementation predictions, Victoria Transport Policy Institute Victoria, Canada2017.

[72] SAE, Taxonomy and Definitions for Terms Related to Driving Automation Systems for On-Road Motor Vehicles, 2018. https://www.sae.org/standards/content/j3016_201806/.

[73] NTSB, Tesla Crash Investigation Yields 9 NTSB Safety Recommendations, 2020. https://www.ntsb.gov/news/press-releases/pages/nr20200225.aspx.

[74] C. Irwin, S. Monement, B. Desbrow, The Influence of Drinking, Texting, and Eating on Simulated Driving Performance, Traffic Injury Prevention 16(2) (2015) 116-123.

[75] N. Deo, M.M. Trivedi, Looking at the Driver/Rider in Autonomous Vehicles to Predict Take-Over Readiness, IEEE Transactions on Intelligent Vehicles 5(1) (2020) 41-52.
[76] R.A. Naqvi, M. Arsalan, G. Batchuluun, H.S. Yoon, K.R. Park, Deep Learning-Based Gaze Detection System for Automobile Drivers Using a NIR Camera Sensor, Sensors 18(2) (2018).
[77] V.J.L. Gan, H. Luo, Y. Tan, M. Deng, H.L. Kwok, BIM and Data-Driven Predictive Analysis of Optimum Thermal Comfort for Indoor Environment, Sensors 21(13) (2021).
[78] S.K. Gupta, S. Atkinson, I. O'Boyle, J. Drogo, K. Kar, S. Mishra, J.T. Wen, BEES: Real-time occupant feedback and environmental learning framework for collaborative thermal management in multi-zone, multi-occupant buildings, Energy and Buildings 125 (2016) 142-152.
[79] M. André, R. De Vecchi, R. Lamberts, User-centered environmental control: a review of current findings on personal conditioning systems and personal comfort models, Energy and Buildings 222 (2020) 110011.
[80] I. Adjabi, A. Ouahabi, A. Benzaoui, A. Taleb-Ahmed, Past, Present, and Future of Face Recognition: A Review, Electronics 9(8) (2020).
[81] M. Indraganti, K.D. Rao, Effect of age, gender, economic group and tenure on thermal comfort: A field study in residential buildings in hot and dry climate with seasonal variations, Energy and Buildings 42(3) (2010) 273-281.
[82] S. Thapa, Insights into the thermal comfort of different naturally ventilated buildings of Darjeeling, India – Effect of gender, age and BMI, Energy and Buildings 193 (2019) 267-288.
[83] M. Indraganti, R. Ooka, H.B. Rijal, Thermal comfort in offices in India: Behavioral adaptation and the effect of age and gender, Energy and Buildings 103 (2015) 284-295.
[84] K. Kang, J. Lin, J. Zhang, BIM- and IoT-based monitoring framework for building performance management, Journal of Structural Integrity and Maintenance 3(4) (2018) 254-261.

[85] J. Teizer, M. Wolf, O. Golovina, M. Perschewski, M. Propach, M. Neges, M. König, Internet of Things (IoT) for Integrating Environmental and Localization Data in Building Information Modeling (BIM), IAARC Publications, Waterloo, 2017, pp. 1-7.

[86] J. Ferreira, R. Resende, S. Martinho, Beacons and BIM models for indoor guidance and location, Sensors 18(12) (2018) 4374.

[87] J.C.P. Putra, A Study of Thermal Comfort and Occupant Satisfaction in Office Room, Procedia Engineering 170 (2017) 240-247.

[88] R.F. Rupp, N.G. Vásquez, R. Lamberts, A review of human thermal comfort in the built environment, Energy and Buildings 105 (2015) 178-205.

[89] D. Ormandy, V. Ezratty, Health and thermal comfort: From WHO guidance to housing strategies, Energy Policy 49 (2012) 116-121.

[90] L. Lan, P. Wargocki, Z. Lian, Quantitative measurement of productivity loss due to thermal discomfort, Energy and Buildings 43(5) (2011) 1057-1062.

[91] C. Karmann, S. Schiavon, E. Arens, Percentage of commercial buildings showing at least 80% occupant satisfied with their thermal comfort, 10th Windsor Conference, Windsor, UK, 2018.

[92] R. Yao, B. Li, J. Liu, A theoretical adaptive model of thermal comfort – Adaptive Predicted Mean Vote (aPMV), Building and Environment 44(10) (2009) 2089-2096.

[93] S.B. Godithi, E. Sachdeva, V. Garg, R. Brown, C. Kohler, R. Rawal, A review of advances for thermal and visual comfort controls in personal environmental control (PEC) systems, Intelligent Buildings International 11(2) (2019) 75-104.

[94] M. Luo, E. Arens, H. Zhang, A. Ghahramani, Z. Wang, Thermal comfort evaluated for combinations of energy-efficient personal heating and cooling devices, Building and Environment 143 (2018) 206-216.

[95] M. Veselý, P. Molenaar, M. Vos, R. Li, W. Zeiler, Personalized heating – Comparison of heaters and control modes, Building and Environment 112 (2017) 223-232.

[96] N.K. Kandasamy, G. Karunagaran, C. Spanos, K.J. Tseng, B.-H. Soong, Smart lighting system using ANN-IMC for personalized lighting control and daylight harvesting, Building and Environment 139 (2018) 170-180.

[97] D. Li, C.C. Menassa, V.R. Kamat, A Personalized HVAC Control Smartphone Application Framework for Improved Human Health and Well-Being, Computing in Civil Engineering 20172017, pp. 82-90.

[98] A. Thomas, C.C. Menassa, V.R. Kamat, A systems simulation framework to realize net-zero building energy retrofits, Sustainable Cities and Society 41 (2018) 405-420.

[99] C. Menassa Carol, R. Kamat Vineet, S. Lee, E. Azar, C. Feng, K. Anderson, Conceptual Framework to Optimize Building Energy Consumption by Coupling Distributed Energy Simulation and Occupancy Models, Journal of Computing in Civil Engineering 28(1) (2014) 50-62.

[100] S. Yang, M.P. Wan, W. Chen, B.F. Ng, S. Dubey, Model predictive control with adaptive machine-learning-based model for building energy efficiency and comfort optimization, Applied Energy 271 (2020) 115147.

[101] EIA, U.S. energy consumption by source and sector, 2021. https://www.eia.gov/tools/faqs/faq.php?id=86&t=1#:~:text=In%202021%2C%20the%20combin

ed%20end,British%20thermal%20units%20(Btu).&text=This%20was%20equal%20to%20about,use%20energy%20consumption%20in%202021.

[102] M. Deng, X. Wang, D. Li, C.C. Menassa, Digital ID framework for human-centric monitoring and control of smart buildings, Building Simulation 15(10) (2022) 1709-1728.

[103] Z. Wang, J. Wang, Y. He, Y. Liu, B. Lin, T. Hong, Dimension analysis of subjective thermal comfort metrics based on ASHRAE Global Thermal Comfort Database using machine learning, Journal of Building Engineering 29 (2020) 101120.

[104] J. Guenther, O. Sawodny, Feature selection and Gaussian Process regression for personalized thermal comfort prediction, Building and Environment 148 (2019) 448-458.

[105] J. Kim, Y. Zhou, S. Schiavon, P. Raftery, G. Brager, Personal comfort models: Predicting individuals' thermal preference using occupant heating and cooling behavior and machine learning, Building and Environment 129 (2018) 96-106.

[106] S. Liu, S. Schiavon, H.P. Das, M. Jin, C.J. Spanos, Personal thermal comfort models with wearable sensors, Building and Environment 162 (2019) 106281.

[107] E. Laftchiev, D. Nikovski, An IoT system to estimate personal thermal comfort, 2016 IEEE 3rd World Forum on Internet of Things (WF-IoT), 2016, pp. 672-677.

[108] A.C. Cosma, R. Simha, Machine learning method for real-time non-invasive prediction of individual thermal preference in transient conditions, Building and Environment 148 (2019) 372-383.

[109] D. Pisinger, S. Ropke, Large Neighborhood Search, in: M. Gendreau, J.-Y. Potvin (Eds.), Handbook of Metaheuristics, Springer US, Boston, MA, 2010, pp. 399-419.

[110] M. Wen, E. Linde, S. Ropke, P. Mirchandani, A. Larsen, An adaptive large neighborhood search heuristic for the Electric Vehicle Scheduling Problem, Computers & Operations Research 76 (2016) 73-83.

[111] B. Funke, T. Grünert, S. Irnich, Local Search for Vehicle Routing and Scheduling Problems: Review and Conceptual Integration, Journal of Heuristics 11(4) (2005) 267-306.

[112] A.A. Kovacs, S.N. Parragh, K.F. Doerner, R.F. Hartl, Adaptive large neighborhood search for service technician routing and scheduling problems, Journal of Scheduling 15(5) (2012) 579-600.

[113] B. Fu, T. Kathuria, D. Rizzo, M. Castanier, X.J. Yang, M. Ghaffari, K. Barton, Simultaneous Human-Robot Matching and Routing for Multi-Robot Tour Guiding Under Time Uncertainty, Journal of Autonomous Vehicles and Systems 1(4) (2022).

[114] A.E. Phillips, H. Waterer, M. Ehrgott, D.M. Ryan, Integer programming methods for large-scale practical classroom assignment problems, Computers & Operations Research 53 (2015) 42-53.

[115] B. Fu, W. Smith, D. Rizzo, M. Castanier, M. Ghaffari, K. Barton, Robust task scheduling for heterogeneous robot teams under capability uncertainty, arXiv preprint arXiv:2106.12111 (2021).

[116] I. Keller, C. Tompkins, An Extension of a Theorem of Dantzig's. Linear Inequalities and Related Systems, Annals of Mathematics Studies 38 (1956) 247-254.

[117] C. Guanquan, S. Jinhua, The Effect of Pre-movement Time and Occupant Density on Evacuation Time, Journal of Fire Sciences 24(3) (2006) 237-259.

[118] L. Arakawa Martins, V. Soebarto, T. Williamson, A systematic review of personal thermal comfort models, Building and Environment 207 (2022) 108502.

[119] M. Karami, G.V. McMorrow, L. Wang, Continuous monitoring of indoor environmental quality using an Arduino-based data acquisition system, Journal of Building Engineering 19 (2018) 412-419.

[120] E. Zender – Świercz, Improvement of indoor air quality by way of using decentralised ventilation, Journal of Building Engineering 32 (2020) 101663.

[121] H. Al-Dmour, A. Salman, M. Abuhashesh, R. Al-Dmour, Influence of social media platforms on public health protection against the COVID-19 pandemic via the mediating effects of public health awareness and behavioral changes: integrated model, Journal of Medical Internet Research 22(8) (2020) e19996.

[122] T.M. Yildirim, H. Eslen-Ziya, The differential impact of COVID-19 on the work conditions of women and men academics during the lockdown, 28(S1) (2021) 243-249.

[123] CDC, The United States Centers for Disease Control and Prevention, 2021. https://www.cdc.gov/coronavirus/2019-ncov/prevent-getting-sick/types-of-masks.html.

[124] OSHA, United States Department of Labor, Occupational Safety and Health Administration, 2021. https://www.osha.gov/coronavirus.

[125] WHO, World Health Organization, 2021. https://www.who.int/news-room/q-a-detail/coronavirus-disease-covid-19-masks.

[126] M. Kaushik, N. Guleria, The impact of pandemic COVID-19 in workplace, European Journal of Business Management 12(15) (2020) 1-10.

[127] D. Spurk, C. Straub, Flexible employment relationships and careers in times of the COVID-19 pandemic, Journal of Vocational Behavior 119 (2020) 103435.

[128] L.T.D. Siqueira, A.P.d. Santos, R.L.F. Silva, P.A.M. Moreira, J.d.S. Vitor, V.V. Ribeiro, Vocal self-perception of home office workers during the COVID-19 pandemic, Journal of Voice (2020).

[129] M. Tysiąc-Miśta, A. Dubiel, K. Brzoza, M. Burek, K. Pałkiewicz, Air disinfection procedures in the dental office during the COVID-19 pandemic, Med Pr 72(1) (2021) 39-48.

[130] M.T. Hall, H.Q. Bui, J. Rowe, T.A. Do, COVID-19 Case and Contact Investigation in an Office Workspace, Military Medicine 185(11-12) (2020) e2162-e2165.

[131] M. Liang, L. Gao, C. Cheng, Q. Zhou, J.P. Uy, K. Heiner, C. Sun, Efficacy of face mask in preventing respiratory virus transmission: A systematic review and meta-analysis, Travel Medicine and Infectious Disease 36 (2020) 101751.

[132] C. Liu, G. Li, Y. He, Z. Zhang, Y. Ding, Effects of wearing masks on human health and comfort during the COVID-19 pandemic, IOP Conference Series: Earth and Environmental Science 531 (2020) 012034.

[133] C.S.W. Law, P.S. Lan, G.H. Glover, Effect of wearing a face mask on fMRI BOLD contrast, NeuroImage 229 (2021) 117752.

[134] Z. Tian, B.-Y. Kim, M.-J. Bae, A study on the effect of wearing masks on stress response, Memory 8 (2020) 12.

[135] Y. Li, H. Tokura, Y.P. Guo, A.S.W. Wong, T. Wong, J. Chung, E. Newton, Effects of wearing N95 and surgical facemasks on heart rate, thermal stress and subjective sensations, International Archives of Occupational and Environmental Health 78(6) (2005) 501-509.

[136] J. Moran, Queuing for beginners: The story of daily life from breakfast to bedtime, Profile Books2010.

[137] Y. Singh, R. Sharma, Individual alpha frequency (IAF) based quantitative EEG correlates of psychological stress, Indian J Physiol Pharmacol 59(4) (2015) 414-421.

[138] P. Tarnowski, M. Kołodziej, A. Majkowski, R.J. Rak, Combined analysis of GSR and EEG signals for emotion recognition, 2018 International Interdisciplinary PhD Workshop (IIPhDW), 2018, pp. 137-141.

[139] T. Kimura, N. Takemura, Y. Nakashima, H. Kobori, H. Nagahara, M. Numao, K. Shinohara, Warmer Environments Increase Implicit Mental Workload Even If Learning Efficiency Is Enhanced, Frontiers in psychology 11(568) (2020).

[140] J. Braithwaite, D. Watson, R. Jones, M. Rowe, A guide for analysing Electrodermal Activity (EDA) & Skin Conductance Responses (SCRs) for psychological experiments (Revised version 2.0), Retrieved (6 April, 2018) from http://www. biopac. com/wp-content/uploads/EDA-SCR-Analysis. pdf (2015).

[141] W. Boucsein, Electrodermal activity, Springer Science & Business Media2012.

[142] C.-C. Carbon, Wearing Face Masks Strongly Confuses Counterparts in Reading Emotions, 11(2526) (2020).

[143] O. Geiss, Effect of Wearing Face Masks on the Carbon Dioxide Concentration in the Breathing Zone, Aerosol and Air Quality Research 21(2) (2021) 200403.

[144] A. Elkhouly, M.F.A. Malek, S. Arza, Effect of Wearing Protective Mask During Exposure to EMF on Body Temperature and Heart Rate, 2019 International Conference on Electrical and Computing Technologies and Applications (ICECTA), 2019, pp. 1-5.

[145] Y. Choi, M. Kim, C. Chun, Effect of temperature on attention ability based on electroencephalogram measurements, Building and Environment 147 (2019) 299-304.

[146] T.L. Smith-Jackson, K.W. Klein, Open-plan offices: Task performance and mental workload, Journal of Environmental Psychology 29(2) (2009) 279-289.

[147] B. Zheng, M.A. Cassera, D.V. Martinec, G.O. Spaun, L.L. Swanström, Measuring mental workload during the performance of advanced laparoscopic tasks, Surgical Endoscopy 24(1) (2009) 45.

[148] Z. Wu, N. Li, J. Peng, J. Li, Effect of long-term indoor thermal history on human physiological and psychological responses: A pilot study in university dormitory buildings, Building and Environment 166 (2019) 106425.

[149] L. Lan, Z. Lian, L. Pan, Q. Ye, Neurobehavioral approach for evaluation of office workers' productivity: The effects of room temperature, Building and Environment 44(8) (2009) 1578-1588.

[150] C. Hocking, R.B. Silberstein, W.M. Lau, C. Stough, W. Roberts, Evaluation of cognitive performance in the heat by functional brain imaging and psychometric testing, Comparative Biochemistry and Physiology Part A: Molecular & Integrative Physiology 128(4) (2001) 719-734.

[151] J. Toftum, D. Wyon, H. Svanekjær, A. Lantner, Remote performance measurement (RPM)–A new, internet-based method for the measurement of occupant performance in office buildings, 10th International Conference on Indoor Air Quality and Climate, 2005, pp. 357-361.

[152] L. Lan, Z. Lian, Use of neurobehavioral tests to evaluate the effects of indoor environment quality on productivity, Building and Environment 44(11) (2009) 2208-2217.

[153] L. Astolfi, F.D.V. Fallani, F. Cincotti, D. Mattia, L. Bianchi, M.G. Marciani, S. Salinari, A. Colosimo, A. Tocci, R. Soranzo, F. Babiloni, Neural Basis for Brain Responses to TV

Commercials: A High-Resolution EEG Study, IEEE Transactions on Neural Systems and Rehabilitation Engineering 16(6) (2008) 522-531.

[154] J.G. Allen, P. MacNaughton, U. Satish, S. Santanam, J. Vallarino, J.D. Spengler, Associations of cognitive function scores with carbon dioxide, ventilation, and volatile organic compound exposures in office workers: a controlled exposure study of green and conventional office environments, Environmental Health Perspectives 124(6) (2016) 805-812.

[155] M. Wilson, People trust black COVID-19 masks more than others. But why?, 2021. https://www.fastcompany.com/90600546/people-trust-black-covid-19-masks-more-than-others-but-why.

[156] U.S. General Services Administration, 6.15 Lighting, 2022. https://www.gsa.gov/node/82715.

[157] W. Su, B. Yang, B. Zhou, F. Wang, A. Li, A novel convection and radiation combined terminal device: Its impact on occupant thermal comfort and cognitive performance in winter indoor environments, Energy and Buildings 246 (2021) 111123.

[158] J. Lee, T. Wan Kim, C. Lee, C. Koo, Integrated Approach to Evaluating the Effect of Indoor CO2 Concentration on Human Cognitive Performance and Neural Responses in Office Environment, Journal of Management in Engineering 38(1) (2022) 04021085.

[159] P. Wargocki, D.P. Wyon, P.O. Fanger, Productivity is affected by the air quality in offices, Proceedings of Healthy Buildings, 2000, pp. 635-40.

[160] Z. Bako-Biro, P. Wargocki, C. Weschler, P.O. Fanger, Personal computers pollute indoor air: effects on perceived air quality, SBS symptoms and productivity in offices, Proceedings of Indoor Air 2 (2002) 249-254.

[161] X. Wang, D. Li, C.C. Menassa, V.R. Kamat, Investigating the Neurophysiological Effect of Thermal Environment on Individuals’ Performance Using Electroencephalogram, Computing in Civil Engineering 20192019, pp. 598-605.

[162] D. Wechsler, Wechsler memory scale (WMS-III), Psychological corporation San Antonio, TX1997.

[163] Z. Jing, A.B. Barreto, C. Chin, L. Chao, Realization of stress detection using psychophysiological signals for improvement of human-computer interactions, Proceedings. IEEE SoutheastCon, 2005., 2005, pp. 415-420.

[164] A.G. Reddy, S. Narava, Artifact removal from EEG signals, International Journal of Computer Applications 77(13) (2013).

[165] T.-P. Jung, S. Makeig, C. Humphries, T.-W. Lee, M.J. McKeown, V. Iragui, T.J. Sejnowski, Removing electroencephalographic artifacts by blind source separation, 37(2) (2000) 163-178.

[166] J.P. Pijn, J. Van Neerven, A. Noest, F.H. Lopes da Silva, Chaos or noise in EEG signals; dependence on state and brain site, Electroencephalography and Clinical Neurophysiology 79(5) (1991) 371-381.

[167] L.J. Christiano, T.J. Fitzgerald, The Band Pass Filter*, International Economic Review 44(2) (2003) 435-465.

[168] J.A. Urigüen, B. Garcia-Zapirain, EEG artifact removal—state-of-the-art and guidelines, Journal of Neural Engineering 12(3) (2015) 031001.

[169] D. Szafir, R. Signorile, An Exploration of the Utilization of Electroencephalography and Neural Nets to Control Robots, in: P. Campos, N. Graham, J. Jorge, N. Nunes, P. Palanque, M.

Winckler (Eds.) Human-Computer Interaction – INTERACT 2011, Springer Berlin Heidelberg, Berlin, Heidelberg, 2011, pp. 186-194.

[170] H. Jebelli, S. Hwang, S. Lee, EEG Signal-Processing Framework to Obtain High-Quality Brain Waves from an Off-the-Shelf Wearable EEG Device, 32(1) (2018) 04017070.

[171] A. Delorme, S. Makeig, EEGLAB: an open source toolbox for analysis of single-trial EEG dynamics including independent component analysis, Journal of Neuroscience Methods 134(1) (2004) 9-21.

[172] F.C. Viola, S. Debener, J. Thorne, T.R. Schneider, Using ICA for the analysis of multi-channel EEG data, 2010.

[173] S. Gurumurthy, V.S. Mahit, R. Ghosh, Analysis and simulation of brain signal data by EEG signal processing technique using MATLAB, International Journal of Engineering Technology 5(3) (2013) 2771-2776.

[174] A. Pedroni, A. Bahreini, N. Langer, Automagic: Standardized preprocessing of big EEG data, NeuroImage 200 (2019) 460-473.

[175] J.N. Saby, P.J. Marshall, The utility of EEG band power analysis in the study of infancy and early childhood, Developmental Neuropsychology 37(3) (2012) 253-273.

[176] E. Combrisson, R. Vallat, J.-B. Eichenlaub, C. O'Reilly, T. Lajnef, A. Guillot, P.M. Ruby, K. Jerbi, Sleep: An Open-Source Python Software for Visualization, Analysis, and Staging of Sleep Data, 11(60) (2017).

[177] N. Jaworska, P. Blier, W. Fusee, V. Knott, Alpha power, alpha asymmetry and anterior cingulate cortex activity in depressed males and females, Journal of Psychiatric Research 46(11) (2012) 1483-1491.

[178] J.A. Coan, J.J.B. Allen, Frontal EEG asymmetry as a moderator and mediator of emotion, Biological Psychology 67(1) (2004) 7-50.

[179] N.L. Fischer, R. Peres, M. Fiorani, Frontal Alpha Asymmetry and Theta Oscillations Associated With Information Sharing Intention, Biological psychology 12(166) (2018).

[180] L. Sun, J. Peräkylä, K.M. Hartikainen, Frontal Alpha Asymmetry, a Potential Biomarker for the Effect of Neuromodulation on Brain's Affective Circuitry—Preliminary Evidence from a Deep Brain Stimulation Study, 11(584) (2017).

[181] F. Morys, L.K. Janssen, E. Cesnaite, F. Beyer, I. Garcia-Garcia, J. Kube, D. Kumral, F. Liem, N. Mehl, K. Mahjoory, A. Schrimpf, M. Gaebler, D. Margulies, A. Villringer, J. Neumann, V.V. Nikulin, A. Horstmann, Hemispheric asymmetries in resting-state EEG and fMRI are related to approach and avoidance behaviour, but not to eating behaviour or BMI, 41(5) (2020) 1136-1152.

[182] iMotions, Electroencephalography-The Complete Pocket Guide, 2019. https://imotions.com/guides/electroencephalography-eeg/.

[183] T.-T. Chen, K.-P. Wang, M.-Y. Cheng, Y.-T. Chang, C.-J. Huang, T.-M. Hung, Impact of emotional and motivational regulation on putting performance: a frontal alpha asymmetry study, PeerJ 7 (2019) e6777.

[184] P.C. Schmid, L.M. Hackel, L. Jasperse, D.M. Amodio, Frontal cortical effects on feedback processing and reinforcement learning: Relation of EEG asymmetry with the feedback-related negativity and behavior, Psychophysiology 55(1) (2018) e12911.

[185] E. Harmon-Jones, P.A. Gable, On the role of asymmetric frontal cortical activity in approach and withdrawal motivation: An updated review of the evidence, 55(1) (2018) e12879.

[186] R.J. Davidson, What does the prefrontal cortex “do” in affect: perspectives on frontal EEG asymmetry research, Biological Psychology 67(1) (2004) 219-234.

[187] C.E. Schaffer, R.J. Davidson, C. Saron, Frontal and parietal electroencephalogram asymmetry in depressed and nondepressed subjects, Biological psychiatry 18(7) (1983) 753–762.

[188] Z. Yin, J. Zhang, Cross-session classification of mental workload levels using EEG and an adaptive deep learning model, Biomedical Signal Processing and Control 33 (2017) 30-47.

[189] V. Menon, S.M. Rivera, C.D. White, G.H. Glover, A.L. Reiss, Dissociating Prefrontal and Parietal Cortex Activation during Arithmetic Processing, NeuroImage 12(4) (2000) 357-365.

[190] A. Gundel, G.F. Wilson, Topographical changes in the ongoing EEG related to the difficulty of mental tasks, Brain Topography 5(1) (1992) 17-25.

[191] Y. Nagai, H.D. Critchley, E. Featherstone, M.R. Trimble, R.J. Dolan, Activity in ventromedial prefrontal cortex covaries with sympathetic skin conductance level: a physiological account of a “default mode” of brain function, NeuroImage 22(1) (2004) 243-251.

[192] H.D. Critchley, R.N. Melmed, E. Featherstone, C.J. Mathias, R.J. Dolan, Volitional control of autonomic arousal: a functional magnetic resonance study, 16 (2002) 909-919.

[193] D. Yeom, J.-H. Choi, S.-H. Kang, Investigation of the physiological differences in the immersive virtual reality environment and real indoor environment: Focused on skin temperature and thermal sensation, Building and Environment 154 (2019) 44-54.

[194] W. Boucsein, D.C. Fowles, S. Grimnes, G. Ben-Shakhar, W.T. roth, M.E. Dawson, D.L. Filion, Publication recommendations for electrodermal measurements, Psychophysiology 49(8) (2012) 1017-34.

[195] M.E. Dawson, A.M. Schell, D.L. Filion, The electrodermal system, Handbook of psychophysiology, 4th ed., Cambridge University Press, New York, NY, US, 2017, pp. 217-243.

[196] H.J. Foy, P. Chapman, Mental workload is reflected in driver behaviour, physiology, eye movements and prefrontal cortex activation, Applied Ergonomics 73 (2018) 90-99.

[197] B. Reimer, B. Mehler, The impact of cognitive workload on physiological arousal in young adult drivers: a field study and simulation validation, Ergonomics 54(10) (2011) 932-942.

[198] T. Chaudhuri, Y.C. Soh, H. Li, L. Xie, Machine learning driven personal comfort prediction by wearable sensing of pulse rate and skin temperature, Building and Environment 170 (2020) 106615.

[199] T.P. Beauchaine, J.F. Thayer, Heart rate variability as a transdiagnostic biomarker of psychopathology, International Journal of Psychophysiology 98(2, Part 2) (2015) 338-350.

[200] A.H. Kemp, D.S. Quintana, The relationship between mental and physical health: Insights from the study of heart rate variability, International Journal of Psychophysiology 89(3) (2013) 288-296.

[201] F. Shaffer, R. McCraty, C.L. Zerr, A healthy heart is not a metronome: an integrative review of the heart's anatomy and heart rate variability, 5(1040) (2014).

[202] J.A. Chalmers, D.S. Quintana, M.J.-A. Abbott, A.H. Kemp, Anxiety Disorders are Associated with Reduced Heart Rate Variability: A Meta-Analysis, 5(80) (2014).

[203] Y.-J. Liu, M. Yu, G. Zhao, J. Song, Y. Ge, Y. Shi, Real-time movie-induced discrete emotion recognition from EEG signals, IEEE Transactions on Affective Computing 9(4) (2017) 550-562.

[204] A.-L. Roos, T. Goetz, M. Voracek, M. Krannich, M. Bieg, A. Jarrell, R. Pekrun, Test Anxiety and Physiological Arousal: A Systematic Review and Meta-Analysis, Educational Psychology Review 33(2) (2021) 579-618.

[205] I. Noy-Meir, D. Walker, W.T. Williams, Data transformations in ecological ordination: II. On the meaning of data standardization, The Journal of Ecology 63(3) (1975) 779-800.

[206] S.S. Shapiro, M.B. Wilk, An analysis of variance test for normality (complete samples), Biometrika 52(3/4) (1965) 591-611.

[207] M.B. Brown, A.B. Forsythe, The small sample behavior of some statistics which test the equality of several means, Technometrics 16(1) (1974) 129-132.

[208] G.V. Glass, P.D. Peckham, J.R. Sanders, Consequences of Failure to Meet Assumptions Underlying the Fixed Effects Analyses of Variance and Covariance, Review of Educational Research 42(3) (1972) 237-288.

[209] H. Liu, Y. Wu, D. Lei, B. Li, Gender differences in physiological and psychological responses to the thermal environment with varying clothing ensembles, Building and Environment 141 (2018) 45-54.

[210] P.R. Boyce, J.A. Veitch, G.R. Newsham, C.C. Jones, J. Heerwagen, M. Myer, C.M. Hunter, Occupant use of switching and dimming controls in offices, 38(4) (2006) 358-376.

[211] M. Franke, C. Nadler, Towards a holistic approach for assessing the impact of IEQ on satisfaction, health, and productivity, Building Research & Information 49(4) (2021) 414-444.

[212] O. Seppanen, W.J. Fisk, A model to estimate the cost effectiveness of the indoor environment improvements in office work (2004).

[213] R. Djukanovic, P. Wargocki, P.O. Fanger, Cost-benefit analysis of improved air quality in an office building, Proceedings of Indoor Air 2002, 2002, pp. 808-813.

[214] M. Brad Shuck, S. Rocco Tonette, A. Albornoz Carlos, Exploring employee engagement from the employee perspective: implications for HRD, Journal of European Industrial Training 35(4) (2011) 300-325.

[215] S. Abraham, Job satisfaction as an antecedent to employee engagement, sies Journal of Management 8(2) (2012).

[216] M.E. Echols, Engaging employees to impact performance, Chief Learning Officer 4(2) (2005) 44-48.

[217] W.B. Schaufeli, A.B. Bakker, M. Salanova, The Measurement of Work Engagement With a Short Questionnaire:A Cross-National Study, 66(4) (2006) 701-716.

[218] S. Ahlfeldt, S. Mehta, T. Sellnow, Measurement and analysis of student engagement in university classes where varying levels of PBL methods of instruction are in use, Higher Education Research & Development 24(1) (2005) 5-20.

[219] G. D. Kuh, Assessing what really matters to student learning inside the national survey of student engagement, The Magazine of Higher Learning, 2001, pp. 10-17.

[220] G. Vecchiato, J. Toppi, L. Astolfi, F. Cincotti, F.D.V. Fallani, A. Maglione, G. Borghini, P. Cherubino, D. Mattia, F. Babiloni, The added value of the electrical neuroimaging for the evaluation of marketing stimuli, Bulletin of the Polish Academy of Sciences: Technical Sciences (2012) 419-426.

[221] I. Papousek, E.M. Weiss, G. Schulter, A. Fink, E.M. Reiser, H.K. Lackner, Prefrontal EEG alpha asymmetry changes while observing disaster happening to other people: Cardiac correlates and prediction of emotional impact, Biological Psychology 103 (2014) 184-194.

[222] K.C.H.J. Smolders, Y. De Kort, P. Cluitmans, Higher light intensity induces modulations in brain activity even during regular daytime working hours, Lighting Research & Technology 48(4) (2016) 433-448.

[223] K.C.H.J. Smolders, Y.A.W. de Kort, P.J.M. Cluitmans, A higher illuminance induces alertness even during office hours: Findings on subjective measures, task performance and heart rate measures, Physiology & Behavior 107(1) (2012) 7-16.

[224] A.-M. Chang, F.A.J.L. Scheer, C.A. Czeisler, D. Aeschbach, Direct Effects of Light on Alertness, Vigilance, and the Waking Electroencephalogram in Humans Depend on Prior Light History, Sleep 36(8) (2013) 1239-1246.

[225] N. Kakitsuba, Comfortable indoor lighting conditions for LEDlights evaluated from psychological and physiological responses, Applied Ergonomics 82 (2020) 102941.

[226] B.-K. Min, Y.-C. Jung, E. Kim, J.Y. Park, Bright illumination reduces parietal EEG alpha activity during a sustained attention task, Brain Research 1538 (2013) 83-92.

[227] J.W.C. Medithe, U.R. Nelakuditi, Study on the impact of light on human physiology and electroencephalogram, Journal of Biomimetics, Biomaterials and Biomedical Engineering, Trans Tech Publ, 2016, pp. 36-43.

[228] J.A. Veitch, R. Gifford, D.W. Hine, Demand characteristics and full spectrum lighting effects on performance and mood, Journal of Environmental Psychology 11(1) (1991) 87-95.

[229] I. Knez, S. Hygge, Irrelevant speech and indoor lighting: effects on cognitive performance and self-reported affect, 16(6) (2002) 709-718.

[230] W.E. Hathaway, Effects of School Lighting on Physical Development and School Performance, The Journal of Educational Research 88(4) (1995) 228-242.

[231] T. Hwang, J.T. Kim, Effects of indoor lighting on occupants' visual comfort and eye health in a green building, Indoor and Built Environment 20(1) (2011) 75-90.

[232] J.-H. Lee, J.W. Moon, S. Kim, Analysis of occupants' visual perception to refine indoor lighting environment for office tasks, Energies 7(7) (2014) 4116-4139.

[233] I. Knez, C. Kers, Effects of indoor lighting, gender, and age on mood and cognitive performance, Environment and Behavior 32(6) (2000) 817-831.

[234] R. Mangkuto, F. Soelami, S. Suprijanto, Study of effect of daylight on Building User's Performance Based on Electroencephalograph Signal, 10th International Seminar on Sustainable Environment and Architecture (10th SENVAR)/1st International Conference on Engineering, Environment, Economic, Safety and Health (1st CONVEEESH), October 26-27, 2009, Manado, Indonesia, 2009, pp. 1-7.

[235] N. Kakitsuba, Comfortable Indoor Lighting Conditions Evaluated from Psychological and Physiological Responses, LEUKOS 12(3) (2016) 163-172.

[236] K. Breevaart, A.B. Bakker, E. Demerouti, J. Hetland, The measurement of state work engagement, European Journal of Psychological Assessment 28(4) (2012).

[237] L.J. McCunn, R. Gifford, Do green offices affect employee engagement and environmental attitudes?, Architectural Science Review 55(2) (2012) 128-134.

[238] A. Feige, H. Wallbaum, M. Janser, L. Windlinger, Impact of sustainable office buildings on occupant's comfort and productivity, Journal of Corporate Real Estate 15(1) (2013) 7-34.

[239] X. Shan, E.-H. Yang, Supervised machine learning of thermal comfort under different indoor temperatures using EEG measurements, Energy and Buildings 225 (2020) 110305.

[240] G. Zheng, K. Li, W. Bu, Y. Wang, Fuzzy comprehensive evaluation of human physiological state in indoor high temperature environments, Building and Environment 150 (2019) 108-118.

[241] X. Zhang, Z. Lian, Y. Wu, Human physiological responses to wooden indoor environment, Physiology & Behavior 174 (2017) 27-34.

[242] Gebs Energy and Environmental Management. http://gebsenergy.co.uk/2013/07/15/lights-on-light-levels-workspace/.

[243] L.J. Trejo, K. Kubitz, R. Rosipal, R.L. Kochavi, L.D. Montgomery, EEG-based estimation and classification of mental fatigue, Psychology 6(05) (2015) 572.

[244] T. Zhang, T. Zhu, P. Xiong, H. Huo, Z. Tari, W. Zhou, Correlated Differential Privacy: Feature Selection in Machine Learning, IEEE Transactions on Industrial Informatics 16(3) (2020) 2115-2124.

[245] H. Li, W. Li, X. Pan, J. Huang, T. Gao, L. Hu, H. Li, Y. Lu, Correlation and redundancy on machine learning performance for chemical databases, 32(7) (2018) e3023.

[246] S. Wold, K. Esbensen, P. Geladi, Principal component analysis, Chemometrics and Intelligent Laboratory Systems 2(1) (1987) 37-52.

[247] N.E. Helwig, Data, Covariance, and Correlation Matrix (2017).

[248] A. Abraham, Artificial Neural Networks, Handbook of Measuring System Design2005.

[249] C. Sammut, G.I. Webb, Encyclopedia of machine learning, Springer Science & Business Media2011.

[250] M. Despenic, S. Chraibi, T. Lashina, A. Rosemann, Lighting preference profiles of users in an open office environment, Building and Environment 116 (2017) 89-107.

[251] J.A. Veitch, G.R. Newsham, Preferred luminous conditions in open-plan offices: research and practice recommendations, 32(4) (2000) 199-212.

[252] G. Newsham, J. Veitch, C. Arsenault, C. Duval, Effect of dimming control on office worker satisfaction and performance, Proceedings of the IESNA annual conference, Citeseer, 2004, pp. 19-41.

[253] H. Zhang, Human thermal sensation and comfort in transient and non-uniform thermal environments, University of California, Berkeley2003.

[254] M. Frontczak, P. Wargocki, Literature survey on how different factors influence human comfort in indoor environments, Building and Environment 46(4) (2011) 922-937.

[255] M. Schweiker, M. André, F. Al-Atrash, H. Al-Khatri, R.R. Alprianti, H. Alsaad, R. Amin, E. Ampatzi, A.Y. Arsano, E. Azar, Evaluating assumptions of scales for subjective assessment of thermal environments–Do laypersons perceive them the way, we researchers believe?, Energy and Buildings 211 (2020) 109761.

[256] Z. Wang, H. Zhang, Y. He, M. Luo, Z. Li, T. Hong, B. Lin, Revisiting individual and group differences in thermal comfort based on ASHRAE database, Energy and Buildings 219 (2020) 110017.

[257] M. Woldeamanuel, D. Nguyen, Perceived benefits and concerns of autonomous vehicles: An exploratory study of millennials' sentiments of an emerging market, Research in Transportation Economics 71 (2018) 44-53.

[258] P. Sun, A. Boukerche, Challenges of Designing Computer Vision-Based Pedestrian Detector for Supporting Autonomous Driving, 2019 IEEE 16th International Conference on Mobile Ad Hoc and Sensor Systems (MASS), 2019, pp. 28-36.

[259] W. Kim, E. Jeon, G. Kim, D. Yeo, S. Kim, Take-Over Requests after Waking in Autonomous Vehicles, Applied Sciences 12(3) (2022).

[260] E. Pakdamanian, S. Sheng, S. Baee, S. Heo, S. Kraus, L. Feng, Deeptake: Prediction of driver takeover behavior using multimodal data, pp. 1-14.

[261] K. Zeeb, A. Buchner, M. Schrauf, Is take-over time all that matters? The impact of visual-cognitive load on driver take-over quality after conditionally automated driving, Accident Analysis & Prevention 92 (2016) 230-239.

[262] J. Ayoub, N. Du, X.J. Yang, F. Zhou, Predicting Driver Takeover Time in Conditionally Automated Driving, IEEE Transactions on Intelligent Transportation Systems 23(7) (2022) 9580-9589.

[263] N. Du, F. Zhou, E. Pulver, D. Tilbury, L.P. Robert, A.K. Pradhan, X.J. Yang, Predicting takeover performance in conditionally automated driving, 2020, pp. 1-8.

[264] N. Du, X.J. Yang, F. Zhou, Psychophysiological responses to takeover requests in conditionally automated driving, Accident Analysis & Prevention 148 (2020) 105804.

[265] E. Pakdamanian, N. Namaky, S. Sheng, I. Kim, J.A. Coan, L. Feng, Toward minimum startle after take-over request: A preliminary study of physiological data, pp. 27-29.

[266] S.A. Mansi, G. Barone, C. Forzano, I. Pigliautile, M. Ferrara, A.L. Pisello, M. Arnesano, Measuring human physiological indices for thermal comfort assessment through wearable devices: A review, Measurement 183 (2021) 109872.

[267] A. Gluck, M. Deng, Y. Zhao, C. Menassa, D. Li, J. Brinkley, V. Kamat, Exploring Driver Physiological Response During Level 3 Conditional Driving Automation, 2022 IEEE 3rd International Conference on Human-Machine Systems (ICHMS), 2022, pp. 1-5.

[268] C.K.L. Or, V.G. Duffy, Development of a facial skin temperature-based methodology for non-intrusive mental workload measurement, Occupational Ergonomics 7(2) (2007) 83-94.

[269] C. Collet, A. Clarion, M. Morel, A. Chapon, C. Petit, Physiological and behavioural changes associated to the management of secondary tasks while driving, Applied Ergonomics 40(6) (2009) 1041-1046.

[270] E.T. Solovey, M. Zec, E.A. Garcia Perez, B. Reimer, B. Mehler, Classifying driver workload using physiological and driving performance data: two field studies, 2014, pp. 4057-4066.

[271] S. Sheng, E. Pakdamanian, K. Han, B. Kim, P. Tiwari, I. Kim, L. Feng, A Case Study of Trust on Autonomous Driving, 2019 IEEE Intelligent Transportation Systems Conference (ITSC), 2019, pp. 4368-4373.

[272] P. Wintersberger, A. Riener, C. Schartmüller, A.-K. Frison, K. Weigl, Let me finish before I take over: Towards attention aware device integration in highly automated vehicles, pp. 53-65.

[273] Q. Meteier, M. Capallera, S. Ruffieux, L. Angelini, O. Abou Khaled, E. Mugellini, M. Widmer, A. Sonderegger, Classification of drivers' workload using physiological signals in conditional automation, Frontiers in psychology 12 (2021) 596038.

[274] R.R. Singh, S. Conjeti, R. Banerjee, A comparative evaluation of neural network classifiers for stress level analysis of automotive drivers using physiological signals, Biomedical Signal Processing and Control 8(6) (2013) 740-754.

[275] H. Mårtensson, O. Keelan, C. Ahlström, Driver Sleepiness Classification Based on Physiological Data and Driving Performance From Real Road Driving, IEEE Transactions on Intelligent Transportation Systems 20(2) (2019) 421-430.

[276] Y. Li, F. Wang, H. Ke, L.-l. Wang, C.-c. Xu, A Driver’s Physiology Sensor-Based Driving Risk Prediction Method for Lane-Changing Process Using Hidden Markov Model, 19(12) (2019) 2670.

[277] M. Soria-Oliver, J.S. López, F. Torrano, Relations between mental workload and decision-making in an organizational setting, Psicologia: Reflexão e Crítica 30 (2017).

[278] M.A. Recarte, L.M. Nunes, Mental workload while driving: effects on visual search, discrimination, and decision making, Journal of experimental psychology: Applied 9(2) (2003) 119.

[279] A. Shantz, K. Alfes, L. Whiley, HRM in healthcare: the role of work engagement, Personnel Review 45(2) (2016) 274-295.

[280] W. Kim, J.A. Kolb, T. Kim, The Relationship Between Work Engagement and Performance:A Review of Empirical Literature and a Proposed Research Agenda, 12(3) (2013) 248-276.

[281] M. Akca, M.T. Küçükoğlu, Relationships between mental workload, burnout, and job performance: a research among academicians, Evaluating Mental Workload for Improved Workplace Performance, IGI Global2020, pp. 49-68.

[282] N. Schaap, R. van der Horst, B. van Arem, K. Brookhuis, The relationship between driver distraction and mental workload, Driver Distraction and Inattention, CRC Press2017, pp. 63-80.

[283] J.K. Muguro, P.W. Laksono, Y. Sasatake, K. Matsushita, M. Sasaki, User Monitoring in Autonomous Driving System Using Gamified Task: A Case for VR/AR In-Car Gaming, 5(8) (2021) 40.

[284] N. Du, F. Zhou, E.M. Pulver, D.M. Tilbury, L.P. Robert, A.K. Pradhan, X.J. Yang, Examining the effects of emotional valence and arousal on takeover performance in conditionally automated driving, Transportation Research Part C: Emerging Technologies 112 (2020) 78-87.

[285] A. Rangesh, N. Deo, R. Greer, P. Gunaratne, M.M. Trivedi, Predicting take-over time for autonomous driving with real-world data: Robust data augmentation, models, and evaluation, arXiv preprint arXiv:2107.12932 (2021).

[286] K. Weigl, C. Schartmüller, P. Wintersberger, M. Steinhauser, A. Riener, The influence of experienced severe road traffic accidents on take-over reactions and non-driving-related tasks in an automated driving simulator study, Accident Analysis & Prevention 162 (2021) 106408.
[287] M. Deng, X. Wang, C.C. Menassa, Investigating the effect of wearing masks on office work in indoor environments during a pandemic using physiological sensing, Building and Environment 221 (2022) 109346.
[288] G. Di Flumeri, G. Borghini, P. Aricò, N. Sciaraffa, P. Lanzi, S. Pozzi, V. Vignali, C. Lantieri, A. Bichicchi, A. Simone, EEG-based mental workload neurometric to evaluate the impact of different traffic and road conditions in real driving settings, Frontiers in human neuroscience 12 (2018) 509.
[289] C. Berka, D.J. Levendowski, M.N. Lumicao, A. Yau, G. Davis, V.T. Zivkovic, R.E. Olmstead, P.D. Tremoulet, P.L. Craven, EEG correlates of task engagement and mental workload in vigilance, learning, and memory tasks, Aviation, space, and environmental medicine 78(5) (2007) B231-B244.
[290] W. Hajek, I. Gaponova, K.H. Fleischer, J. Krems, Workload-adaptive cruise control – A new generation of advanced driver assistance systems, Transportation Research Part F: Traffic Psychology and Behaviour 20 (2013) 108-120.
[291] R.F. Woolson, Wilcoxon Signed-Rank Test, Wiley Encyclopedia of Clinical Trials2008, pp. 1-3.
[292] D.G. Pereira, A. Afonso, F.M. Medeiros, Overview of Friedman's Test and Post-hoc Analysis, Communications in Statistics - Simulation and Computation 44(10) (2015) 2636-2653.
[293] M. Hollander, D.A. Wolfe, E. Chicken, Nonparametric statistical methods, John Wiley & Sons2013.

[294] N. Cliff, Dominance statistics: Ordinal analyses to answer ordinal questions, Psychological bulletin 114(3) (1993) 494.

[295] G. Macbeth, E. Razumiejczyk, R.D. Ledesma, Cliff's Delta Calculator: A non-parametric effect size program for two groups of observations, Universitas Psychologica 10(2) (2011) 545-555.

[296] M. Evin, A. Hidalgo-Munoz, A.J. Béquet, F. Moreau, H. Tattegrain, C. Berthelon, A. Fort, C. Jallais, Personality trait prediction by machine learning using physiological data and driving behavior, Machine Learning with Applications 9 (2022) 100353.

[297] X. Wang, C.-J. Liang, C. Menassa Carol, R. Kamat Vineet, Interactive and Immersive Process-Level Digital Twin for Collaborative Human–Robot Construction Work, Journal of Computing in Civil Engineering 35(6) (2021) 04021023.

[298] C.-J. Liang, X. Wang, R. Kamat Vineet, C. Menassa Carol, Human–Robot Collaboration in Construction: Classification and Research Trends, Journal of Construction Engineering and Management 147(10) (2021) 03121006.

[299] H. Yu, V.R. Kamat, C.C. Menassa, W. McGee, Y. Guo, H. Lee, Mutual physical state-aware object handover in full-contact collaborative human-robot construction work, Automation in Construction 150 (2023) 104829.